Maria Catarina Coutinho Varela da Silva

Licenciada em Ciências da Engenharia Química e Bioquímica

Effect of surfactant on PDLC films with and without permanent memory effect

Dissertação para obtenção do Grau de Mestre em

Engenharia Química e Bioquímica

Orientador: Prof. Doutor João Carlos da Silva Barbosa Sotomayor

DQ-FCT/UNL

FACULDADE DE CIÊNCIAS E TECNOLOGIA
UNIVERSIDADE NOVA DE LISBOA

September 2013

Maria Catarina Coutinho Varela da Silva

Licenciada em Ciências da Engenharia Química e Bioquímica

Effect of surfactant on PDLC films with and without permanent memory effect

Dissertação para obtenção do Grau de Mestre em

Engenharia Química e Bioquímica

Orientador: Prof. Doutor João Carlos da Silva Barbosa Sotomayor
DQ-FCT/UNL

Setembro, 2013

"Effect of surfactant on PDLC films with and without permanent memory effect"

Copyright, Maria Catarina Coutinho Varela da Silva, FCT/UNL

Indicação dos direitos de cópia
A Faculdade de Ciências e Tecnologia e a Universidade Nova de Lisboa têm o direito, perpétuo e sem limites geográficos, de arquivar e publicar esta dissertação através de exemplares impressos reproduzidos em papel ou de forma digital, ou por qualquer outro meio conhecido ou que venha a ser inventado, e de a divulgar através de repositórios científicos e de admitir a sua cópia e distribuição com objectivos educacionais ou de investigação, não comerciais, desde que seja dado crédito ao autor e editor.

Copyright
Faculdade de Ciências e Tecnologia and Universidade Nova de Lisboa have the perpetual right with no geographical boundaries, to archive and publish this dissertation through printed copies reproduced on paper or digital form or by any means known or to be invented, and to divulge through scientific repositories and admit your copy and distribution for educational purposes or research, not commercial, as long as the credit is given to the author and editor

Ao meu Avô

Acknowlegements

First of all , I would like to thank Professor João Sotomayor for the opportunity to collaborate on this project, for the participation in " XXIII National Meeting of the Portuguese Society of Chemistry " , with a poster , and for all the techniques that had the opportunity to expand during this work . I also want to thank him for his kindness and support, forcing me to develop a critical attitude towards my experimental results and autonomy at work in the laboratory .

I also wish to thank Ana Mouquinho for all her help in the laboratory, in particular in the use of the polarized light microscopy and the electro-optical testing .

To Professor João Figueirinhas , IST , for the great help and patience with the electro-optical testing and preparing the kinetic model used in this work .

I must also thank to D. Idalina and D. Conceição for their assistance with some laboratory equipment and by the company at lunch hours .

I would like to thank to Professor Madalena Dionísio and Gonçalo Santos for the explanation of the use of the DSC technique and helps in the interpretation of results .

At Daniela Nunes and Professor Pedro Barquinha, CENIMAT, for her help in the SEM technique .

I would also like to thank Alexandra Costa and Noémi Jordão by sympathy and support.

A special thanks to my friends who always accompanied, including Mariana Lopes , Inês Vieira zalthough in Ireland , ever present since 20 years ago) , Sónia Marques , Francisco Raposo, Joana Clero , Inês Melo , Hugo Moreira , João Costa among others .

Last but not least , I thank my family for their patience , support and friendship.

Abstract

The main goal of this work is to optimize the performance of the PDLC films with the introduction of an additive, in this case the triton X100.

The polymer matrix of the PDLC is based on monomers, such as Tri(ethylene glycol) dimethacrylate and poly(ethylene glycol) dimethacrylate with molecular weight of 875 $gmol^{-1}$ which were thermal polymerized using α,α-azobisisobutyronitrile as initiator.

Different aspects were investigated, such as the study of the dynamics of the transition ON/OFF state using a high-frequency alternate voltage and the attempt to minimize the liquid crystal anchorage force to the polymer matrix observed. The polymer morphology and the composites synthesized were analyzed by scanning electron microscopy.

The PDLC films were also analyzed resorting to additional studies of differential scanning calorimetry, polarized optical microscopy and Fourier transform Infrared spectroscopy

.

Finally, the kinetic behavior of the PDLC films was studied. This part of the work was done with the goal to understand what was the impact of the increase amount of TX100 on the orientation and disorientation time of the LC molecules. Additionally, a fitting model was developed in order to describe the orientation and disorientation kinetic of the system.

It was verified that the increase amount of TX100 modifies the initial anchorage force of the LC molecules to the polymeric matrix, decreasing it. This reflects on the increase of the permanent memory effect and decrease of the E90 of the PDLC films, verified also with the decrease of the average elastic constant, K, of the PDLC film. On this work, the best value for the permanent memory effect was 96% with an E90 of 2V/μm.

However, this work also demonstrates that the kinetic of the system is independent of the amount of TX100, which means that the LC molecules orientate and disorientate at practically the same time with or without additive.

Resumo

O objectivo principal deste trabalho é o de optimizar o rendimento dos filmes do PDLC com a introdução de um aditivo, neste caso, o Triton X100.

A matrix polimérica dos filmes de PDLC é baseada em monómeros, como por exemplo tri (etileno-glicol) e dimetacrilato de poli (etilenoglicol) dimetacrilato, com peso molecular de 875 $gmol^{-1}$ cuja polimerização foi realizada termicamente utilizando α,α-azobisisobutyronitrile como iniciador.

Foram investigados diferentes aspectos, tais como o estudo da dinâmica de transição estado ON / OFF usando uma tensão alternada de alta frequência e a tentativa de minimizar a força de ancoragem de cristal líquido com a matriz de polímero observada quando a tensão é aplicada. A morfologia de polímeros e os compostos sintetizados foram analisados por microscopia eletrónica de varrimento.

Os filmes de PDLC também foram analisados recorrendo a estudos adicionais de calorimetria de varrimento diferencial,varrimento de temperatura em microscopia de luz polarizada e espectroscopia de infravermelho com transformada de Fourier.

Finalmente, foi estudado o comportamento cinético dos filmes de PDLC. Esta parte do trabalho foi feita com o objetivo de entender qual o impacto do aumento de quantidade de TX100 no tempo de orientação e desorientação das moléculas de cristal líquido. Adicionalmente, um modelo cinético foi desenvolvido de forma a aferir a cinética de orientação e desorientação do sistema.

Verificou-se que o aumento da quantidade de TX100 modifica a força inicial de ancoragem das moléculas de cristal líquido com a matriz polimérica, diminuindo-a. Isto reflecte-se no aumento do efeito de memória permanente e na diminuição do E90 dos filmes de PDLC, comprovado também com a diminuição da constante elástica média, K, do filme de PDLC. Neste trabalho, o melhor valor para o efeito de memória permanente foi de 96% com um E90 de 2V/μm.

No entanto, este trabalho demonstra, também, que a cinética do sistema é independente da quantidade de TX100, o que significa que as moléculas de LC orientam-se e desorientam-se praticamente no mesmo tempo com ou sem aditivo.

This work was supported by Fundação para a Ciência e Tecnologia through the Project PTDC/CTM-POL/122845/2011.

Table of Contents

Figure Index

Chapter 1

Chapter 2

Chapter 3

Chapter 6

Graphs Index

Chapter 3

Chapter 6

Tables Index

Chapter 2

Chapter 3

Chapter 6

Symbols and Abbreviations

AIBN - α,α-azobisisobutyronitrile

BSE - Backscattered electrons

DSC - Differential Scanning Calorimetry

$\boldsymbol{E90}$ - Electric field required to achieve 90% of maximum transmittance

EO - Electro-Optical Study

FTIR - Fourier Transform Infrared Spectroscopy

IR - Infrared

LC - Liquid Crystal

PDLC - Polymer Dispersed Liquid Crystal

PIPS - Polymer-induced phase separation

PME - Permanent Memory Effect

POLYEGDMA875 - Poly(ethylene glycol) dimethacrylate 875

POM - Polarized Optical Microscopy

SEM - Scanning Electron Microscopy

SIPS - Solvent-induced phase separation

TIPS - Temperature-induced phase separation

$\mathbf{T_g}$ - Glass Transition Temperature

$\boldsymbol{T_{ON}}$ - The transmittance when the voltage is applied

$\boldsymbol{T_{OFF}}$ - The transmittance when the voltage is removed

$\boldsymbol{TNI}$ - Nematic-Isotropic Temperature

TRIEGDMA - Tri(ethylene glycol) dimethacrylate

TX100 - Triton X-100

$\boldsymbol{\Delta V}$ - Effective Applied Voltage

$\vec{\boldsymbol{\Gamma}}_{\boldsymbol{viscous}}$ - Moment of Viscous Force

$\vec{\boldsymbol{\Gamma}}_{\boldsymbol{elastic}}$ -Moment of Elastic Force

$\vec{\boldsymbol{\Gamma}}_{\boldsymbol{electric}}$ - Moment of Electric Force

$\boldsymbol{\gamma}$- Rotational Viscosity of the Director

$\boldsymbol{\lambda}$ - Ratio between LC Volume and polymer Volume

$\boldsymbol{d}$ - Thickness of the liquid crystal

$\vec{\boldsymbol{E}}$ - Electric Field of LC

$\boldsymbol{F}$ - Elastic Energy Density of the nematic LC

$\vec{\boldsymbol{h}}$ - Molecular Field

$\boldsymbol{I_0}$ - Intensity of Light Incident on the Sample

$\boldsymbol{I}$ - Transmitted Light Intensity

$\boldsymbol{K}$- Average Elastic Constant

$\boldsymbol{k_d}$ - Rate constant for dissociation of the initiator

$\boldsymbol{k_i}$ - Rate constant for the initiation step

$\boldsymbol{k_p}$ - Rate constant for the propagation step

$\boldsymbol{k_{tc}}$- Rate constant for the termination step by combination

$\boldsymbol{k_{td}}$ - Rate constant for the termination step by disproportionation

$\overline{\boldsymbol{MM}}$ - Average Molar Mass

$\vec{\boldsymbol{n}}$ - Vector Director

$\boldsymbol{n_{air}}$ - Refractive Index of the air=1

$\boldsymbol{n_e}$ - Extraordinary index of LC

$\boldsymbol{n_{glass}}$ - Refractive Index of the glass≈1,51

$\boldsymbol{n_o}$ - Ordinary index of LC

$\boldsymbol{n_p}$ - Refractive index of the polymer

$\boldsymbol{S}$ - Degree Order of the molecules on the liquid crystal

$\boldsymbol{T_0}$ - The initial reference transmittance

$\boldsymbol{t_{10}}$ - Necessary time to reach 10% of the PDLC final transmittance after removing the applied voltage

$\boldsymbol{t_{90}}$ - Necessary time to reach 90% of the maximum transmittance when applying voltage

$\vec{\mu}$ - Permanent Dipole Moment

1. Introduction

1.1 Liquid Crystals

The majority of the substances exist only in three states: solid, liquid and gas. However, certain organic materials do not show a single transition from solid to liquid, but rather a cascade of transitions involving new phases. The mechanical properties and the symmetry properties of these phases are intermediate between those of liquid and those of a crystal. For this reason, they have been often called *liquid crystals (LC).* A more proper name is "mesomorphic phases". In order to understand the significance of these new states of matter, it may be useful to recall the distinction between a crystal and a liquid first.

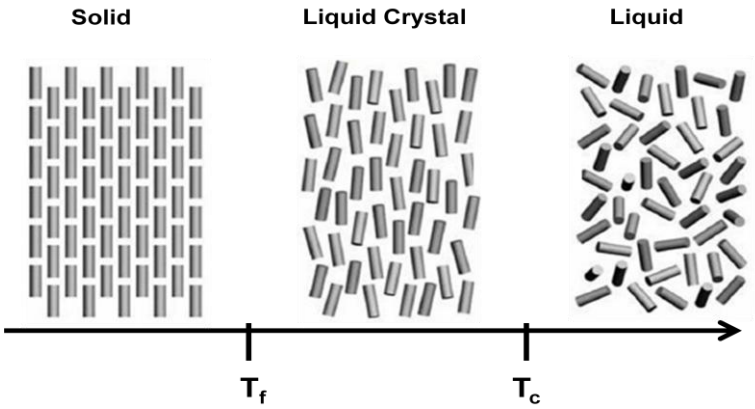

Figure 1.1 - The different states of matter according to the temperature [1]

In the crystalline solid state, as represented in Figure 1.1[1], the molecules are arranged in regular positions, with a regularly repeating pattern in all directions. The molecules are held in fixed positions by intermolecular forces, meaning that the molecules have positional and orientational order. As the temperature of a matter increases, its molecules vibrate more vigorously.When these vibrations overcome the forces that hold the molecules in place, the molecules start to move. In the liquid state, this motion overcomes the intermolecular forces that maintain a crystalline state, and the molecules move into random positions, losing both positional and orientational order.

On the materials that form liquid crystals, the intermolecular forces are not the same in all directions: they are weaker in some directions than in others. As such material is heated, the increased molecular motion overcomes the weaker forces first, but its molecules remain bound by the stronger forces. This produces a molecular arrangement that is random in some directions

and regular in others, meaning that the positional order gets lost, but some orientational order is kept. The arrangement of molecules in one type of liquid crystal is represented in Figure 1.1. According to the molecular structure, these materials can go through one or more mesophase before becoming isotropic liquids. These transitions can be observed by changing the temperature (thermotropic mesophase) or in the presence of an adequate solvent (lyotropic mesophase).

Most of electro optical devices use thermotropic liquid crystals. Thus, in this paper we will focus on this type of liquid crystal, which will then be restricted to a more specific type that will be use on the experimental work.

- Thermotropic liquid crystals

In thermotropic liquid crystals, phase transitions occur by temperature variation. Molecules of this type of liquid crystal display various forms, which make it possible to classify them. Thermotropic liquid crystals can be classified by the different shapes molecules present. These shapes can be: rod-like, disc-like, pyramid and tetrahedron; originating the following mesophases, respectively: calamitic, discotic, pyramidal and tetrahedral.

All mesophases can be grouped in three major categories: nematic , cholesteric and smectic phase . What distinguishes these different states of matter is the molecules' organization, which originates different macroscopic symmetries and physical properties. One of the simplest ways to distinguish between the different mesophases is through the observation of the respective textures using a polarized light microscope, as shown in Figure 1.2[2].

Figure 1.2 - Examples of liquid crystals textures observed through the polarized microscope: (a) - nematic phase; (b) - cholesteric phase; smecitc phase[2]

NEMATIC PHASE

The nematic phase is characterized by molecules with no positional order but tend to align in the same direction. They align through a preferred axis, wich is defined by a vector n, that translates its local orientation. This vector is called director. Because there its magnitude has no significance, it is considered to be the unit vector. The director has no physical significance and therefore $n = -n$ are equivalent. Optically, a nematic behaves as a uniaxial material with a center of symmetry.

CHOLESTERIC PHASE

On the cholesteric phase the molecules have the long-range orientation order characteristic of the nematic phase but no long-range order in positions of the centers of mass of molecules. Unlike the nematic phase, on the cholesteric phase the director varies throughout the medium in a regular way. This leads to the formation of layers with the director in ecah layer twisted with respect to those above and below. The variation of the director tends to be periodic.

SMECTIC PHASE

The biggest different between the smectic phase and the nematic phase is the fact that in the smectic phase the molecules are arranged in layers and exhibit some correlations in their positions in addition to the orientational order. This phase presents a stratification of the molecules. The smectic phase can be divided in several classes: smectic phase A, smectic phase B and smectic pahse C. In the type of smectic A the molecules are arranged perpendicularly to the plane of the layers; in the smectic of type C the molecules are arranged obliquely to the layers; and in the smectic phase B there is hexagonal crystalline order within the layers.

Liquid crystals possess many of the mechanical properties of an isotropic liquid, such as, high fluidity and the inability to support shear, but on the other hand they have some properties similar to crystalline solids such as optical anisotropy (birefringence).

On the liquid crystalline state the molecules tend to point along a common axis, called the director vector which is represented by n. The director gives the direction of the preferred orientation of the liquid crystal molecules, being directions, +n and -n equivalent. The important

thing is the direction that the molecules are pointing, except for molecules with permanent dipole moments.

Liquid crystals possess more order than the liquids but less than the solids since molecular orientations are not perfect due to fluctuations. This value is quantified by the degree order parameter, defined S, which varies between 0 and 1. In a perfect oriented system, $S = 1$, and in an isotropic liquid state, with no orientational order, $S = 0$.

$$S = \frac{1}{2}3(\cos^2\Theta - 1)$$

In the mesophase, this value ranges between 0,3 and 0,9, as temperatures decreases. To simplify, it is assumed that in a liquid crystal phase, $S = 0{,}5$[2].

The anisotropic structure of the LC is due to the fact that its molecules have a molecular axis of different dimension than the others. On an anisotropic material the propagation velocity of the light beam in the medium isn't uniform, and depends on the direction and the polarization of the light beam that crosses it, as shown in Figure 1.3 [1]. As a result, the liquid crystals present more than one refractive index . These refractive indices are called the ordinary and the extraordinary indices, n_o and n_e, respectively. These is called optical anisotropic or birefringence. The first one is measured perpendicularly to the optic axis and the second one is measured parallel to the same axis.

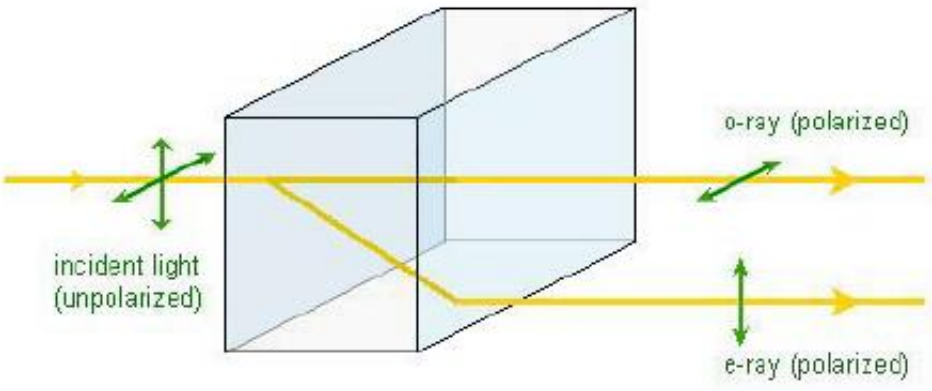

Figure 1.3 - Light traveling through a birefringent medium will take one of two paths depending on its polarization [1]

These refraction indices of the material can be defined as the ratio between the speed of light in vacuum and the speed of light in the material:

$$n_e = \frac{c}{v_{parallel}} \quad and \; n_o = \frac{c}{v_{perpendicular}}$$

The maximum value for the birefringence is given by:

$$\Delta n = n_e - n_o$$

For a typical nematic liquid crystal, n_o is around 1,5 and the maximum difference, Δn, may range between 0,05 and 0,5[3]. In the case of uniaxial liquid crystals the optic axis coincides with the director n.

The degree of orientational order in liquid crystal varies with temperature. Therefore, the refractive index also change. At a temperature higher than the TNI (nematic isotropic temperature) the mesophase melts into an isotropic liquid, losing all the positional and orientational order and the two indices become together in value (Figure 1.4[4]).

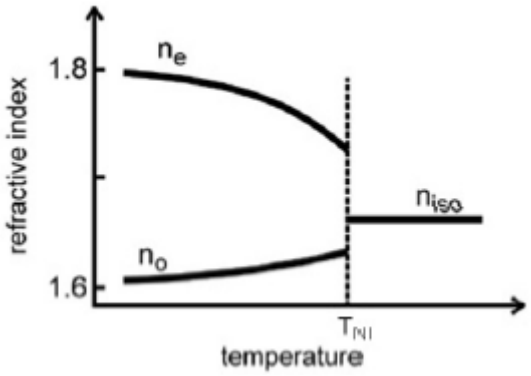

Figure 1.4 - Temperature dependence on refractive index of a thermotropic liquid crystal [4]

Beside the optical anisotropy, liquid crystals also exhibit a dielectric anisotropy. Dielectric anisotropy defines the director alignment and, consequently, the orientation of the liquid crystal molecules in the presence of an electric field. This anisotropy is characterized by the dielectric constants, measured perpendicularly and parallel to the longitudinal axis of the liquid crystal molecule. Therefore, dielectric anisotropy is given by:

$$\Delta\varepsilon = \varepsilon_{parallel} - \varepsilon_{perpendicular}$$

This difference measures the tendency of the director of the molecules to align parallel or perpendicular to the applied electric field. This interest of the application of this material on EO devices is mostly due this interaction of the LC molecules with the electric (or magnetic) filed. This action induce alterations on the LC orientation, allowing a control of its macroscopic properties.

The LC molecules can be polar or non -polar. On the case of the polar molecules there is an irregular distribution of the electric charges, resulting in an area where the molecule is positive and another where it is negative, producing a permanent dipole moment, $\vec{\mu}$. This separation occurs because there is a difference of electro negativity between the different atoms. On the case of non-polar molecules, they acquire an electric dipole induced by the application of an external electric field, causing a slightly separation of the positive and negative charges of the molecule.

Without an electric field, the molecules are preferentially oriented on the director direction. When an electric field is applied, these molecules tend to align according to the direction of the electric field and if the dipole moment of the molecule is normal to the director, as shown in Figure 1.5[5], the molecules tend to align perpendicularly to the direction of the electric field.

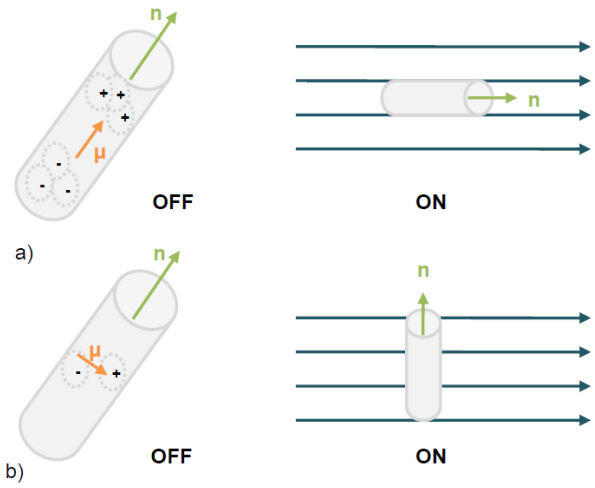

Figure 1.5 - Effects of an electric field in a liquid crystal molecule; (a) Δε>0, (b)Δε<0 (adapted[5])

1.2 Polymer Dispersed Liquid Crystals

1.2.1 The PDLC paradigm

Polymer dispersed liquid crystals (PDLC) films are a mixed phase of nematic liquid crystals (LC) dispersed as inclusions in a solid polymer. They have a remarkable electro-optical behaviour since they can be switched from an opaque to a transparent state simply by application of an electric (or magnetic) field.

The unifying theme in polymer dispersed liquid crystals is the formation of systems with a high surface-to-volume ratios. Traditional liquid crystal devices are formed as thin films between two parallel substrates. The substrates are usually treated to obtain a uniform alignment of the liquid crystal in each surface. While the director field may vary in direction from one substrate to the other, laterally the director orientation is quite uniform. Anchoring effects are relegated to the two bounding substrates.

PDLC systems differ in several fundamental ways from other types of liquid crystal devices. First, there is a large increase in the relative surface are in PDLC systems, around 15 times more. This increase will make interfacial effects quite important in PDLC devices. One obvious example of the interfacial effects that can be expected to be important is the anchoring properties of the liquid crystal at the surface.

Unlike parallel-plate geometries, the internal surfaces in PDLC films are curved. Curved surfaces leads to alignment and defect structures not found in parallel-plate liquid crystal devices. Wide variations in the internal polymer structure are found in PDLC material. The liquid crystal may exist as either discrete droplets, as an interpenetrating network with the polymer, or something in between.

The polymer network inside the PDLC films leads to another major difference between most PDLC systems and conventional liquid crystals films which is the average volume of uniformly-oriented liquid crystal. In many types of liquid crystal devices the director field is oriented uniformly over large volumes. In contrast, each domain of LC in a PDLC film can possess an a alignment independent of other droplets. The rapid variation in liquid crystal alignment throughout the film provides the scattering properties seen in many PDLC devices.

1.2.2 History

Dispersed Liquid Crystals have been object of occasional study in the literature for many decades[6]. Liquid crystal tactoids (cigar-shaped droplets) were noted by Zocher and others. In the 1950's, Frank and Pryce proposed a "spherulite" structure for cholesteric droplets. Meyer reported the bipolar droplet structure in 1969, while later that year Dubois-Violette and Parodi published a theoretical paper considering the energetic of different director configurations within the droplets. Candau examined the effect of magnetic fields on bipolar, radial, and sherulitic droplets in the early 1970's. Lens-shaped droplets floating on water were studied by Press and Arrot un 1974. The early 1979's aksi saw several papers published on the structure of nematic and smectic liquid crystals in capillary tubes. These cylindrical systems were interesting as they allowed for the observation of "escaped" defect structures, which formed as a low-energy alternative to a line defect.

Some liquid crystal/polymer composites were reported in the 1970's as electrically-controllable displays. The use of a polymer binder to support large area liquid crystal displays was proposed by Shanks , although the concept did not extend beyond the electro-optical effects known at the time. Phase methods of forming dispersed liquid crystal systems exhibiting the dynamic scattering effect were proposed by Taylor. None of these systems proved of any lasting influence, presumably because the electro-optic effects were impractical to use in real devices.

The situation changed dramatically is 1981 when Fergason disclosed novel electro-optical effects in a polymer dispersed liquid crystal system. The films were made by emulsifying a nematic liquid crystal into an aqueous solution of polyvinyl alcohol, casting this film onto a conductive substrate to form the device. The film was highly scattering at zero field but became transparent when a sufficiently strong electric field was applied across the film. If the liquid crystal contained a dichroic dye, the film possessed a controllable absorbance as well as scattering. These materials possessed the basic properties for which present-day PDCL devices are known.

In 1982, Craighead reported a scattering-based device formed by taking a porous membrane, filling the membrane with liquid crystal, and placing the membrane between conducting substrates. At zero field were highly scattering but became transparent when an electric field was applied.

One of the hallmarks of early PDLC films was that they operate at substantially higher voltages than nematic devices. Devices voltages ranging from 60 V to 120V (or higher) were common

for early PDLC devices. In recent years, improvement in polymer materials gas advanced to the point where many groups can produce films which operate in the 5-10 V range. The lowered voltage makes active-matrix PDLC devices both possible and attractive.

1.2.3 PDLC morphology

It is known from the literature that the PDLC films can exhibit essentially two types of morphology known as "Swiss Cheese" and "Polymer Ball". Both can be electrically switched from the light scattering (OFF) to a transparent (ON) state. The different configurations can be explained by the conditions under which phase separation occurs.

- "Swiss Cheese" Morphology

This morphology presents liquid crystal droplets embedded in the polymer matrix. The LC found in the interior can present different configurations which depend on several factors such as the size and shape of the domains. The radial configuration can be observed when the LC molecules are found with an orientation perpendicular to the polymer surface. When the LC molecules are oriented perpendicularly to the polymer walls but with a low anchorage force, we have an axial configuration. If the LC possesses a parallel orientation relatively to the polymer surface, two punctual defects are created on the polar of the domains, and in this case we have a bipolar configuration. These three configurations are schematized on the Figure 1.6.

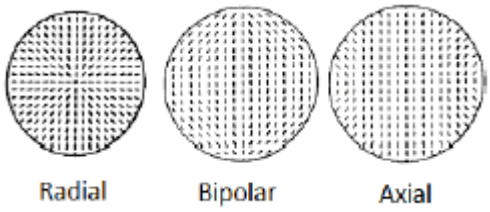

Figure 1.6 - Possible configurations of the LC molecule inside a micro domain

On the next figure there is a SEM image of the "Swiss Cheese" morphology.

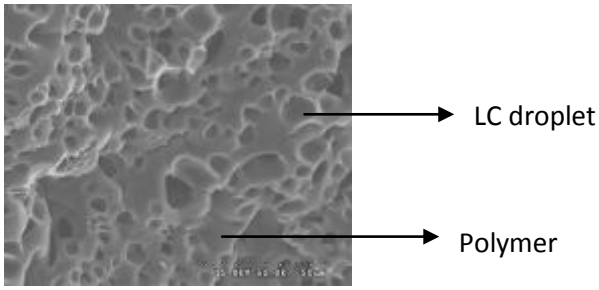

Figure 1.7 - SEM image of the "Swiss Cheese" morphology[7]

- "Polymer Ball" Morphology

The “polymer ball” morphology has a continuous liquid crystal phase embedded in a polymer bead matrix. The nuclei of the insoluble component form a discontinuity, in this configuration the discontinuous phase is the polymer[7]. It is characterized by asymmetric voids in the polymer matrix in which the liquid crystal exists. The polymer phase appears as a collection of agglomerated microspheres forming an irregular network within the nematic fluid[2].

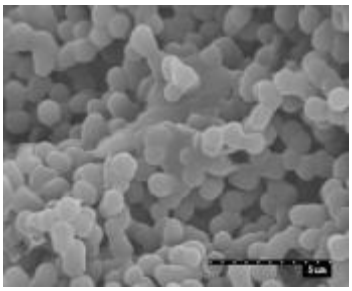

Figure 1.8 - SEM image of the "Polymer Ball" morphology[2]

In the “Swiss cheese” morphology the memory effect is not found, but in the “polymer ball” morphology it is. This means that after voltage removal the liquid crystal alignment is maintained. Moreover, liquid crystal alignment induced by anchoring on the micro sized polymer balls surface appears to affect other liquid crystal molecules nearby, so they align collectively along the same direction. Since the liquid crystal is not isolated, this collective alignment may occur without increasing elastic energy. The memory effect depends strongly on the surface anchoring effects on the polymer balls surface. The PDLCs with a higher surface-to-volume ratio and complicated structure exhibit stronger memory effect[8].

1.2.4 PDLC films transmittance

The polymer matrix is optically having a single refractive index (n_p). However, the microdomains of LC have an ordinary refractive index (n_o) and an extraordinary refractive index (n_e).

In an electrical off-condition, PDLC film is opaque (when $\Delta\varepsilon>0$ - figure 1.5) because of the light scattering caused by the refractive index mismatch between the LC droplets and the polymer matrix. In an electrical on-condition, PDLC film becomes transparent because the alignment of the LC is parallel to the applied electric field and the ordinary refractive index of the LC matches the refractive index of the polymer. It has been found that the electro-optic

property of PDLC films is influenced by the size and morphology of LC domains, the compositions ratios, separation degree and other parameters.

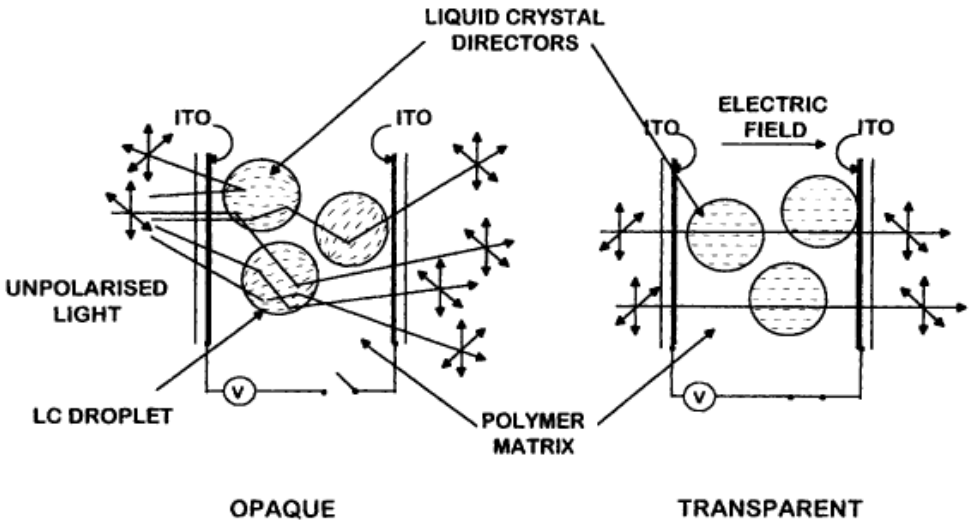

Figure 1.9 - Schematic PDLC in OFF and ON state[9]

PDLC films can be prepared by several techniques such as thermally induced phase separation (TIPS), solvent induced phase separation (SIPS) and polymerization induced phase separation (PIPS), as described in sector 2.2.1 .

1.2.5 Electro-Optical Properties of PDLC films

EO response of PDLC films is usually studied measuring the behavior of these films by ramping a PDLC up and down in voltage and comparing the optical response at each voltage.

One of the factors used to evaluate the PDLC efficiency is $E90$, which is defined as the electric field required to achieve 90% of maximum transmittance. The ideal value is a small as possible, hence it means that the PDLC will switch from an opaque state to a transparent state more easily.

Usually the PDLC most common response reported in the literature is when submitting a PDLC film to a certain voltage and removing it, the decreasing voltage curve and the increasing voltage curve are equal, as shown in Figure 1.10 [2].

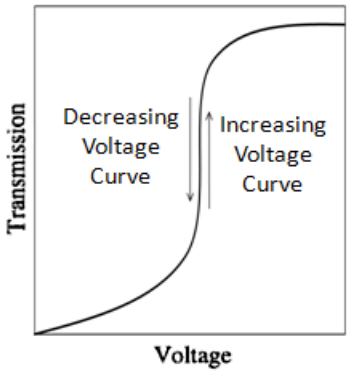

Figure 1.10 - PDLC electro-optic study with no hysteresis [2]

Although in some PDLC films, when an voltage is applied and then removed the cell returns to an opaque state to a different path. In this case, the PDLC film EO response exhibit an hysteresis and can be defined as the difference between the increasing voltage curve and the decreasing voltage curve.

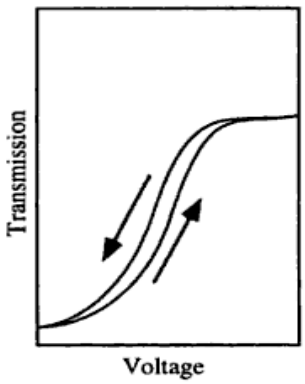

Figure 1.11 - PDLC electro-optic study with hysteresis effect [2]

In particular cases, not only the transmission with increasing voltage is lower than the transmission voltage is decreased, but also a transparency state is obtained for a long period time at room temperature even after the applied voltage has been removed. This is called permanent memory effect and it is represented in Figure 1.12 [2].

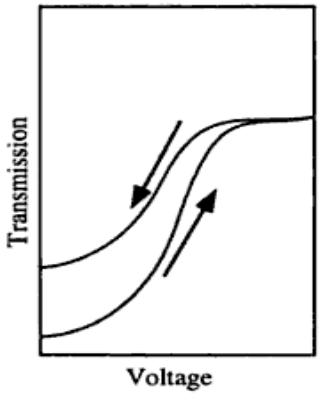

Figure 1.12 - PDLC electro-optic study with permanent memory effect [2]

The percentage of memory effect can be defined as:

$$\boldsymbol{PME}\ (\%) = \frac{T_{OFF} - T_0}{T_{ON} - T_0} \times 100$$

where:

T_{ON} (%) - The transmittance when the voltage is applied

T_{OFF} (%) - The transmittance when the voltage is removed

T_0 (%) - The initial reference transmittance

The contrast ratio of the memory state and the value of E90 are important factors to the functioning of a polymer dispersed liquid crystal display. A higher ratio is the desired aspect of any display and can be calculated by the following equation:

$$State\ Memory\ Contrast = \boldsymbol{T_{OFF} - T_0}$$

E90 is defined as the electric field required to achieve 90% of maximum transmittance an the desire value is as low as possible.

1.2.6 Factors that influence the PDLC performance

There are several factors that influence the PDLC performance, and therefore the PME. The most important is the anchorage force [10] [11] [12]. The molecules nearest the surface remain anchored to the substrate surface, when energy is supplied or taken, while the other molecules suffer an alignment or misalignment. If it is considered the LC domain as been constituted of an interfacial shell of immobilized molecules due to the anchoring interaction with the polymer surface, this interfacial shell holds in its interior anchored molecules that will influence the orientation of the adjacent ones through the elastic restoring forces arising in the deformed nematic. Before applying any field the inclusions are randomly distributed. When an electric field is applied, the molecules in the bulk reorient along the field but the anchored molecules at the interface impair a full homeotropic alignment. Above that field, the anchoring of the molecules to the polymeric surface is broken and the molecules on the surface adopt an alignment towards the field direction that tends to persist after removal. The alignment at the surface determines the orientation of the remaining liquid crystal giving rise to a higher transparency state even in the off sate, is defined as permanent memory effect (**PME**). These

anchorage links are easily broken by increase of temperature. This effect is represented in Figure 1.13[13].

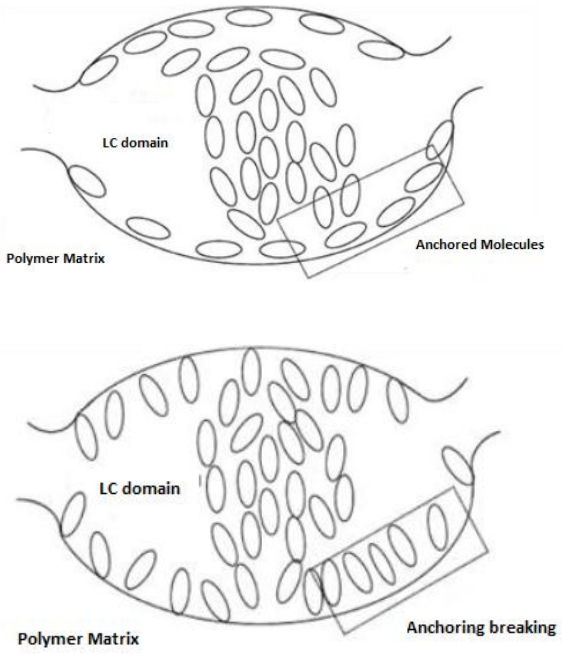

Figure 1.13 - Surface anchorage when E=0 and when E≠0, respectively [13]

This anchoring force is affected by the presence of an additive. *Chung et at*.[14] proved that the addition of a surfactant modifies the original anchoring force of the liquid crystal molecules to the surface of the polymer. It is argued that the modification presented, would result on a less rigid interface between the polymer and the LC interface. Figure 1.14[13] shows a scheme that represents the interaction between the surfactant (additive) molecules and the polymer matrix.

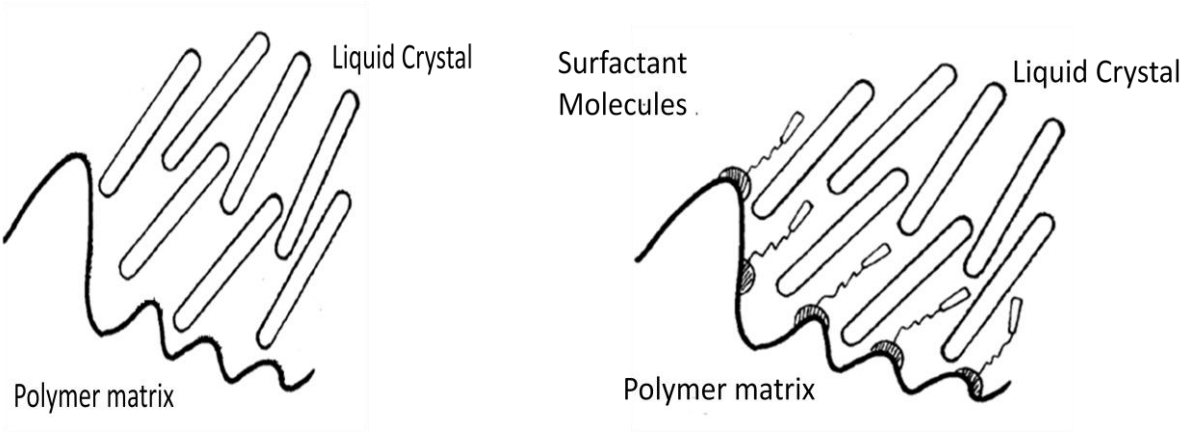

Figure 1.14 - Interaction between the molecules with and without an additive[14]

Without an additive the liquid crystal molecules are anchoraged to the surface of the polymeric matrix with a certain force. When a surfactant is added, such as TX100, it tends to place itself between the polymeric matrix and the liquid crystal molecules. This modifies the original anchoring force of liquid crystal molecules to the surface of the polymer, reducing it[14]. Therefore the LC molecules are more mobile and tend to orientate with a lower applied voltage. When removing this applied voltage, because the anchoring force is not as strong as without TX100, it is expected that the PME increases and the E90 decreases.

1.2.7 Applications

PDLCs have a wide variety of applications due to their peculiar electro-optical and mechanical properties. Such properties allow the use of PDLC in situations where other devices cannot be used. Here it is summarized some PDLC characteristics useful in one or more applications:

- PDCLs do not require rigid boundaries (glass plates) so they can be easily produced in large, flexible films.
- The amount of LCs in a PDLC film is lower than in other LC-based devices, with economic advantages since LC is an expensive material.

The application of PDLC films on "smart windows" is one of the first and, perhaps, the most popular PDLC application. Placing a PDLC film between two glass panes with conducting surface treatment, it is possible to switch the appearance of the window between a transparent and an opalescent state by applying a high-frequency voltage across conducting electrodes, as shown in Figure 1.15. Such device can be used for privacy or light protection.

Figure 1.15 - Example of a smart window

Another interesting application is related to PDLC films with permanent memory effect. These materials seem to be promising for the development of new optical digital memories [15] [16], as

they can be used for electrically write information, optically read the written information and they can be thermally erased back to the initial scattered state. For example, taking a pixel display, below, (in this example 6 pixels), we can WRITE information in a digital way by applying voltage to selected pixels (transparent or opaque, 0 or 1), we can READ information, for instance with a laser measuring transmittance, and we can ERASE information by heating to a temperature higher than the composite clearing temperature.

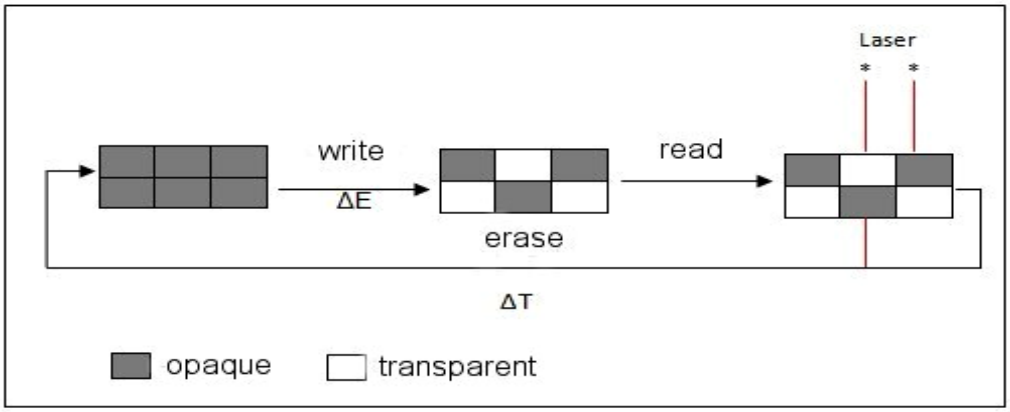

Figure 1.16 - Example of the operation of an optical memory device [15],[16]

2. Materials and Techniques

2.1 Materials

In this chapter will be described the materials and methods used during this work. Here, it is referred to all the components that are a part of the PDLC films preparation, such as monomers, polymerization initiators, liquid crystal and additive in study.

2.1.1 Monomers

In this work, the two monomers used are tri(ethylene glycol) dimethacrylate - TRIEGDMA - and poly(ethylene glycol) dimethacrylate 875 - POLYEGDMA$_{875}$ - from *Fluka* and *Aldrich*, respectively. In the figures bellow, it is shown the chemical structure and molecular formula of both monomers.

The monomer TRIEGDMA, has a molecular weight of 286.33 $\mathrm{g\,mol^{-1}}$ and a density of $\mathrm{d}_4^{20} = 1.075$. Product details information can be found under CAS number 109-16-0.

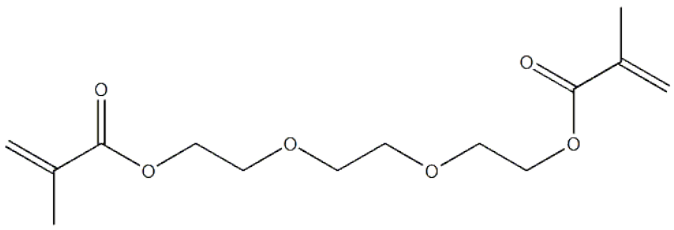

$C_{14}H_{22}O_6$

Figure 2.1 - Chemical structure and molecular formula of TRIEGDMA

The oligomer POLYEGDMA$_{875}$, from *Aldrich* has typical molecular weight of 875 $g\mathrm{mol^{-1}}$ and a density of $\mathrm{d}_4^{20} = 1.099$. Product detailed information can be found under CAS number 25852-47-5.

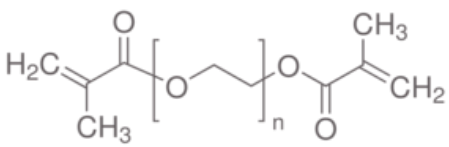

$C_8H_{10}O_3(C_2H_4O)_n \qquad n \cong 16.5$

Figure 2.2 - Chemical structure and molecular formula of POLYEGDMA$_{875}$

2.1.2. Polymerization Initiators

The polymerization is initiated through the use of agents capable of forming free radicals, which are referred to polymerization initiators as described in the section 2.2.1. The initiator is a thermal initiator , α,α-azobisisobutyronitrile (AIBN). This initiator, from Merck, has a molecular weight of 164.21 $gmol^{-1}$ and a melting point of 103~105 ºC. **In the presence of heat, AIBN originates two free radicals (at about 64ºC) and nitrogen**. Product information can be found under CAS number 78-67-1. The chemical structure and molecular formula of AIBN is shown in the figure 2.3.

.

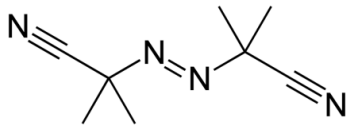

Figure 2.3 - Chemical structure of AIBN

2.1.3. Liquid Crystal

The liquid crystal used, table 2.1, is a blend of various compounds forming a nematic liquid crystal, cyanobiphenyl mixture, known as E7 manufactured and commercially available from *Merck*, division of Licrystal.

Table 2.1 - Composition of nematic liquid crystal E7

IUPAC Name	Chemical Structure and Molecular Formula
4-cyano-4'-n-pentyl-1,1'-biphenyl **(5CB)**	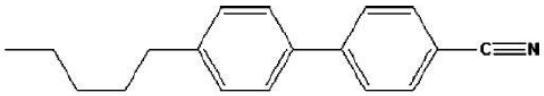 $C_{18}H_{19}N$
4-cyano-4'-n-heptyl-1,1'-biphenyl **(7CB)**	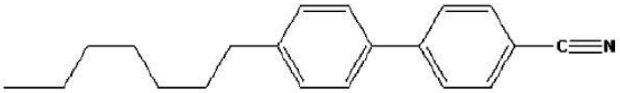 $C_{20}H_{23}N$
4-cyano-4'-n-octyloxy-1,1'-biphenyl **(8OCB)**	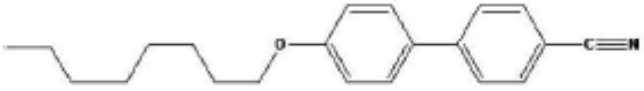 $C_{21}H_{25}NO$
4-cyano-4''-n-penthyl-1,1',1''-terphentyl **(5CT)**	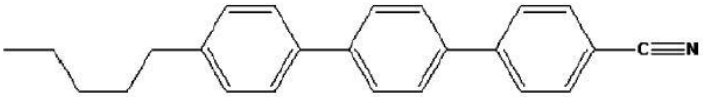 $C_{24}H_{23}N$

In this table is illustrated the chemical structures of E7 components with all its constituents. E7 it is a mixture with different proportions of three cyanobiphenyl molecules (51% of 5CB, 25% of 7CB and 16% of 8OCB) and one cyanoterphenyl molecule (8% of 5CT).

E7 is widely used in polymer dispersed liquid crystals, and it was selected to be studied in this work, because it offers a wide range of operating temperatures in which it maintains anisotropic characteristics. It exhibits a nematic to isotropic transition at nearly TNI=58ºC (this value is supplied by *Merck*). At room temperature it still exhibits a nematic phase and no other transitions between 58 and -62ºC, where it shows a glass transition (these values are given by the company *Merck)*. Therefore, liquid crystalline properties are extended down to the glass transition.

2.1.4. Additives

In previous studies a few additives were tested, such as octanoic acid, ethyleneglycol, Triton X100 (TX100), cetyl trimethyl ammonium bromide and sodium dodecyl sulphate. From all of them Triton X100 was the best additive to format the shape and the size of the liquid crystal micro droplets and to avoid its coalescence and, therefore, optimizing the performance of the device as being able to electro-optical application[17].

Therefore, aiming to test the additive effects in polymer dispersed liquid crystals, this study was only focused on TX100. TX100, a non-ionic surfactant, has a typical molecular weight of $647\ gmol^{-1}$ and a density of $d_4^{20} = 1.065$. Product detailed information can be found under CAS number 9002-93-1.

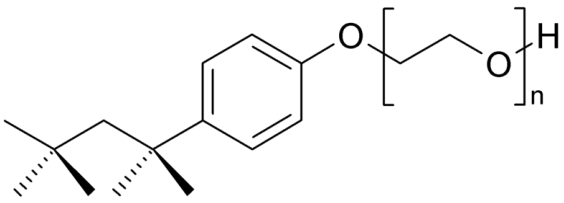

Figure 2.4 - Chemical Structure of TX100

2.1.5. Indium Tin Oxide Cells

The cells used as PDLC films support are constituted for a glass covered with a small layer of indium and tin conductive oxide. A schematic illustration of an indium tin oxide cell is present in Figure 2.5[18].

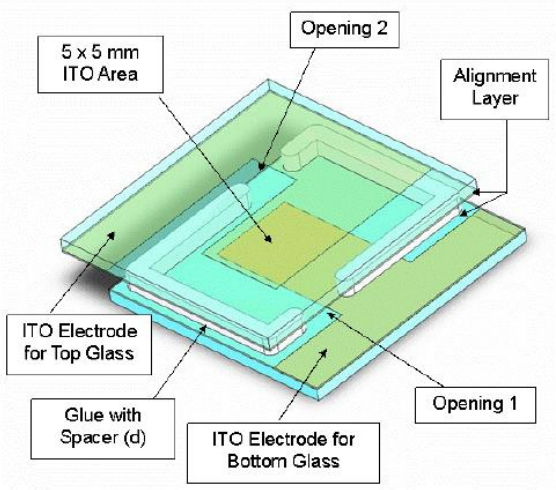

Figure 2.5 - ITO cell [18]

2.2 Techniques

2.2.1 Preparation of solutions

In our studies, the PDLC devices synthesized consist on a polymerized mixture of liquid crystal, monomer, initiator and some also have TX100 in different proportions. Table 2.2 shows a resume of the solutions that were prepared. Each solution has in total 0,5 g (%w/w), the additive in solution corresponds to a determined percentage of the total weight and the rest is distributed between the monomer, liquid crystal and initiator. The initiator is about 1%w/w relative to the monomer.This solutions are weighed on a scale RADWAG analytical balance with four decimal digits. The solutions are prepared in eppendorf tubes and stored at 4 $^{\circ}C$.

The monomers are commercialized with an inhibitor of polymerization (specifically hydroquinone and monomethyl ether hydroquinone) so that the monomers do not polymerize on storage. So, before preparing the solutions for polymerization, it is necessary to remove this inhibitor. In order to do so, specific columns for each monomer are available. It consists on a column filled with a resin, polystyrene divinylbenzene, and supplied by *Merck*. Further information on the product can be found under CAS number 9003-70-7.

Table 2.2 - Solutions prepared to use in the PDLC devices

Additive (% w/w)	Monomer (% w/w)	Liquid Crystal (% w/w)	Initiator (% w/w)
0	50	50	1
	40	60	
	30	70	
	20	80	
	10	90	
0,2	30	70	
1	30	70	
2	30	70	
3	30	70	
5	30	70	
10	30	70	
20[(1)]	30	70	

[(1)] - This amount of additive was only use in the case of the $POLYEGDMA_{875}$

This procedure is very simple: add the monomer to an addition funnel above the column and then let it dropwise through the column, collecting the monomer (now without inhibitor) in an appropriate container. In Figure 2.6 it is shown the type of column and scale used.

Figure 2.6 - Extraction Column and Analytical Balance

Before transferring the solutions into an indium tin oxide cell it is necessary to mix the components on a vortex so that the solution stays as much homogenous as possible and form a single-phase solution of LC , monomer and additive.

2.2.1 PDLC preparation techniques

The PDLC preparation techniques can be grouped in two main classes depending on whether it starts with an emulsion of the LC in the polymer (or corresponding monomer) or with a single-phase solution of LC , monomer and additive. In the first case, it is called "emulsion techniques" and the LC droplets are formed in the liquid phase, while in the second case, the "phase separation techniques", are formed later during the film solidification. In our studies it was chosen to prepare the PDLC films through a phase separation technique.

In this technique, the PDLC is obtained starting with a homogenous liquid single phase mixture containing both the LC, monomer additive. During the polymer solidification, almost all LC molecules are "expelled" from the polymer (phase separation) and aggregated in droplets or domains which remain embedded in the polymer matrix.

The separation phase can be induced in several ways:

- Temperature-induced phase separation (**TIPS**)

The LC is mixed with a melted thermoplastic polymer, the liquid is placed between two transparent conducting electrodes and phase separation is induced by polymer solidification, obtained by cooling the sample at a controlled rate.

- Solvent-induced phase separation (**SIPS**)

A solution is prepared with the polymer, the solvent and the required amount of LC. The liquid placed over a single transparent conducting electrode. After the solvent has evaporated, thus inducing droplet formation, a second transparent conducting electrode is placed over the PDLC film.

- Polymer-induced phase separation (**PIPS**)

The monomer is mixed with the required amount of LC in a single phase liquid. The liquid is placed between two transparent conducting electrodes and the polymerization process is started, by heating (thermally, using a thermal initiator) or photo-initiator with ultraviolet light.

In our studies the phase separation technique applied was PIPS, inducing polymerization using AIBN as a thermal initiator. This type of thermal polymerization was widely studied in previous works, allowing to conclude that a slower kinetic of polymerization presents better results.

So, the PDLC preparation was done slowly in a store during night at 74ºC. Figure 2.7 shows the stove used in polymerization. This temperature ensures the formation of free radicals to initiate polymerization.

Figure 2.7 - Stove used in thermal polymerization

Polymerization occurs by adding (or growing chain), characterized by breaking a reactive double bond. The break of a double bound, which begins the process, requires the presence of a radical, therefore called free radical reaction. This process goes on until the reaction is over.
The reaction mechanism of free radical polymerization is composed of three main steps: initiation, propagation and termination[19].

- **Initiation:**

The initiation step involves two reactions: the production of free radicals and its addition to the monomer.

1) Dissociation

$$I \xrightarrow{k_d} 2R\bullet$$

(where k_d rate constant for dissociation of the initiator)

Equation 2.1 - Dissociation of the initiator

2) Addition of the radical initiator to the first monomer molecule

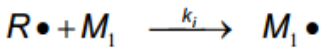

(where k_i is the rate constant for the initiation step)

Equation 2.2 - Initiation step

- **Propagation:**

In the propagation step, there is a fast growing by successive additions of monomer molecules. Each addition gives rise to a new radical with the same identity as the radical that gave it origin. The equation that reflects the propagation is:

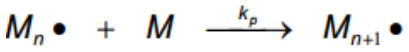

(where k_p is the rate constant for the propagation step)

Equation 2.3 - Propagation step

- **Termination:**
-

The polymer chain ends and terminates their growth. Termination can occur by simple interaction between two active species and -M_n e M_m - termination by combination - or disproportionation, where one active center is neutralized by transfer of a hydrogen atom of an active species to another:

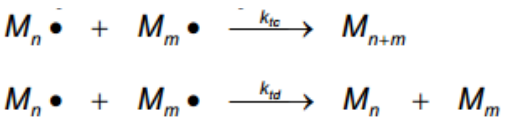

(where k_{tc} is the rate constant for the termination step by combination and k_{td} is the rate constant for the termination step by disproportionation)

Equation 2.4 - Termination step

2.3 Characterization Methods

2.3.1. LC characterization

- **Polarized Optical Microscopy**

A polarized optical microscope is a special microscope that uses polarized light for investigating the optical properties of species. POM images were obtained directly from PDLC films with a Olympus BH-2 microscope with crossed polarisers, equipped with a Olympus Carmedia C-5060 camera. A polarizer is a filter that only allows the light oriented in a specific direction with its polarizing direction to pass through. There are two polarisers in a polarized optical microscope (Figure 2.8[20]) and they are designed to be oriented at right angle to each other, which is termed as cross polar.

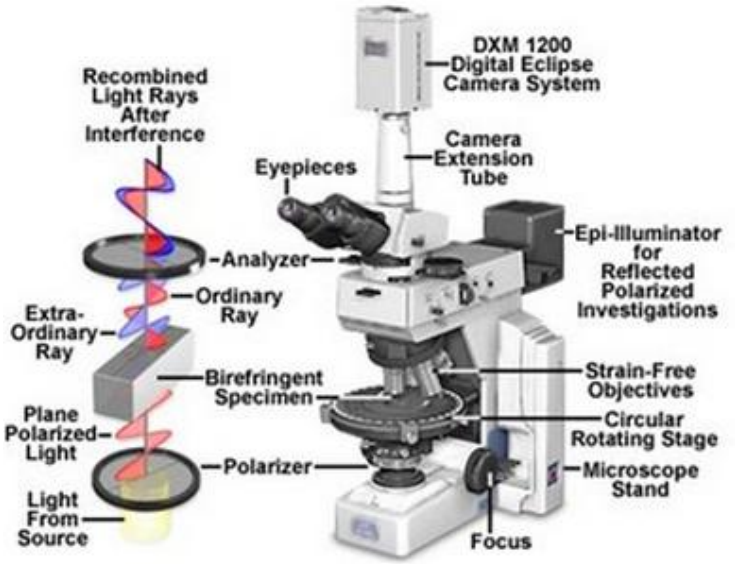

Figure 2.8 - The basic configuration of polarized optical microscopy[20]

The fundamental of cross polar is illustrated in figure 2.9 [20], the polarizing direction of the first polarizer is oriented vertically to the incident beam, so only the waves with vertical direction can pass through it. The passed wave is blocked by the second polarizer, since the polarizer is oriented horizontally to the incident wave.

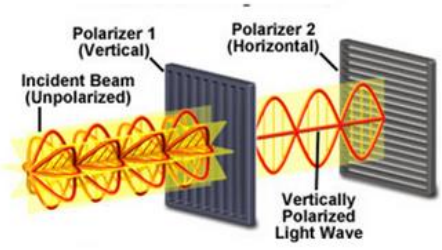

Figure 2.9 - A schematic representation of the polarization of light wave[20]

2.3.2. Polymer Matrix characterization

- **Scanning Electron Microscopy**

The scanning electron microscope (SEM) uses a focused beam of high-energy electrons to generate a variety of signals at the surface of solid specimens. The signals that derive from electron sample interactions reveal information about the sample including external morphology (texture), chemical composition and crystalline structure and orientation of material making up the sample. In most applications, data are collected over a selected area of the surface of the sample, and a 2-dimensional image is generated that displays spatial variations in these properties. Areas ranging from 1 cm to 5 microns in width can be imaged in a scanning mode using conventional SEM techniques. The SEM is also capable of performing analyses of selected point locations on the sample. In SEM, accelerated electrons carry significant amounts of kinetic energy and this energy is dissipated as a variety of signals produced by electron sample interactions when the incident electrons are decelerated in the solid sample. These signals include secondary electrons (that produce SEM images), backscattered electrons (BSE), diffracted backscattered electrons (EBSD that are use to determine crystal structures and orientations of minerals), photons (characteristic X-rays, that are used for elemental analysis and continuum X-rays), visible light (cathodoluminescence-CL) and heat. Secondary electrons and backscattered electrons are commonly used for imaging samples; secondary electrons are most valuable for showing morphology and topography on samples and backscattered electron are most valuable for illustrating contrasts in multiphase samples. In our studies, it was aimed to determinate the morphology of our PDLC films, so in our case, secondary electrons and backscattered electrons are the most important ones.

Scanning Electron microscope (SEM) images were acquired with a Carl Zeiss Auriga crossbeam (SEM-FIB) workstation instrument equipped with a Oxford energy dispersive X-Ray spectrometer. The SEM images have been carried out with an acceleration voltage of 5kV and aperture size of 30 μm.

Figure 2.10 - SEM apparatus at CENIMAT, FCT-UNL[21]

- Sample Preparation

The samples were prepared on Teflon plates and the sample was polymerized in the stove at 74 ° C for several hours. After polymerization, the samples were washed with acetonitrile in order to remove the liquid crystal. The washing process must be performed in a very careful way to ensure that all (or nearly all) the liquid crystal is removed. After washing, the samples were placed in a desiccator for several days. The goal of the desiccator is evaporating the solvent of the sample.

Subsequently, a piece of each sample was placed on a conductive metal glued with adhesive tape carbon double sided. Lastly all samples were placed on a gold bath to ensure that all the sample is conductive.

By SEM it was tried to obtain images of the surface of the sample, amplified 5000 times.

- **Fourier Transform Infrared Spectroscopy**

The principle of FTIR is based on the fact that bonds and groups of bonds vibrate at characteristic frequencies. A molecule that is exposed to infrared rays absorbs infrared energy at frequencies which are characteristic to that molecule. Molecules with a dipole moment allow infrared photons to interact with the molecule causing excitation to higher vibration states. During FTIR analysis, a spot on the specimen is subjected to a modulated IR beam. The specimen's transmittance and reflectance of the infrared rays at different frequencies is translated into an IR absorption plot consisting of reverse peaks. The resulting FTIR spectral pattern is then analyzed and matched with known signatures of identified materials in the FTIR library.

The spectra were analyzed in an ATI Mattson/Unicam Genesis Series FTIR™ as shown in Figure 2.11.

Figure 2.11 - FTIR apparatus

- Sample Preparation

In this work we analysed through FTIR samples before polymerization and after polymerization. In the first case, two disks of KBr were prepared and between them, it was placed a drop of the mixture. This sample is placed in a proper support and analysed by FTIR in order to obtain a spectrum before polymerization. The same mixture is placed on a Teflon board and left to polymerize during about 5 hours. After polymerization the solutions, now in a form of a powder are analysed through FTIR. It is prepared a disk containing the mixture and KBr in a proportion of about 1/3. The objective is to compare the spectrums before and after polymerization.

The FTIR measures the variation of transmittance with the wave number. These values of transmittance were converted to absorbance resorting to the Lambert-Beer law. The spectra shown were all normalized to the peak value of E7.

2.3.3. PDLC characterization

- **EO study**

1) EO study at selected time

PDLC electro-optical (EO) study is based on the voltage dependence of the light transmission coefficient that gives important parameters such as the minimum and maximum transmission as well as the applied voltage. This method also allows us to identify which PDLCs possess hysteresis and/or permanent memory effect (PME). To determine these parameters an apparatus such as the one on Figure 2.12 was used[22].

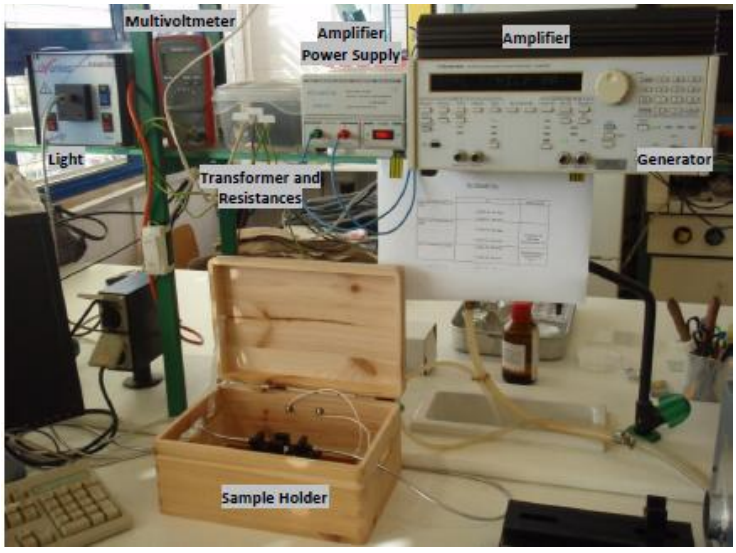

Figure 2.12 - Electro-Optic system[22]

This system has the purpose of acquisition the variation of transmittance with applied voltage. It consists of several parts as shown in Figure 2.12 [20]. The optical part has a diode array Avantes spectrophotometer (AvaLight-DHS and Ava Spec 2048) using 633 nm light by means a halogen lamp and optical fibber cables that carries the light to the sample holder. The signal generator (Wavetek 20MHz Synthesized Function Generator Model 90) creates a 1 kHz sine wave with its amplitude varying between 1 mV and 10 V. This signal is, then, converted to an electrical power signal, with a small voltage gain, by an audio amplifier (Vtrek TP-430) which allows the output sine wave to be applied to the transformer's secondary coil. The audio amplifier is connected to the transformer's secondary coil because it was used a conventional 230V:9V step-down transformer. With the transformer connected in reverse, one can achieve a 24x voltage gain.

The first resistance (1Ω) has the purpose of securing the amplifier form short-circuits and the second resistance's (150kΩ) purpose is to standardize the voltage wave. The amplifier's power supply is a Kiotto KPS 1310. The output detector (AvaSpec-2048) is connected to data acquisition computer software.

Since there is no voltage sensor installed in parallel with the PDLC film, the transformer's output voltage has to be estimated by the following equation, obtained by calibration method:

$$\boldsymbol{y = 0,1961\, x^2 + 39,04x,}$$

Where "x" is the amplitude value given by the wave generator and "y" is the transformer's output voltage and, consequently, the applied voltage to the PDLC film. The study was divided into three cycles, which corresponds to 1/3, 2/3 and 3/3 of the maximum applied voltage (400 V). Each cycle consists of 35 experimental points and each point is made in 1.2 seconds. The pulse is applied to the sample activated after 10 ms and lasts for 200 ms and, later, takes 1000 ms to apply again the pulse. The apparatus originates transmittances measured at five different times, three during the pulse and two after removal of the wrist. For the analysis of experimental data was considered the experimental broadcast at 180 ms. This value of time was chosen because it was at this time the PDLC presented the highest maximum transmittance.

2) EO study time dependent

On Figure 2.13 there is the experimental setup of the electro-optic system used to measure the orientation and disorientation time of the molecules of LC and analyse the kinetic behavior of the PDLC films.

Figure 2.13 - Electro-Optic system at IST-UTL prof. Jão Figueirinhas Lab.

The experimental setup is composed of four parts; one optical bench with a polarized laser light source and a photo-diode detector to monitor the samples optical transmittance, an electrical excitation and measurement unit including a function generator, a voltage amplifier and a digitizing scope. This unit supplies a suitable voltage to the sample and registers the applied voltage and current going through it. The system setup also comprises a temperature controlled oven and the acquisition computer. The time dependence of the light transmittance for different voltage pulses applied to the sample is registered with the photo diode connected to digitizing scope. The voltage pulses coming from the computer controlled function generator are conveniently amplified and fed to the sample. The samples temperature is kept constant by the temperature controlled oven. The acquisition computer drives the setup and registers the data.

The objective of this EO study was to understand the PDLC behavior with increasing voltage and to develop a theoretical kinetic model to fit the experimental data. This model is described in the appendix 2 and it was done in collaboration with professor João Figueirinhas from UTL-IST.

- ## Differential Scanning Calorimetry

Differential scanning calorimetry (DSC) is an analytical tool to characterize the physical properties of compounds. DSC enables determination of melting, crystallization, and mesomorphic transition temperatures, and the corresponding enthalpy and entropy changes, and characterization of glass transition and other effects that show either changes in heat capacity or a latent heat as shown in Figure 2.14 [23].

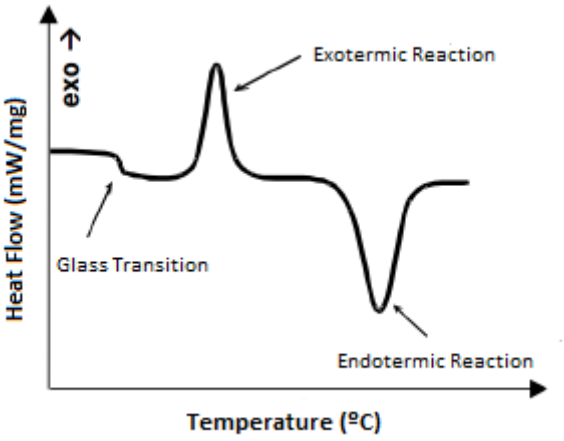

Figure 2.14 -Variation of heat flow versus temperature (adapted [23])

On this work, this technique was applied to determine the glass transition temperature (T_g) of the nematic Liquid Crystal E7 and if possible of the polymers and the Nematic-Isotropic temperature (TNI). We can define T_g as the temperature at which occurs the transition from glassy state to the liquid state. Amorphous polymers have a characteristic T_g, although in the case of highly crystalline polymers this value can be very difficult to measure. All the polymers are solid, rigid and stiff to very low temperatures. When temperature rises, there is an increase in the thermal energy available and the mobility of the polymer molecules increases. From a certain temperature value, the polymeric substances can behave like a viscous liquid. Below the glass transition temperature of the polymer behaves as a rigid and brittle.

- Sample Preparation

The preparation of the samples is very simple: the material is weighted into an aluminium crucible, which is closed in case of negative temperatures. The assays are performed under an atmosphere of N_2. The samples were submitted to a sequence of a first cooling from 40ºC until -90ºC, a heating from -90ºC until 120ºC , and then a second cooling from 120ºC until -90ºC and a second heating from -90ºC until 120ºC, equilibrating at the end at 40ºC, at a speed of 10ºC.min^{-1}. In the case of the polymer TRIEGDMA and POLYEGDMA$_{875}$ the samples were submitted of a first cooling from 40ºC until -90ºC, a heating from -90ºC until 220ºC, and then a second cooling from 220ºC until -90ºC and a second heating from -90ºC until 220ºC, equilibrating at the end at 40ºC, at a speed of 10ºC.min^{-1}. It was used a final higher temperature in the assay, because the objective was to determine the T_g of the polymers, and from the literature, the glass transition temperature for TRIEGDMA is known to be around 145ºC.

3. Experimental Results and Analysis

In this chapter, it will be described and analyzed the experimental results obtained.

This work is focused on the influence of TX100 in the performance of PDLC films formed with TRIEGDMA and POLYEGDMA$_{875}$. The polymerization was performed thermally and the PDLCs were studied using different techniques, as described in chapter 2.3, such as electro-optical studies, polarized optical microscopy, Fourier transform infrared spectroscopy, differential scanning calorimetry and scanning electron microscopy.

Also, in this work, a kinetic study was done in order to have a general understanding of the behavior of the PDLCS films with increasing amounts of TX100. The experimental results were compared with a theoretical model developed in collaboration with professor Dr. João Figueirinhas from IST-UTL.

Because it was studied several samples with TX100 in different proportions, in this chapter it is presented only the experimental results for PDLC without TX100 and with proportions of 1, 5 and 10% all of them in the proportion of 30/70% ($w_{monomer}/w_{LC}$), the remain ones are presented at the appendix 1.

3.1 Chemical Analysis

First of all, an EO study of the PLC formed was done, aiming to determine several PDLC characteristics, namely if it has an EO response or not, if it presents permanent memory effect (PME) , what is the value of the parameter E90 and the memory state contrast (C).

The PME can be calculated through the following expression:

$$\boldsymbol{PME}\ (\%) = \frac{\boldsymbol{T_{OFF} - T_0}}{\boldsymbol{T_{ON} - T_0}}$$

where:

T_0 (%) - Initial reference transmittance

T_{ON} (%) - Maximum transmittance when the voltage is applied

T_{OFF} (%) -Transmittance when the voltage is removed

The parameter E90 is defined as the electric field required to achieve 90% of maximum transmittance.

The memory state contrast can be determined through the following expression:

$$\boldsymbol{C}\ (\%) = \boldsymbol{T_{OFF} - T_0}$$

Secondly, a temperature ramp, followed by POM was made to observe the clarification temperature of the PDLC films and also analyse their morphologies. In this case, it was analysed their morphologies, before applying the voltage, after applying the voltage and at room temperature after reaching the clarification temperature. At the case of the monomer TRIEGDMA with PME, the clarification temperature is not enough to completely remove the memory effect. Therefore, in these cases the PDLC was heated at the stove at 74ºC for another 15 minutes and then the PDLC morphology was, once again, analysed through POM. Photographs are taken with crossed polarisers at a magnification of 10X and 10X eyepiece lens.

The PDLC morphology was also analysed resorting to a SEM analysis. For each PDLC film it is presented one picture illustrating its morphology.

In this work we also analysed the PDLC films through FTIR before polymerization and after polymerization with the goal of comparing the spectrums obtained.

In the next graph it is possible to see the absorption spectrum for each compound, when considered in separate.

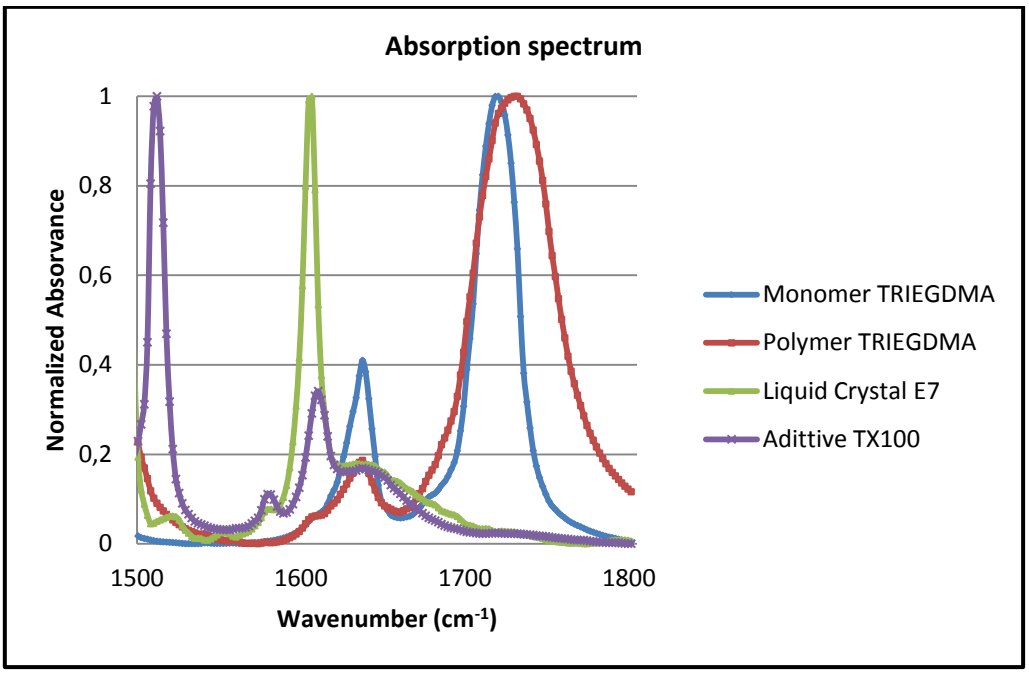

Graph 3.1 - Absorption Spectrum of all compounds when considered in separate

After the polymerization, a decrease on the 1638 cm^{-1} band can be seen, related to the disappearance of the $C=C$ double bond of the vinyl group of the methacrylate in the TRIEGDMA . The original 1720 cm^{-1} band of the carbonyl group appears approximately in the same place . There is a third band characteristic of the liquid crystal at 1605 cm^{-1} and a fourth band at around 1600 cm^{-1} characteristic of the TX100. In PDLC films with $POLYEGDMA_{875}$ the bands appear at similar wavenumbers.

In the table 3.1 are the POM photographs taken of the changes of the liquid crystal E7, contained in a cell of ITO, with gradual increase in temperature. For this, we performed polarized light microscopy and made a scanning temperature from 58,7 to 61,6 ° C at a rate of 1° C/min. Photographs are taken with crossed polarisers at a magnification of 10X and 10X eyepiece lens.

Table 3.1 - Temperature Scanning followed by POM for nematic liquid crystal E7

Temperature (ºC)	POM observation
58,7	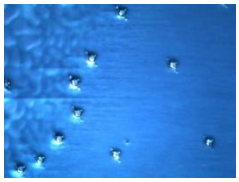
59,2	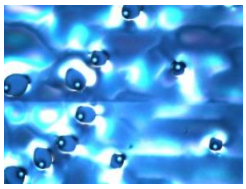
59,4	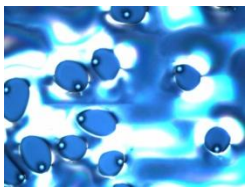
59,9	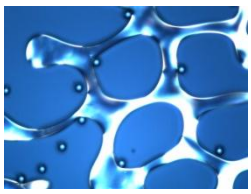
60,1	
60,8	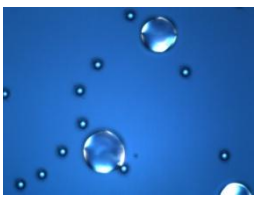
61,4	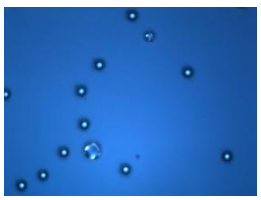
61,6	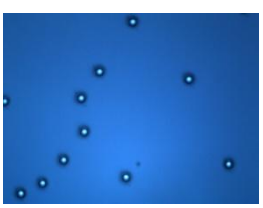

In this work, several DSC studies were also performed. This method was used as a support for the results obtained; by this method it was possible to measure the T_g of the polymer $POLYEGDMA_{875}$, TNI and T_g of the liquid nematic crystal E7 and also see if the amount of TX100 had an influence on this values. In the next graphs it is possible to see the DSC studies for all the compounds when considered in separate.

- DSC study for nematic liquid crystal E7

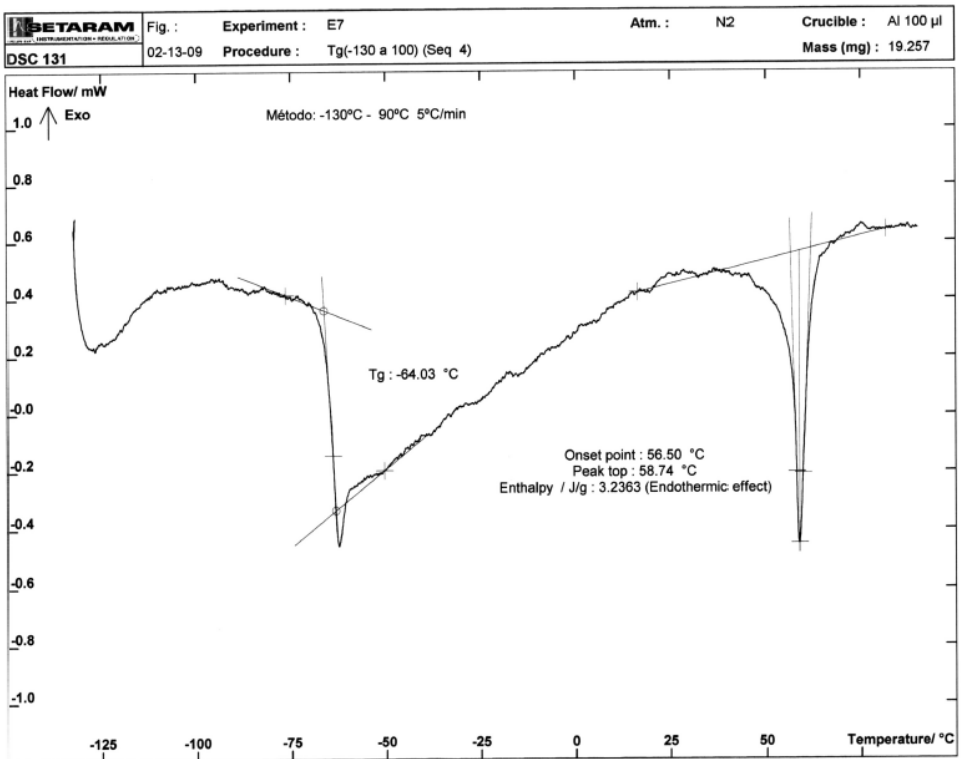

Graph 3.2 - DSC study for nematic liquid crystal E7

From the DSC study for the nematic liquid crystal E7 it is possible to see that $T_g = -64{,}03$ ºC and the TNI has an onset point at 56,50ºC and a midpoint at 58,74ºC which is in concordance with the value obtained through the POM technique and with the value indicated in literature.

- DSC study for polymer TRIEGDMA

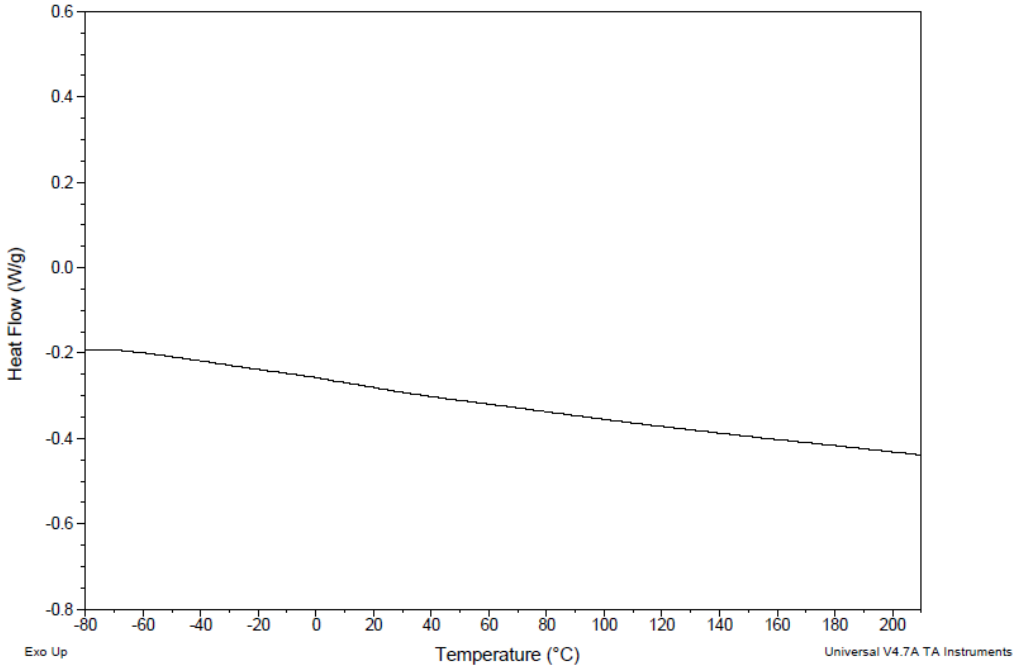

Graph 3.3 - DSC study for polymer TRIEGDMA

On this type of polymer is very difficult to detect the T_g because highly cross-linked polymers form, for high polymerization degrees, a dense network that broadens the region of the glass transition due to a structural heterogeneity increase and a concomitant Tg increase. For some systems, the chain stiffness can impair the emerging of a thermal event in a DSC experiment and the glass transition can even be suppressed /not detected[24]. *C.M. Yakacki et al.*[25] determined the T_g for several PEGDMA polymers and presented the folowing graph:

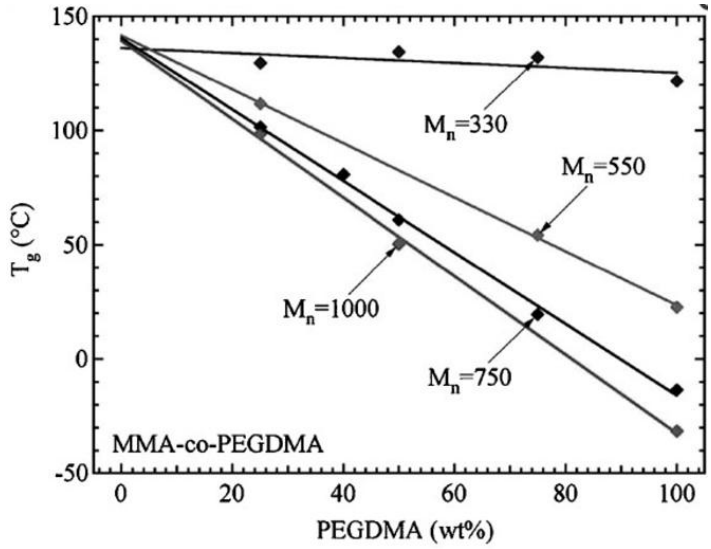

Graph 3.4 - Variation of Tg for MMA-co-PEGDMA polymers [25]

Considering that the mixture only has PEGDMA polymer, then from the graph shown below it is possible to draw the following values:

Table 3.2 - Tg variation for PEGDMA polymers

$\overline{MM}$ (PEGDMA) $gmol^{-1}$	T_g (ºC)
330	125
550	20
750	-15
1000	-35

The variation of Tg with the increase of molecular weight is showed on the graph 3.5.

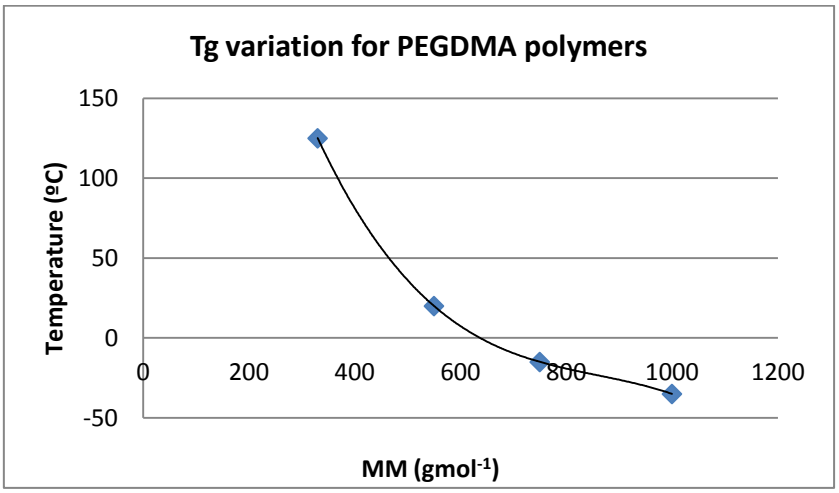

Graph 3.5 - Tg variation for several PEGDMA polymers

Since the monomer used to form the PDLC films used in this work has an average molecular weight of 286,33 g/mol from the graph presented it is possible to estimate the glass transition for TRIEGDMA that it will be around 146 ºC.

- DSC study for polymer $POLYEGDMA_{875}$

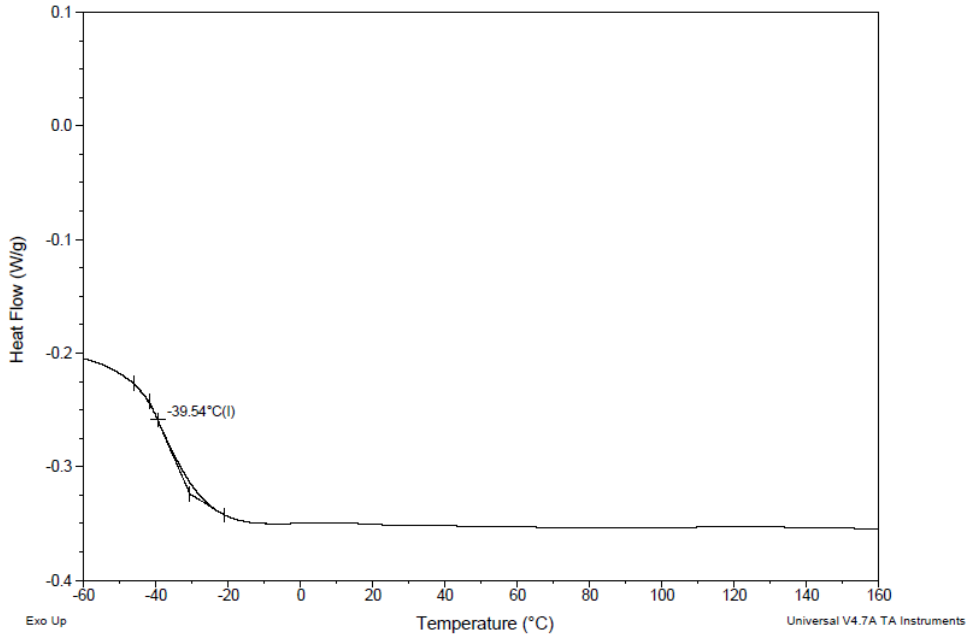

Graph 3.6 - DSC study for polymer $POLYEGDMA_{875}$

From the DSC study for the polymer $POLYEGDMA_{875}$ it is possible to see that $T_g - 39{,}54ºC$.

- DSC study for TX100

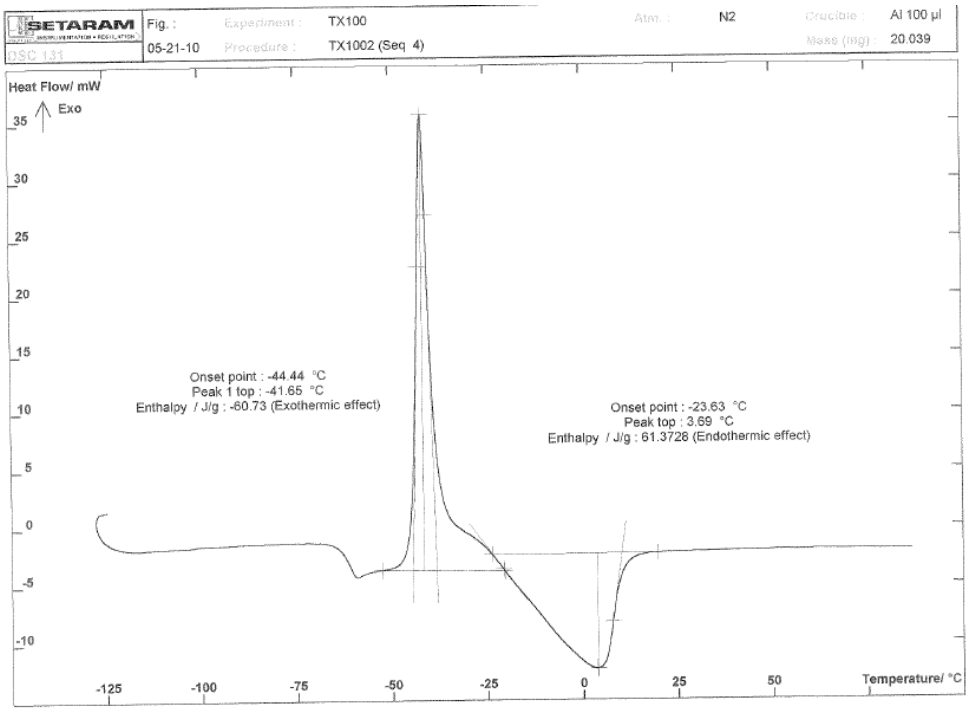

Graph 3.7 - DSC study for TX100

This DSC study presents the glass transition of TX100 at -61ºC, the melting temperature at 3,69ºC and the cold crystalization at -41,65ºC.

3.1.1 PDLC with TRIEGDMA

The following table shows the values obtained for TNI as well as the pictures taken with crossed polarisers for all of the PDLC films synthesised with the monomer TRIEGDMA.

Table 3.3 - Temperature Scanning followed by POM for polymer TRIEGDMA

E7/ Monomer (%w/w)	Additive (%total solution)	Clarification Temperature (°C)
50/50	0	56,4
60/40	0	59,0
70/30	0	58,4
	0,2	53,2
	1	56,0
	2	54,7
	3	53,8
	5	47,5
	10	43,4
80/20	0	56,7
90/10	0	54,6

3.1.1.1 TRIEGDMA without TX100

Graph 3.8 presents the EO response of the PDLC formed with polymer TRIEGDMA (1%AIBN) and LC in the proportion of 30/70% (w/w) without TX100.

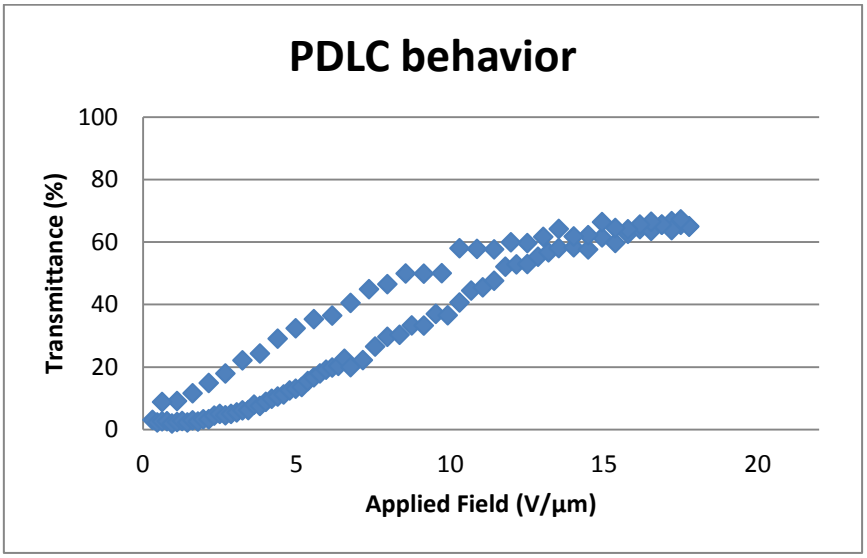

Graph 3.8 - EO response of the system polymer TRIEGDMA (1%AIBN) and LC in the proportion 30/70% (w/w) without TX100

Through the graph it can be concluded that initially the device has a transmittance of about 3%, meaning that it is opaque. When the electric field is applied, the PDLC achieves a maximum transmittance of about 65%. After removal of the electric field remains the PDLC with a transmittance of about 9%, which means that this device has permanent memory effect (PME) of about 9% and an E90 of 14 V/µm. The memory state contrast value obtained was 6%.

The analysis of the morphology of this PDLC is shown in Figure 3.1:

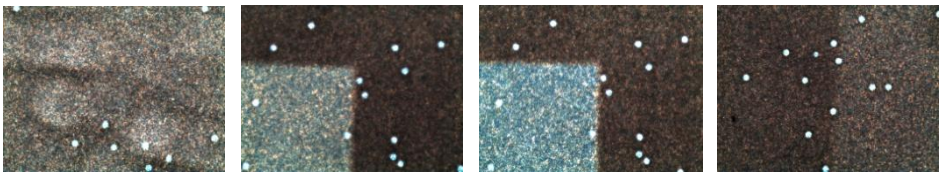

Figure 3.1 - POM micrograph for polymer TRIEGDMA (1%AIBN) and LC in the proportion 30/70% (w/w) without TX100

As shown in figure 3.1 the sample is homogeneous in its totality, the area where the voltage is applied is in a brighter tonality, not visible before applying the voltage. In this PDLC it is necessary to heat the sample on the stove in order to obtain an homogeneous matrix again.

3.1.1.2 TRIEGDMA with TX100

- **TRIEGDMA (1%AIBN) + E7 with 30/70% (w/w) and 1%TX100 of the total solution**

Graph 3.9 presents the EO response of the PDLC formed with polymer TRIEGDMA (1%AIBN) and LC in the proportion of 30/70% (w/w) with 1% of TX100 of the total solution.

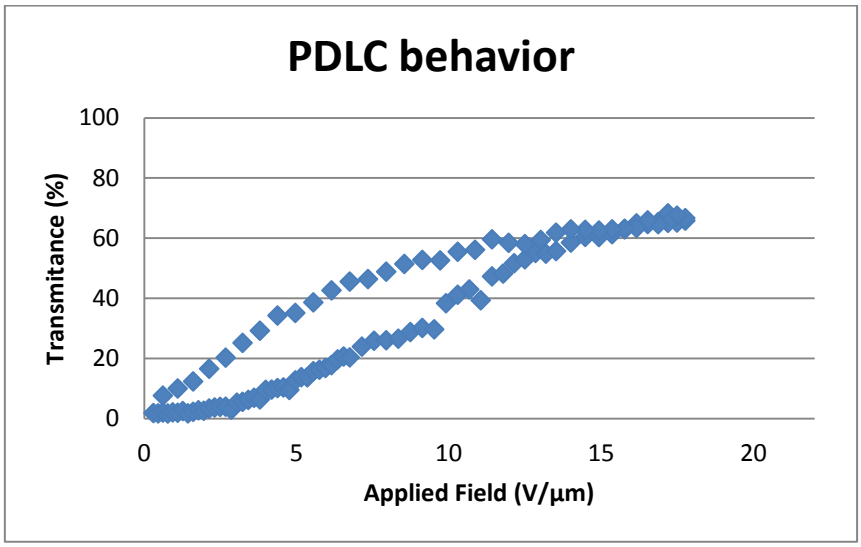

Graph 3.9 - EO response of the system polymer TRIEGDMA (1%AIBN) and LC in the proportion 30/70% (w/w) with 1%TX100 of the total solution

From the graph it can be concluded that initially the device has a transmittance of about 2%, meaning that it is opaque. When the electric field is applied, the PDLC achieves a maximum transmittance of about 66%. After removal of the electric field remains the PDLC with a transmittance of about 8%, which means that this device has permanent memory effect (PME) of about 9% and an E90 of 14 V/µm. The memory state contrast value obtained was 6%.

The analysis of the morphology of this PDLC is shown in Figure 3.2:

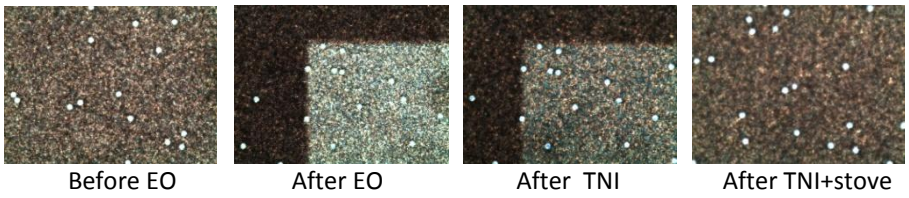

Figure 3.2 - POM micrograph for polymer TRIEGDMA (1%AIBN) and LC in the proportion 30/70% (w/w) with 1% of TX100 of the total solution

As shown in figure 3.2 the sample is homogeneous in its totality, the area where the voltage is applied is in a brighter tonality, not visible before applying the voltage. As in the pure PDLC TRIEGDMA, in this PDLC it is also necessary to heat the sample on the stove in order to obtain an homogeneous matrix again .

The analysis of the morphology by SEM is shown in figure 3.3:

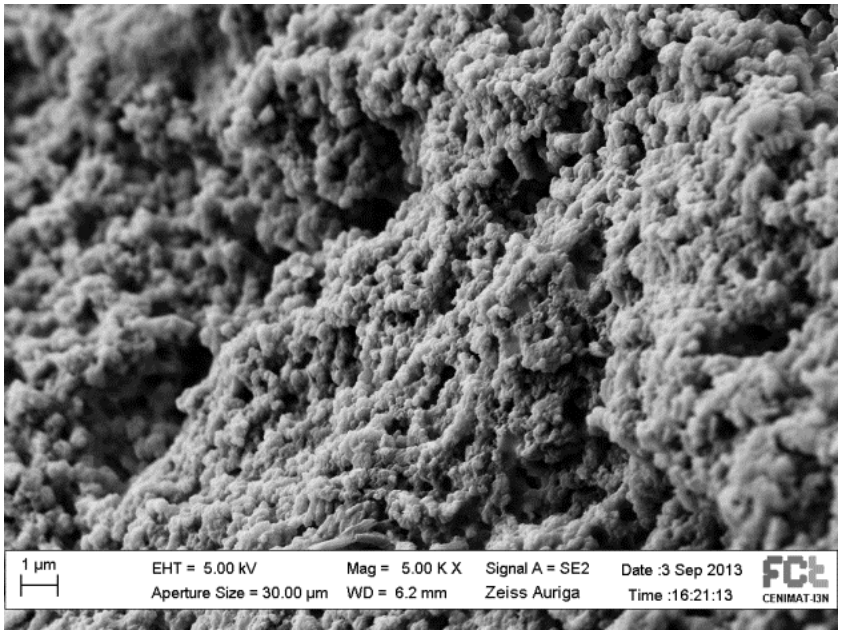

Figure 3.3 - SEM analysis for polymer TRIEGDMA (1%AIBN) and LC in the proportion 30/70% (w/w) with 1% of TX100 of the total solution

The FTIR spectra obtained for this PDLC composition is shown in the Graph 3.10. Before and after the polymerization it can be seen a decrease on the 1638 cm^{-1} band related to the disappearance of the C = C double bond of the vinyl group of the methacrylate in the TRIEGDMA . The original 1720 cm^{-1} band of the carbonyl group appears approximately in the same place. There is a third band characteristic around 1600 cm^{-1}. This band corresponds to a sum of the band of liquid crystal with the band of TX100.

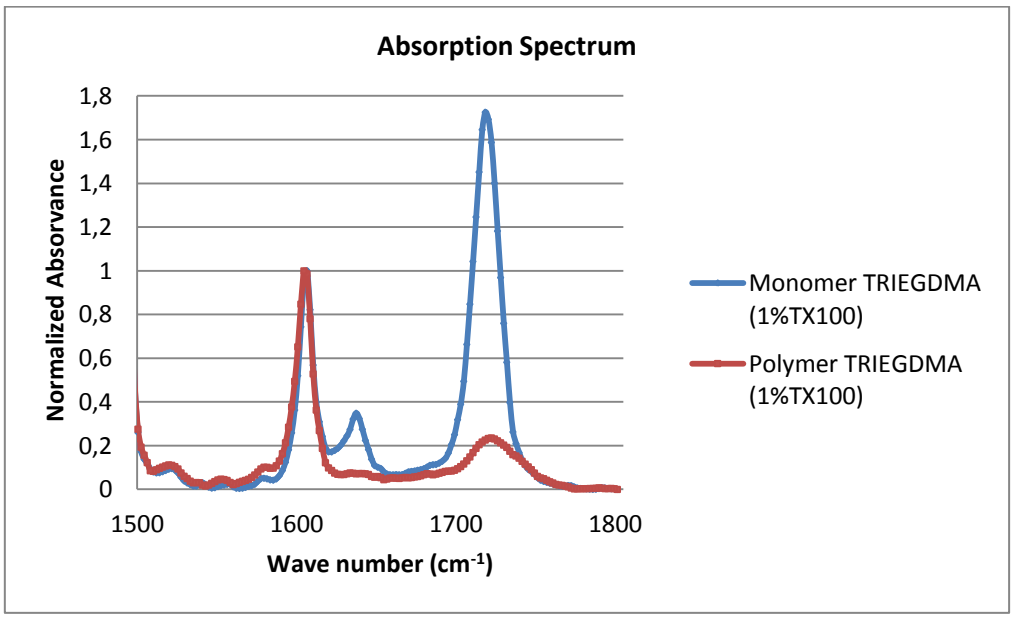

Graph 3.10 - FTIR spectra variation for the PDLC film with polymer TRIEGDMA and LC in the proportion of 30/70% (w/w) and 1%TX100 of the total solution

The following results show the DSC study for the mixture of TRIEGDMA and LC in the proportion of 30/70% (w/w) and 1% of TX100 of the total solution for the first and second heating stage.

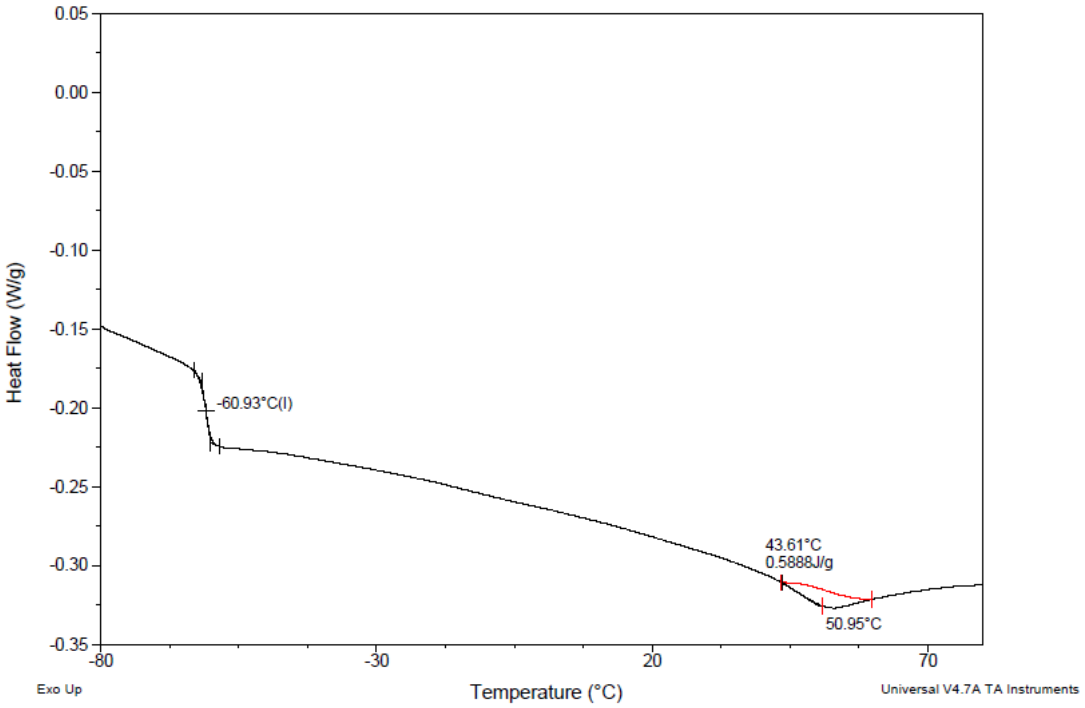

Graph 3.11 - DSC - First heating stage of the mixture of TRIEGDMA and LC in the proportion of 30/70% (w/w) and 1% of TX100 of the total solution

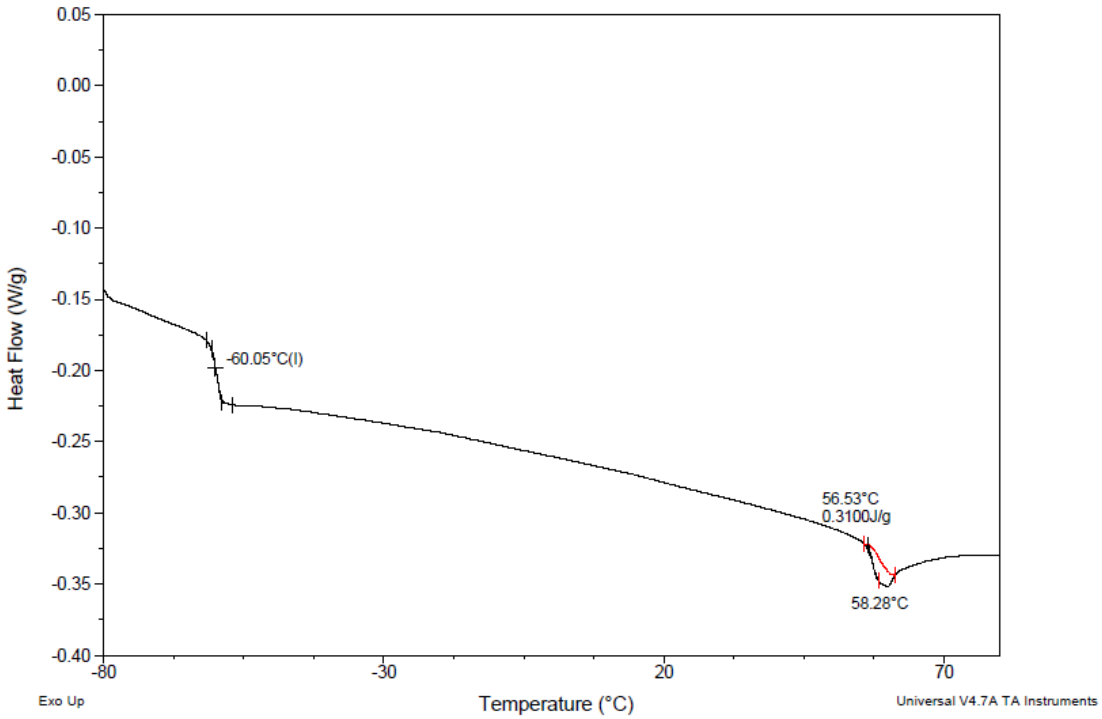

Graph 3.12 - Second heating stage of the mixture of TRIEGDMA and LC in the proportion of 30/70% (w/w) and 1% of TX100 of the total solution

From the DSC study is possible to identify the temperature transitions:

Table 3.4 - DSC study for polymer TRIEGDMA and LC 30/70 (%w/w) and 1% of TX100 of the total solution

Temperature Transitions	Temperature (ºC)	
	First Heating Cycle	Second Heating Cycle
T_g	-60,96	-60,05
Pick	50,94	58,48

The T_g is characteristic of the glass transition of the nematic liquid crystal E7; the pick is probably the one that shows the nematic isotropic transition of liquid crystal E7, although it occurs at a lower temperature than the one presented on the DSC study for the liquid crystal without been mixed with the polymer and the additive, showed in Graph 3.2.

- **TRIEGDMA (1%AIBN) + E7 with 30/70% (w/w) and 5%TX100 of the total solution**

Graph 3.13 presents the EO response of the PDLC formed with polymer TRIEGDMA (1%AIBN) and LC in the proportion of 30/70% (w/w) with 5% of TX100 of the total solution.

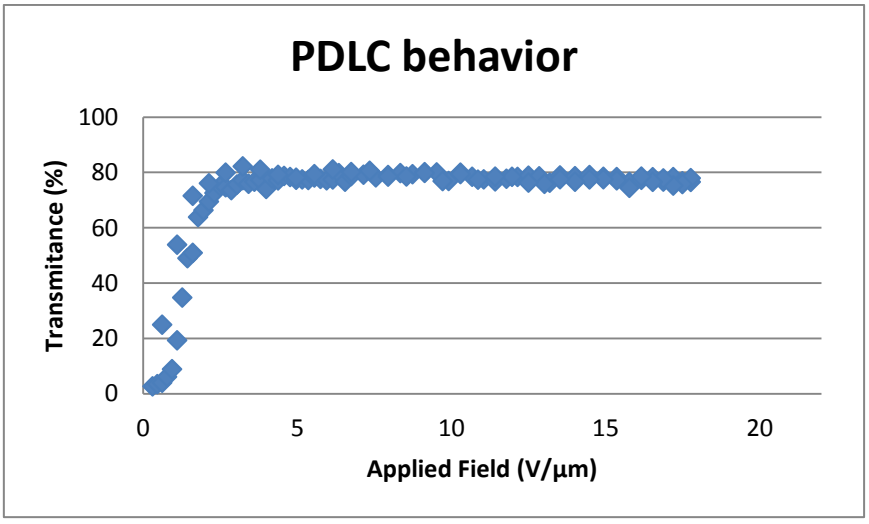

Graph 3.13 - EO response of the system polymer TRIEGDMA (1%AIBN) and LC in the proportion 30/70% (w/w) with 5%TX100 of the total solution

From the graph it can be concluded that initially the device has a transmittance of about 2%, meaning that it is opaque. When the electric field is applied, the PDLC achieves a maximum transmittance of about 80%. After removal of the electric field remains the PDLC with a transmittance of about 25%, which means that this device has permanent memory effect (PME) of about 29% and an E90 of 2 V/µm. The memory state contrast value obtained was 22%.

The analysis of the morphology of this PDLC is shown in Figure 3.4:

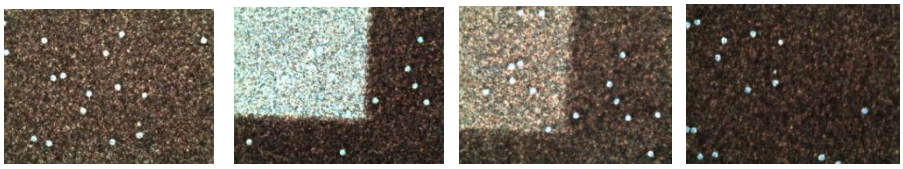

Figure 3.4 - POM micrograph for polymer TRIEGDMA (1%AIBN) and LC in the proportion 30/70% (w/w) with 5% of TX100 of the total solution

As shown in figure 3.4 the sample is homogeneous in its totality, the area where the voltage is applied is in a brighter tonality, not visible before applying the voltage. As in the pure PDLC TRIEGDMA, in this PDLC it is also necessary to heat the sample on the stove in order to obtain an homogeneous matrix again .

The analysis of the morphology by SEM is shown in Figure 3.5:

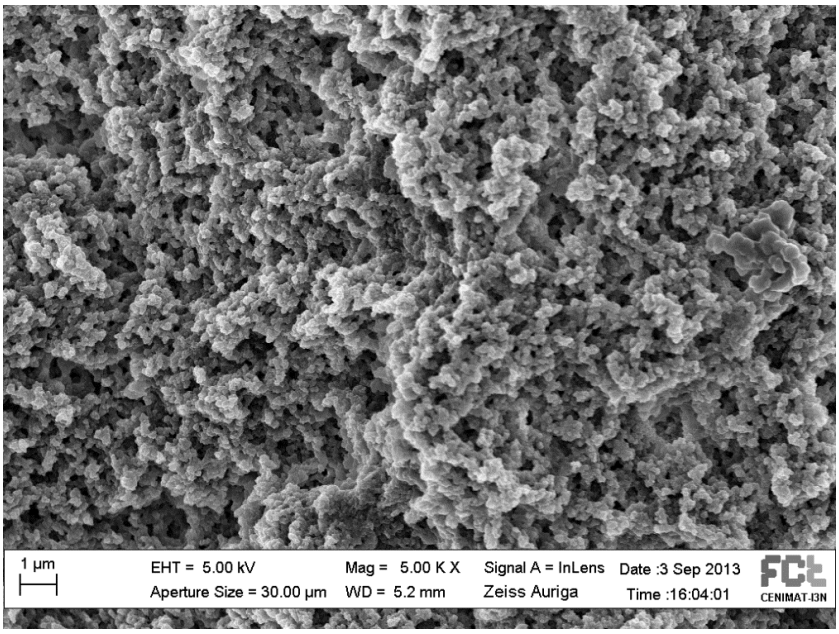

Figure 3.5 - SEM analysis for polymer TRIEGDMA (1%AIBN) and LC in the proportion 30/70% (w/w) with 5% of TX100 of the total solution

The FTIR spectra obtained for this PDLC composition is shown in Graph 3.14. As refered before it is possible to identify three bands: the =C double bond band, the band of the carbonyl group and the band correspondent to a sum of the band of liquid crystal with the band of TX100.

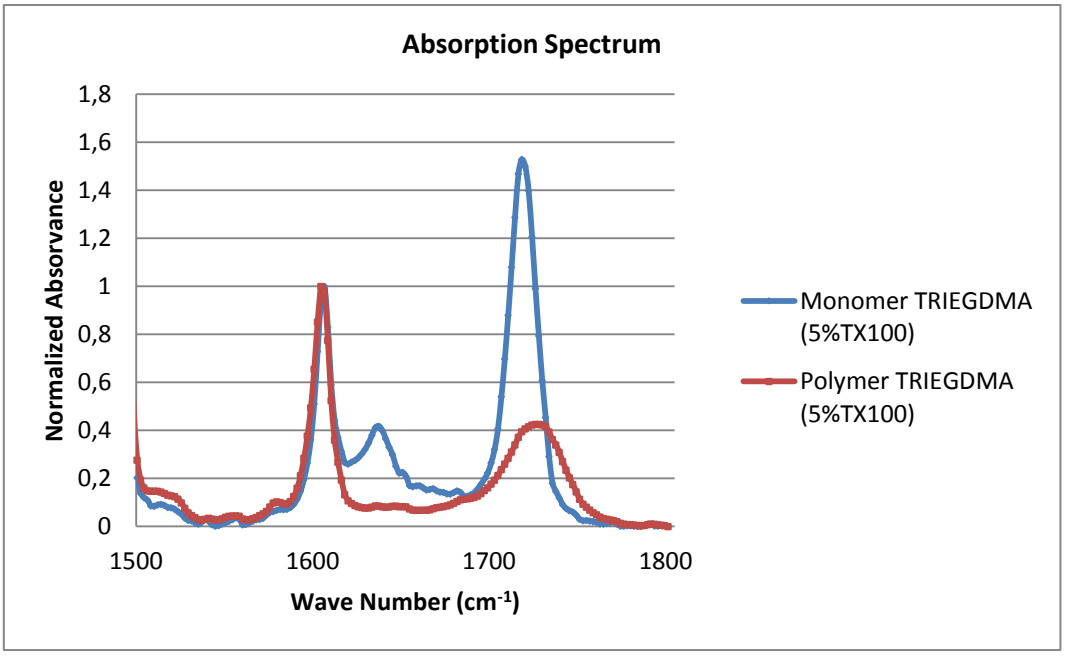

Graph 3.14 - FTIR spectra variation for the PDLC film with polymer TRIEGDMA and LC in the proportion of 30/70% (w/w) and 5%TX100 of the total solution

The following results show the DSC study for the mixture of TRIEGDMA and LC in the proportion of 30/70% (w/w) and 5% of TX100 of the total solution for the first and second heating stage.

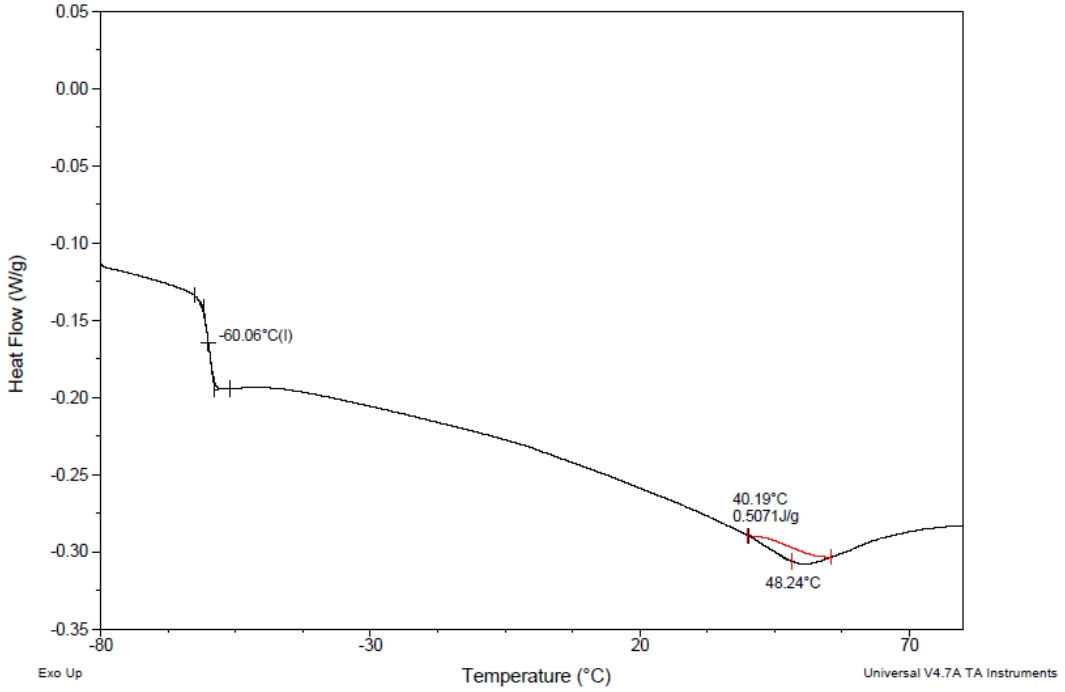

Graph 3.15 - First heating stage of the mixture of polymer TRIEGDMA and LC in the proportion of 30/70% (w/w) and 5% of TX100 of the total solution

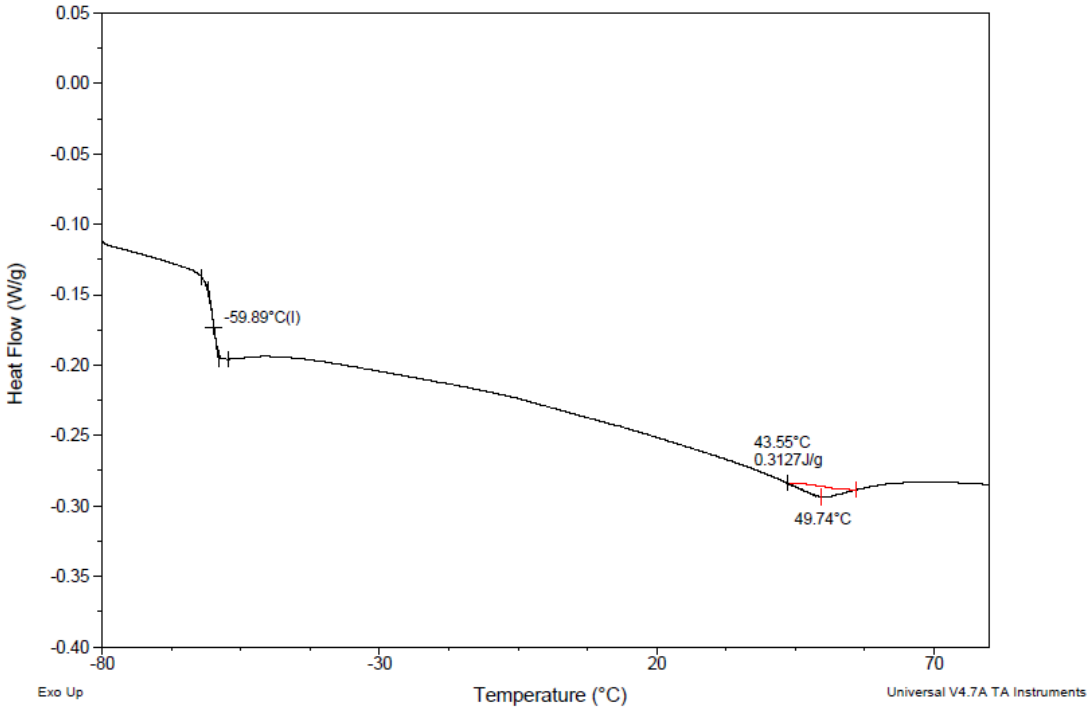

Graph 3.16- Second heating stage of the mixture of polymer TRIEGDMA and LC in the proportion of 30/70% (w/w) and 5% of TX100 of the total solution

From the DSC study is possible to identify the following temperature transitons:

Table 3.5 - DSC study of polymer TRIEGDMA and LC, 30/70 (%w/w) and 5% of TX100 of the total solution

Temperature Transitions	Temperature (ºC)	
	First Heating Cycle	Second Heating Cycle
T_g	-60,06	-59,89
Pick	48,24	49,74

The T_g is characteristic of the glass transition of the nematic liquid crystal E7; the pick is probably the one that shows the nematic isotropic transition of liquid crystal E7, although it occurs at a lower temperature than the one presented on the DSC study for the liquid crystal without been mixed with the polymer and the additive, showed in Graph 3.2.

- **TRIEGDMA (1%AIBN) + E7 with 30/70% (w/w) and 10%TX100 of the total solution**

Graph 3.17 presents the EO response of the PDLC formed with polymer TRIEGDMA (1%AIBN) and LC in the proportion of 30/70% (w/w) with 10% of TX100 of the total solution.

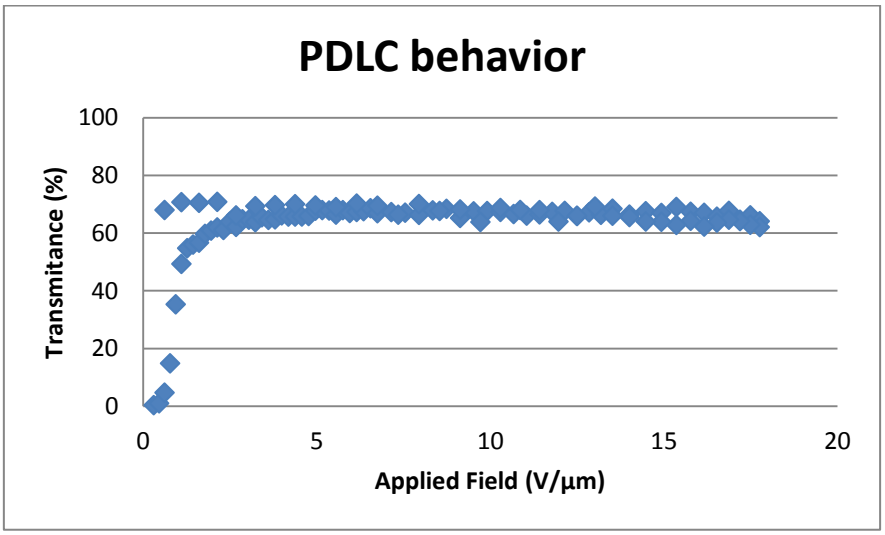

Graph 3.17- EO response of the system polymer TRIEGDMA (1%AIBN) and LC in the proportion 30/70% (w/w) with 10%TX100 of the total solution

From the graph it can be concluded that initially the device has a transmittance of about 0%, meaning that it is opaque. When the electric field is applied, the PDLC achieves a maximum transmittance of about 71%. After removal of the electric field remains the PDLC with a transmittance of about 68%, which means that this device has permanent memory effect (PME) of about 96% and an E90 of 2 V/µm. The memory state contrast value obtained was 68%.

The analysis of the morphology of this PDLC is shown in Figure 3.6:

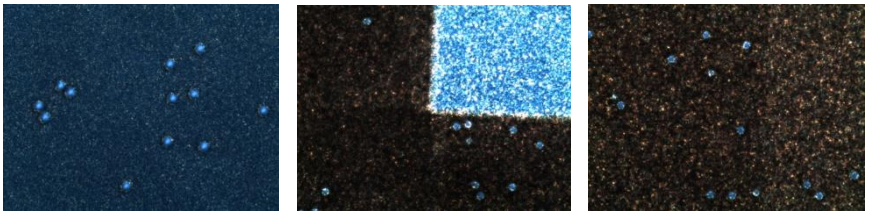

Figure 3.6 -POM micrograph for polymer TRIEGDMA (1%AIBN) and LC in the proportion 30/70% (w/w) with 10% of TX100 of the total solution

As shown in figure 3.6 the sample is homogeneous in its totality, the area where the voltage is applied is in a brighter tonality, not visible before applying the voltage. In this case is not necessary to heat the sample in the stove after the TNI because the sample is already an homogenous matrix.

The analysis of the morphology by SEM is shown in Figure 3.7:

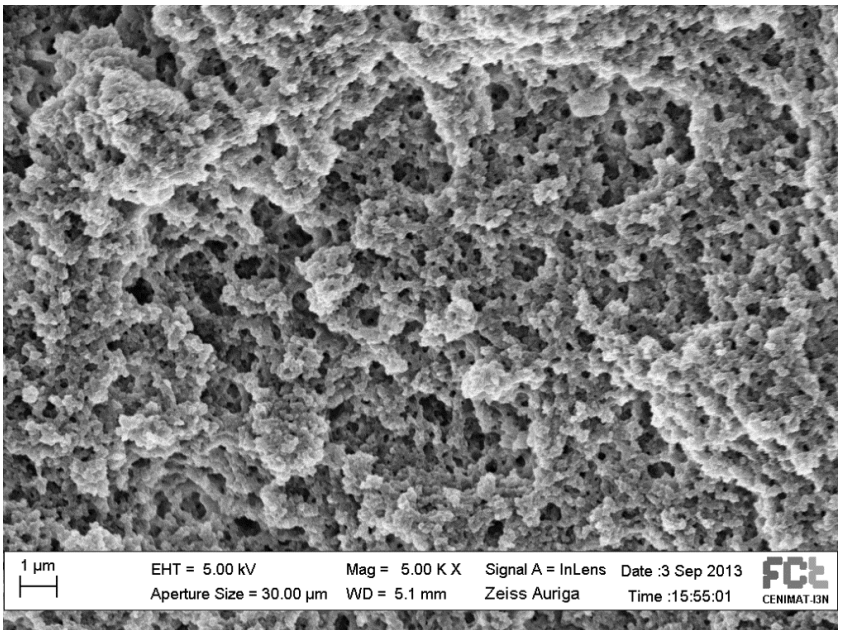

Figure 3.7 - SEM analysis for polymer TRIEGDMA (1%AIBN) and LC in the proportion 30/70% (w/w) with 10% of TX100 of the total solution

The FTIR spectra obtained for this PDLC composition is shown in Graph 3.18. As refered before it is possible to identify three bands: the =C double bond band, the band of the carbonyl group and the band correspondent to a sum of the band of liquid crystal with the band of TX100.

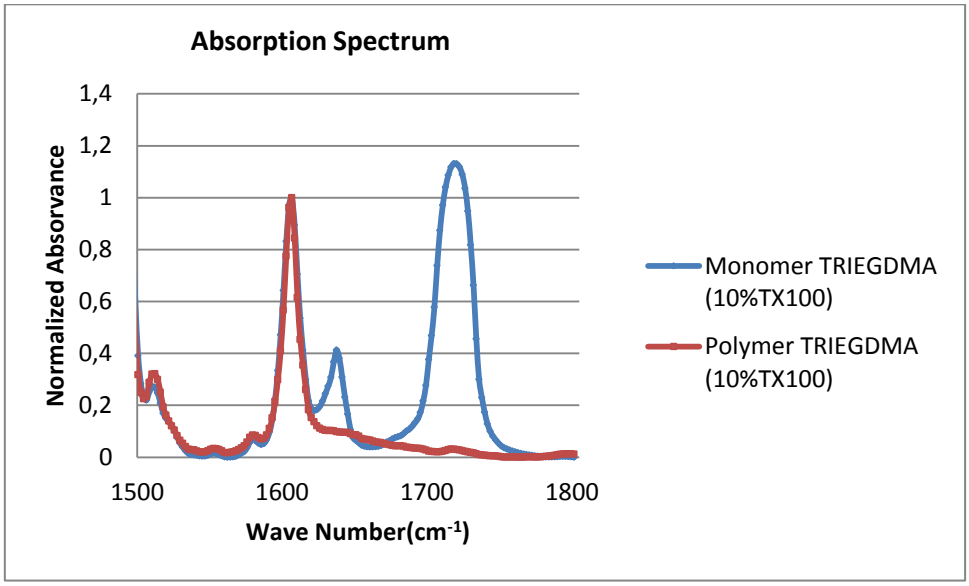

Graph 3.18- FTIR spectra variation for the PDLC film with polymer TRIEGDMA and LC in the proportion of 30/70% (w/w) and 10%TX100 of the total solution

The following results show the DSC study for the mixture of TRIEGDMA and LC in the proportion of 30/70% (w/w) and 10% of TX100 of the total solution for the first and second heating stage.

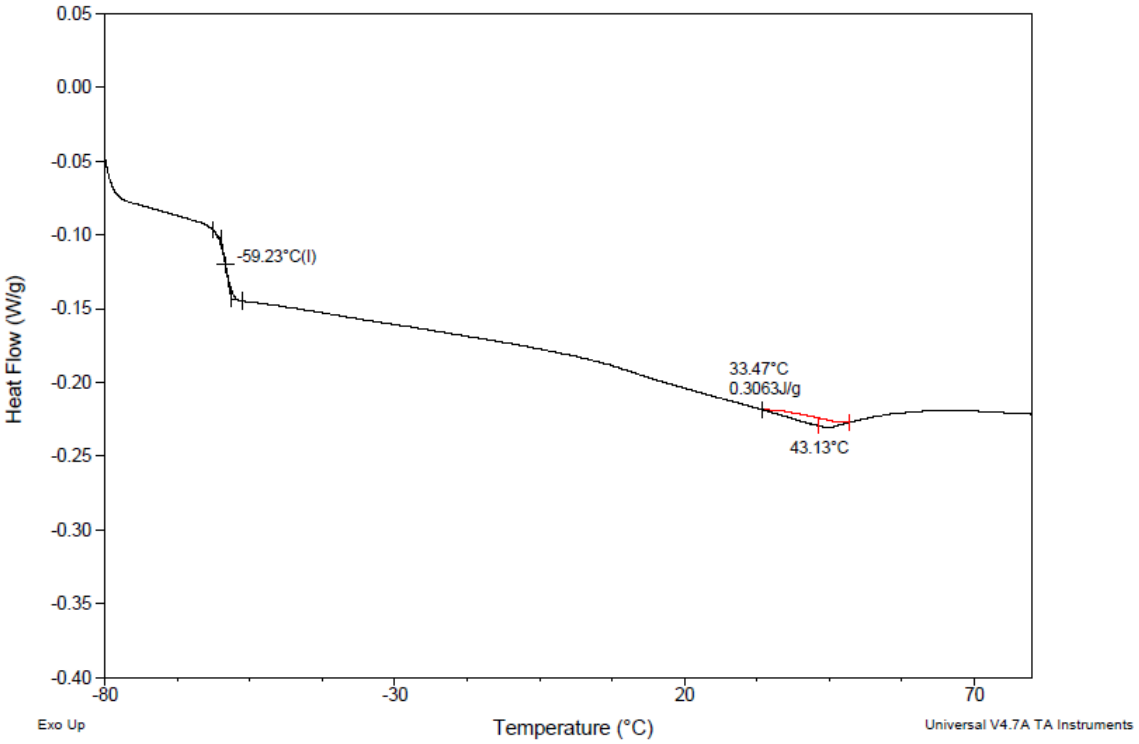

Graph 3.19 -First heating stage of the mixture of TRIEGDMA and LC in the proportion of 30/70% (w/w) and 10% of TX100 of the total solution

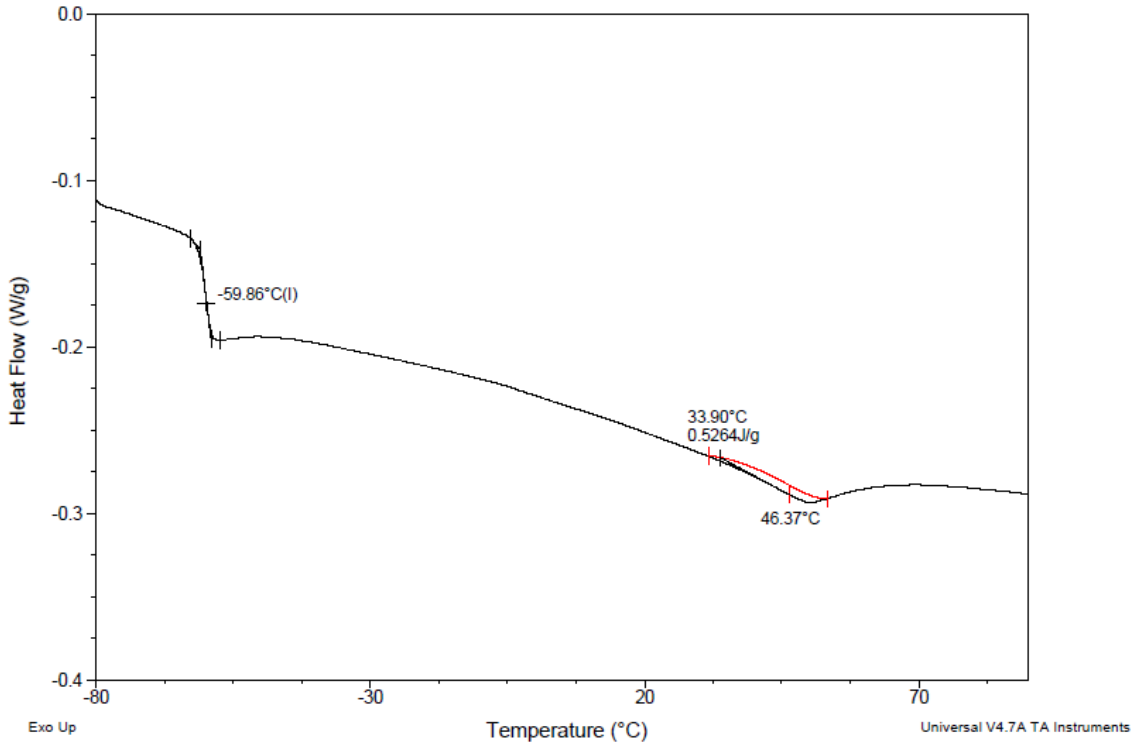

Graph 3.20 - Second heating stage of the mixture of TRIEGDMA and LC in the proportion of 30/70% (w/w) and 10% of TX100 of the total solution

From the DSC study is possible to identify the following temperature transitions:

Table 3.6 - DSC study of polymer TRIEGDMA and LC, 30/70 (%w/w) and 10% of TX100 of the total solution

Temperature Transitions	Temperature (ºC)	
	First Heating Cycle	Second Heating Cycle
T_g	-59,23	-59,86
Pick	43,13	43,7

The T_g is characteristic of the glass transition of the nematic liquid crystal E7; the pick is probably the one that shows the nematic isotropic transition of liquid crystal E7, although it occurs at a lower temperature than the one presented on the DSC study for the liquid crystal without been mixed with the polymer and the additive, showed in Graph 3.2.

3.1.2 PDLC with POLYEGDMA$_{875}$

The following table shows the values obtained for TNI as well as the pictures taken with crossed polarisers for all of the PDLC films synthesised with the oligomer POLYEGDMA$_{875}$.

Table 3.7 - Temperature Scanning Followed by POM for polymer POLYEGDMA$_{875}$

E7/Monomer (%w/w)	Additive (%total solution)	Clarification Temperature (°C)
50/50	0	58,5
60/40	0	58,9
70/30	0	59,8
	0,2	60,4
	1	56,7
	2	53,5
	3	51,0
	5	45,1
	10	36,2
	20	42,9
80/20	0	58,1
90/10	0	58,3

3.1.2.1 POLYEGDMA$_{875}$ without TX100

Graph 3.21 presents the EO response of the PDLC formed with polymer POLYEGDMA$_{875}$ (1%AIBN) and LC in the proportion of 30/70% (w/w) without TX100.

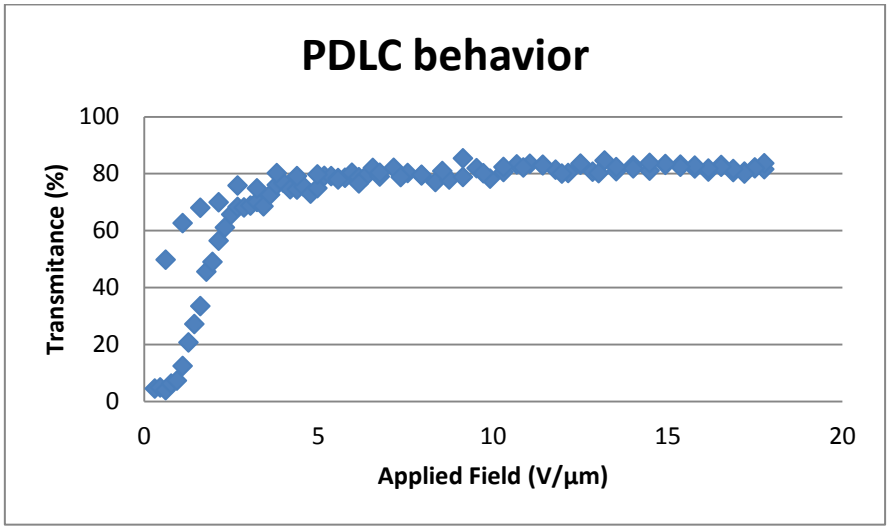

Graph 3.21 - EO response of the system polymer POLYEGDMA$_{875}$ (1%AIBN) and LC in the proportion 30/70% (w/w) without TX100

Through the graph it can be concluded that initially the device has a transmittance of about 4%, meaning that it is opaque. When the electric field is applied, the PDLC achieves a maximum transmittance of about 83%. After removal of the electric field remains the PDLC with a transmittance of about 50%, which means that this device has permanent memory effect (PME) of about 58% and an E90 of 5 V/µm. The memory state contrast obtained was 45%.

The analysis of the morphology of this PDLC is shown in Figure 3.8:

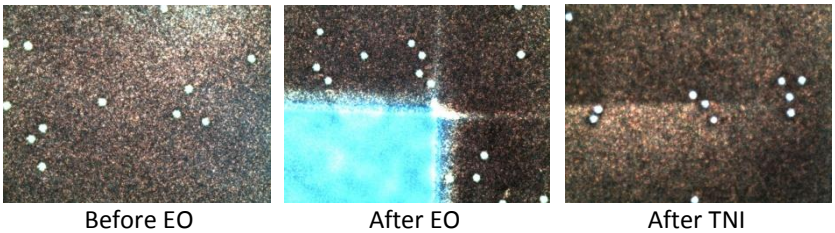

Figure 3.8 - POM micrograph for polymer POLYEGDMA$_{875}$ (1%AIBN) and LC in the proportion 30/70% (w/w) without TX100

As shown in figure 3.8 the sample is homogeneous in its totality, the area where the voltage is applied is in a brighter tonality, not visible before applying the voltage. After reaching the TNI the sample becomes an homogeneous matrix like in the beginning.

3.1.2.2 POLYEGDMA$_{875}$ with TX100

- **POLYEGDMA$_{875}$ (1%AIBN) + E7 with 30/70% (w/w) and 1%TX100 of the total solution**

Graph 3.22 presents the EO response of the PDLC formed with polymer POLYEGDMA$_{875}$ (1%AIBN) and LC in the proportion of 30/70% (w/w) with 1% of TX100 of the total solution.

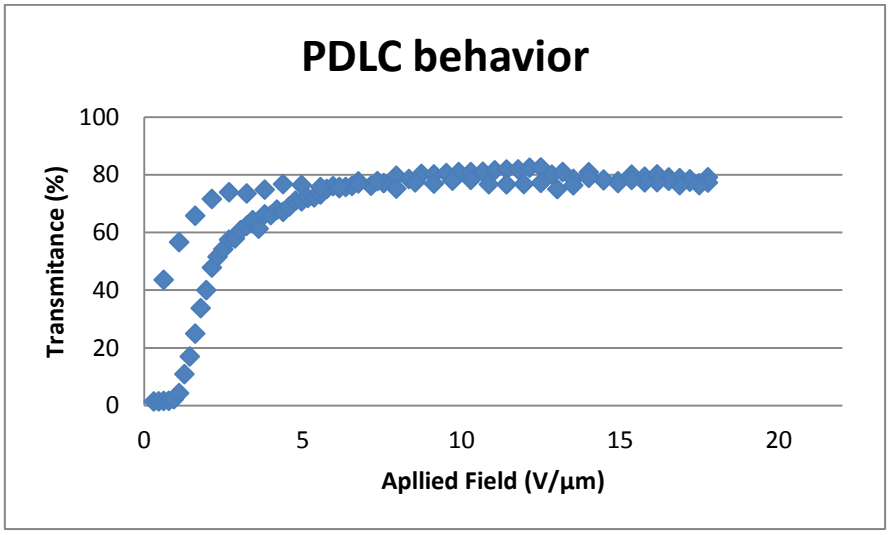

Graph 3.22 - EO response of the system polymer POLYEGDMA$_{875}$ (1%AIBN) and LC in the proportion 30/70% (w/w) with 1%TX100 of the total solution

Through the graph it can be concluded that initially the device has a transmittance of about 1%, meaning that it is opaque. When the electric field is applied, the PDLC achieves a maximum transmittance of about 80%. After removal of the electric field remains the PDLC with a transmittance of about 44%, which means that this device has permanent memory effect (PME) of about 54% and an E90 of 5 V/µm. The memory state contrast obtained was 42%.

The analysis of the morphology of this PDLC is shown in figure 3.9:

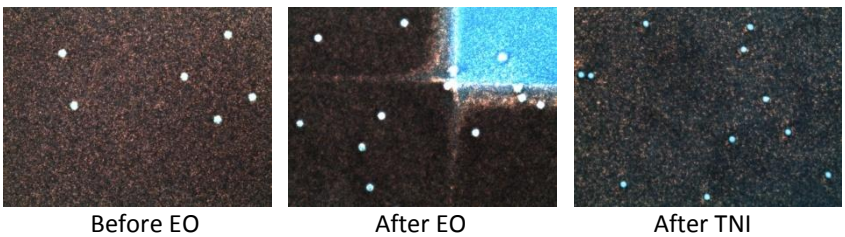

Figure 3.9 - POM micrograph for polymer POLYEGMDA$_{875}$ (1%AIBN) and LC in the proportion 30/70% (w/w) with 1% of TX100 of the total solution

As shown in figure 3.9 the sample is homogeneous in its totality, the area where the voltage is applied is in a brighter tonality, not visible before applying the voltage. After reaching the TNI the sample becomes an homogeneous matrix like in the beginning.

The analysis of the morphology by SEM is shown in Figure 3.10:

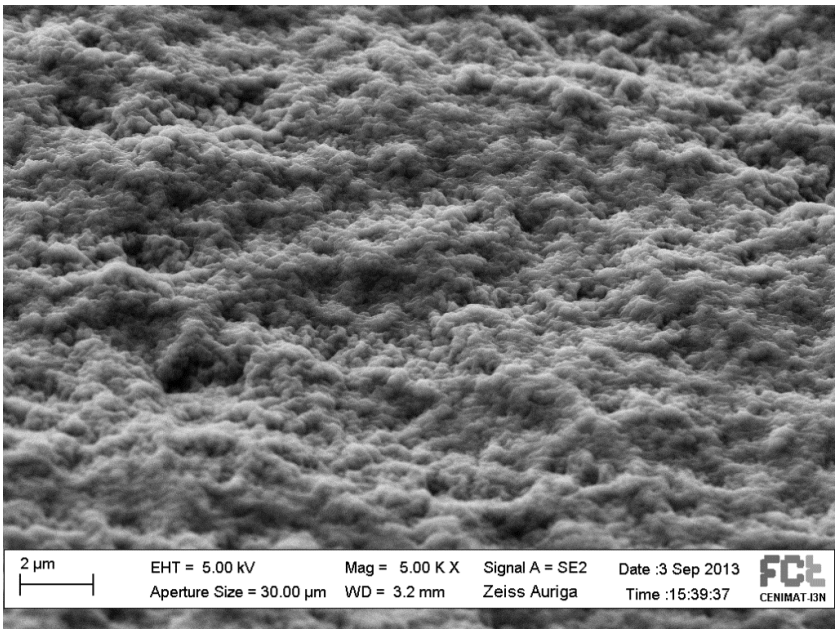

Figure 3.10 - SEM analysis for polymer POLYEGMDA$_{875}$ (1%AIBN) and LC in the proportion 30/70% (w/w) with 1% of TX100 of the total solution

The FTIR spectra obtained for this PDLC composition is shown in the Graph 3.23. Before and after the polymerization it can be seen a decrease on the 1638 cm^{-1} band related to the disappearance of the $C=C$ double bond of the vinyl group of the methacrylate in the POLYEGDMA$_{875}$. The original 1720 cm-1 band of the carbonyl group appears approximately in the same place, but smaller. There is a third band around 1600 cm-1. This band corresponds to a sum of the band of liquid crystal with the band of TX100.

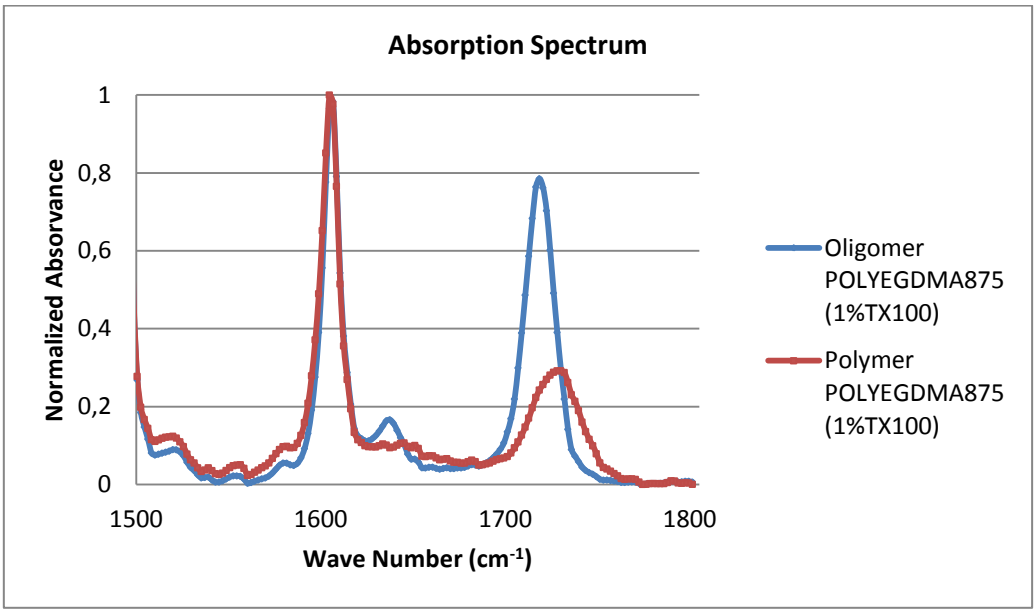

Graph 3.23 - FTIR spectra variation for the PDLC film with polymer POLYEGDMA$_{875}$ and LC in the proportion of 30/70% (w/w) and 1%TX100 of the total solution

The following results show the DSC study for the mixture of POLYEGDMA$_{875}$ and LC in the proportion of 30/70% (w/w) and 1% of TX100 of the total solution for the first and second heating stage.

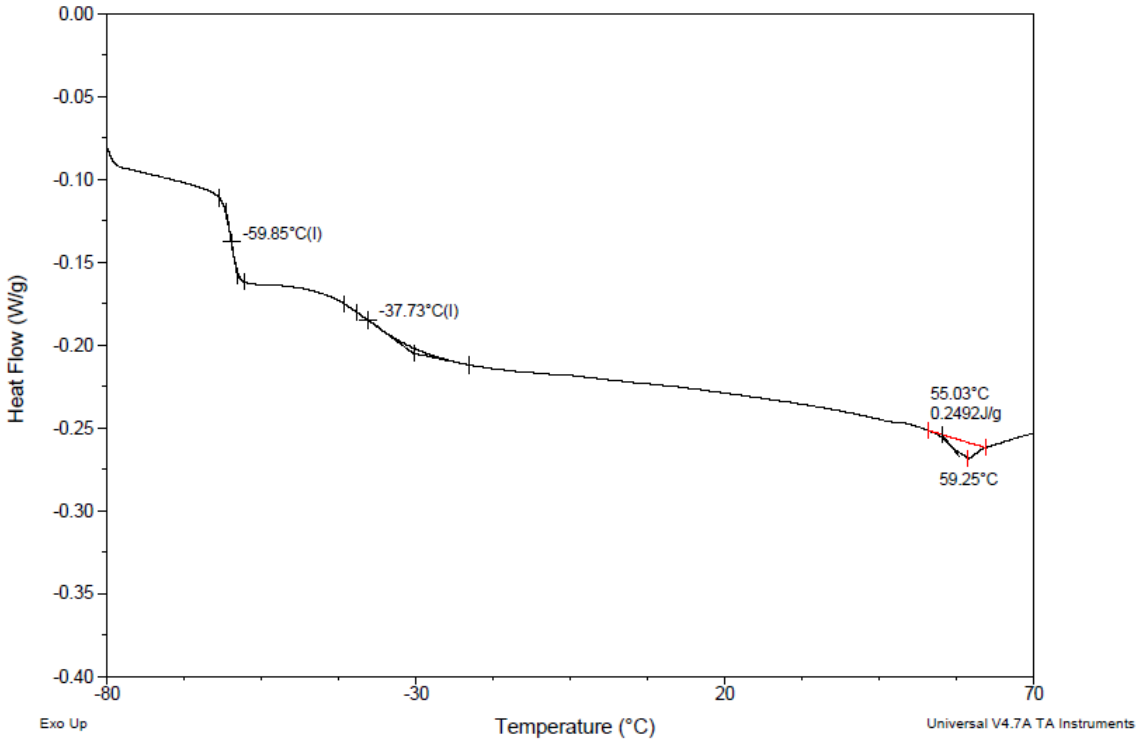

Graph 3.24 - First heating stage of the mixture of POLYEGDMA$_{875}$ and LC in the proportion of 30/70% (w/w) and 1% of TX100 of the total solution

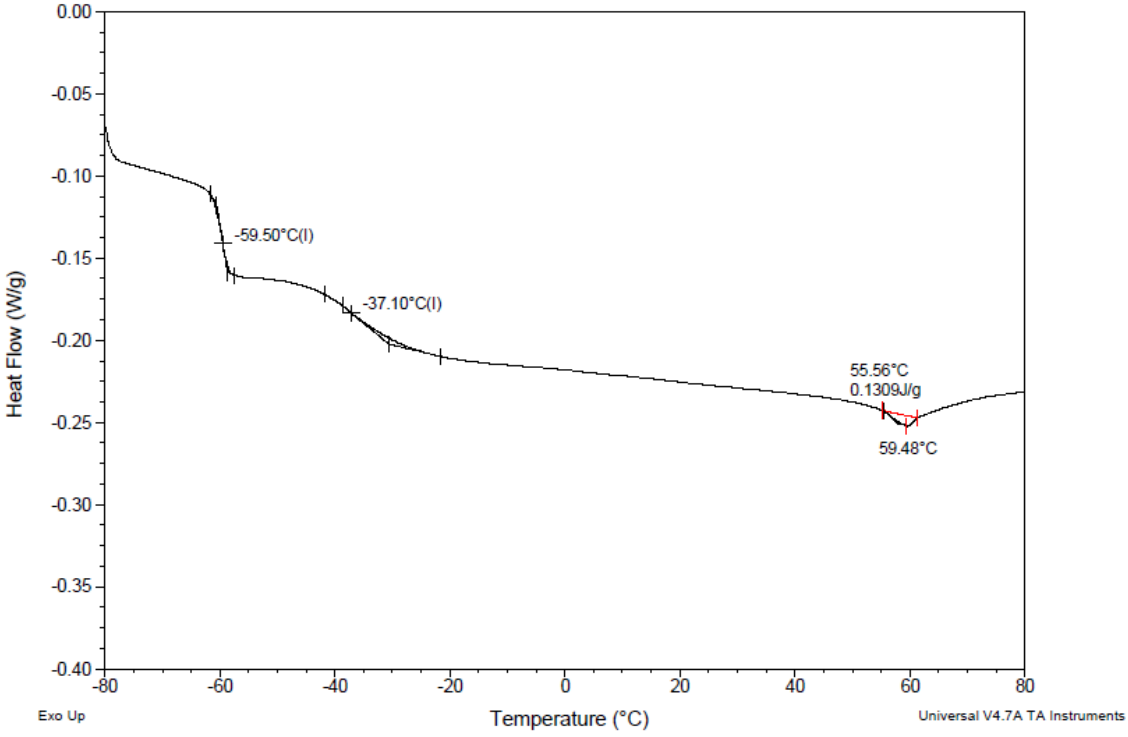

Graph 3.25 - Second heating stage of the mixture of POLYEGDMA$_{875}$ and LC in the proportion of 30/70% (w/w) and 1% of TX100 of the total solution

From the DSC study is possible to identify the following temperature transitions:

Table 3.8 - DSC study of polymer POLYEGDMA$_{875}$ and LC, 30/70 (%w/w) and 1% of TX100 of the total solution

Temperature Transitions	Temperature (ºC)	
	First Heating Cycle	Second Heating Cycle
$T_{g,1}$	-59,85	-59,50
$T_{g,2}$	-37,73	-37,10
Pick	59,25	59,48

The $T_{g,1}$ is characteristic of the glass transition of the nematic liquid crystal E7; the $T_{g,2}$ is characteristic of the glass transition of the polymer POLYEGDMA$_{875}$; the pick is probably the one that shows the nematic isotropic transition of liquid crystal E7, although it occurs at a lower temperature than the one presented on the DSC study for the liquid crystal without been mixed with the polymer and the additive, showed Graph 3.2.

- **POLYEGDMA$_{875}$ (1%AIBN) + E7 with 30/70% (w/w) and 5%TX100 of the total solution**

Graph 3.26 presents the EO response of the PDLC formed with polymer POLYEGDMA$_{875}$ (1%AIBN) and LC in the proportion of 30/70% (w/w) with 5% of TX100 of the total solution.

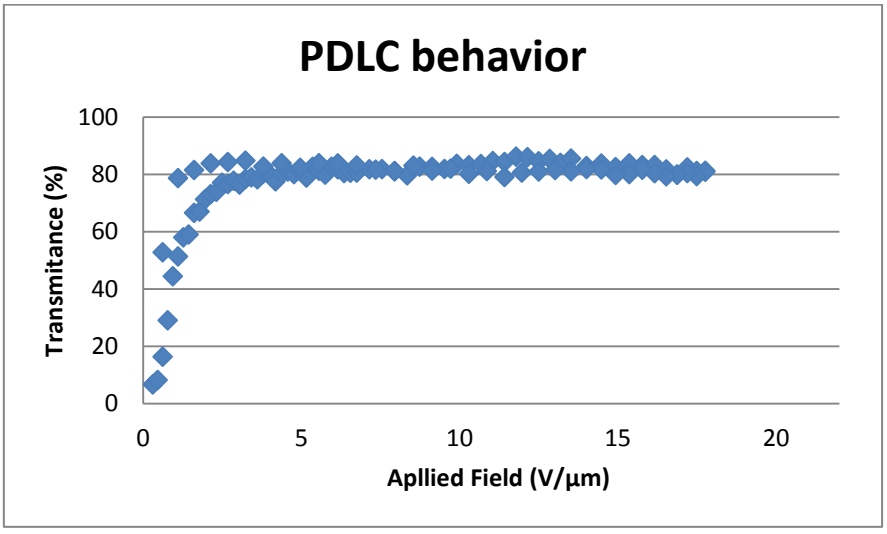

Graph 3.26 - EO response of the system polymer POLYEGDMA$_{875}$ (1%AIBN) and LC in the proportion 30/70% (w/w) with 5%TX100 of the total solution

Through the graph it can be concluded that initially the device has a transmittance of about 6%, meaning that it is opaque. When the electric field is applied, the PDLC achieves a maximum transmittance of about 84%. After removal of the electric field remains the PDLC with a transmittance of about 53%, which means that this device has permanent memory effect (PME) of about 60% and an E90 of 2 V/µm. The memory state contrast value obtained was 46%.

The analysis of the morphology of this PDLC is shown in Figure 3.11:

Figure 3.11 - POM micrograph for polymer POLYEGMDA$_{875}$ (1%AIBN) and LC in the proportion 30/70% (w/w) with 5% of TX100 of the total solution

As shown in figure 3.11 the sample is homogeneous in its totality, the area where the voltage is applied is in a brighter tonality, not visible before applying the voltage. After reaching the TNI the sample becomes an homogeneous matrix like in the beginning.

The analysis of the morphology by SEM is shown in Figure 3.12:

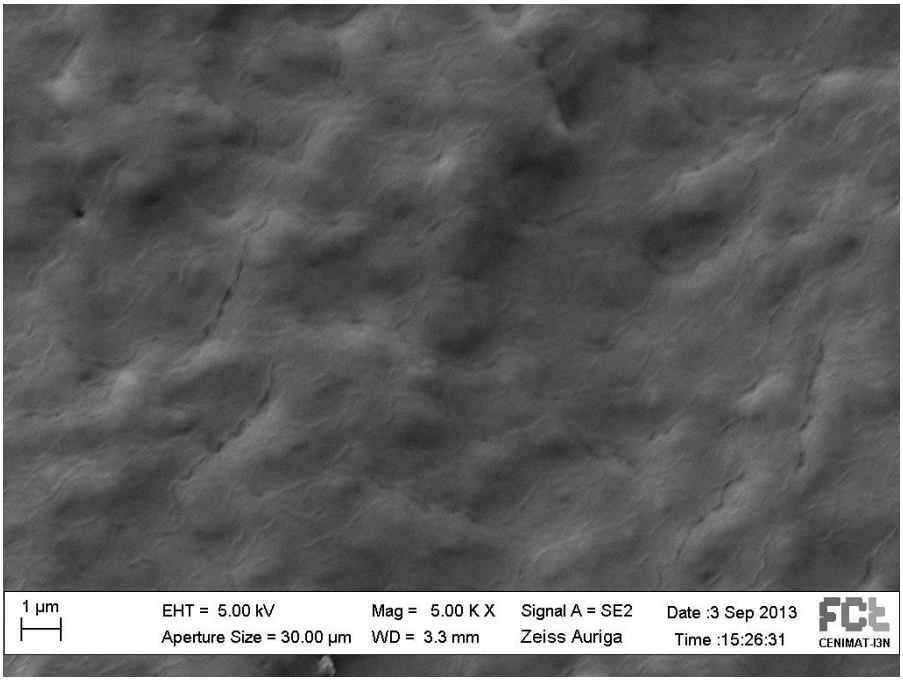

Figure 3.12 -SEM analysis for polymer POLYEGMDA$_{875}$ (1%AIBN) and LC in the proportion 30/70% (w/w) with 5% of TX100 of the total solution

The FTIR spectra obtained for this PDLC composition is shown in Graph 3.27. As refered before it is possible to identify three bands: the C=C double bond band, the band of the carbonyl group and the band correspondent to a sum of the band of liquid crystal with the band of TX100.

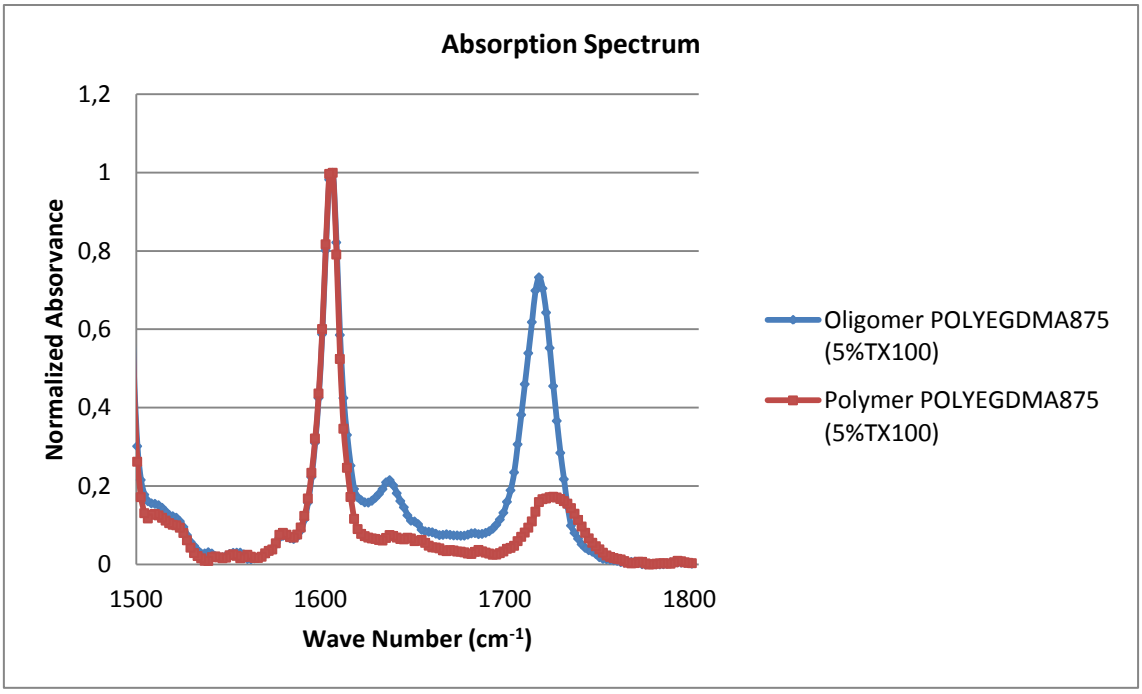

Graph 3.27 - FTIR spectra variation for the PDLC film with polymer POLYEGDMA$_{875}$ and LC in the proportion of 30/70% (w/w) and 5%TX100 of the total solution

The following results show the DSC study for the mixture of POLYEGDMA$_{875}$ and LC in the proportion of 30/70% (w/w) and 5% of TX100 of the total solution for the first and second heating stage.

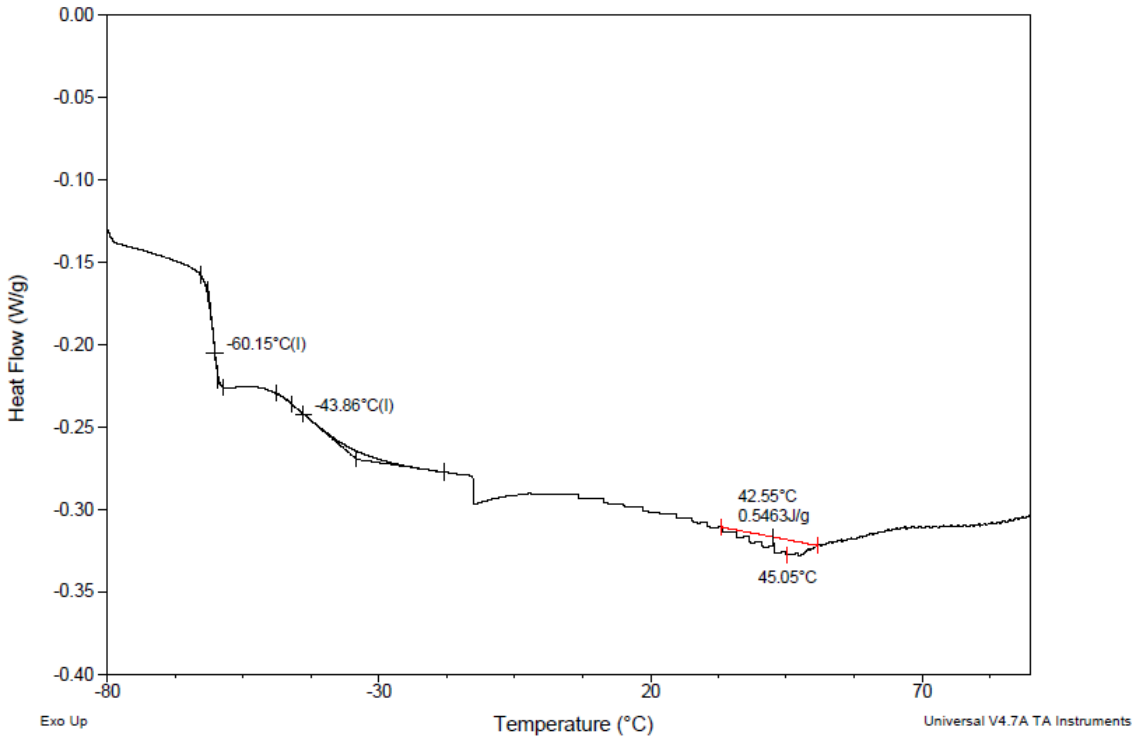

Graph 3.28 - First heating stage of the mixture of POLYEGDMA$_{875}$ and LC in the proportion of 30/70% (w/w) and 5% of TX100 of the total solution

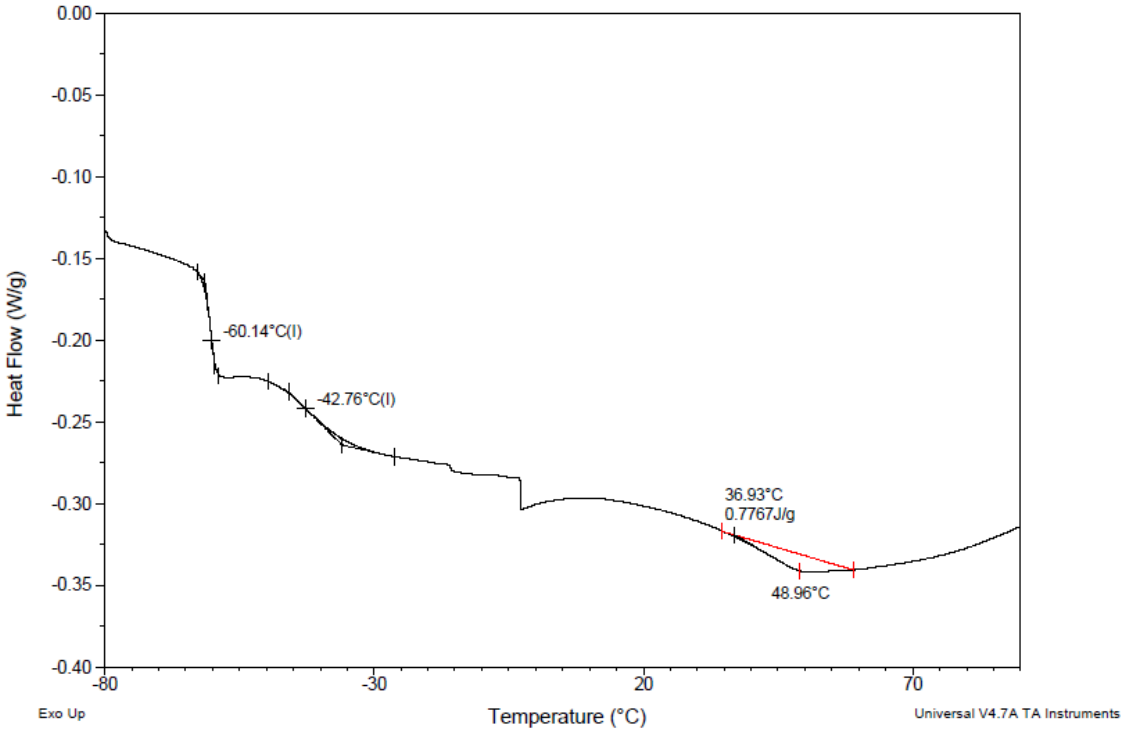

Graph 3.29 - Second heating stage of the mixture of POLYEGDMA$_{875}$ and LC in the proportion of 30/70% (w/w) and 5% of TX100 of the total solution

From the DSC study is possible to identify the following temperature transitions:

Table 3.9 - DSC study of polymer POLYEGDMA$_{875}$ and LC, 30/70 (%w/w) and 5% of TX100 of the total solution

Temperature Transitions	Temperature (ºC)	
	First Heating Cycle	Second Heating Cycle
$T_{g,1}$	-59,62	-59,57
$T_{g,2}$	-43,33	-44,35
Pick	37,00	37,06

The $T_{g,1}$ is characteristic of the glass transition of the nematic liquid crystal E7; the $T_{g,2}$ is characteristic of the glass transition of the polymer POLYEGDMA$_{875}$; the pick is probably the one that shows the nematic isotropic transition of liquid crystal E7, although it occurs at a lower temperature than the one presented on the DSC study for the liquid crystal without been mixed with the polymer and the additive, showed Graph 3.2.

- **POLYEGDMA$_{875}$ (1%AIBN) + E7 with 30/70% (w/w) and 10%TX100 of the total solution**

In the Graph 3.30 is presented the EO response of the PDLC formed with polymer POLYEGDMA$_{875}$ (1%AIBN) and LC in the proportion of 30/70% (w/w) with 10% of TX100 of the total solution.

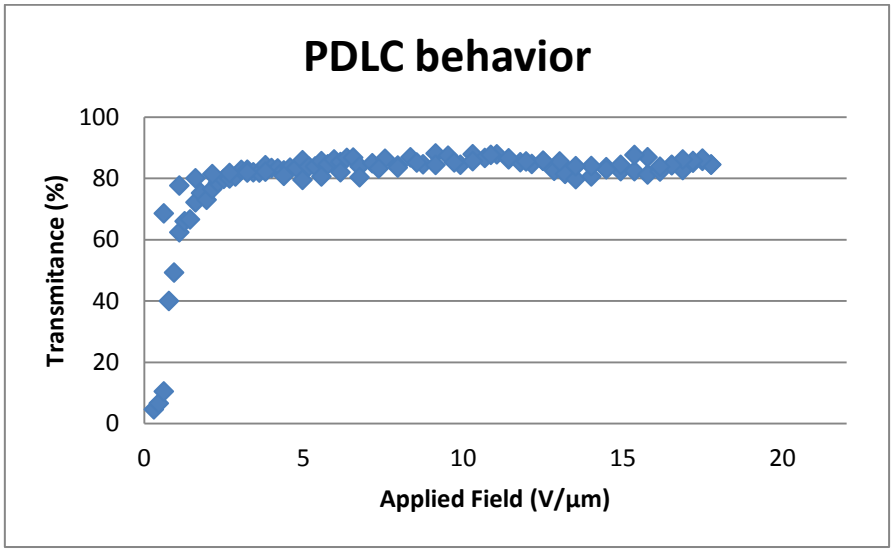

Graph 3.30 - EO response of the system polymer POLYEGDMA$_{875}$ (1%AIBN) and LC in the proportion 30/70% (w/w) with 10%TX100 of the total solution

Through the graph it can be concluded that initially the device has a transmittance of about 5%, meaning that it is opaque. When the electric field is applied, the PDLC achieves a maximum transmittance of about 87%. After removal of the electric field remains the PDLC with a transmittance of about 69%, which means that this device has permanent memory effect (PME) of about 78% and an E90 of 2 V/µm. The memory state contrast value obtained was 70%.

The analysis of the morphology of this PDLC is shown in Figure 3.13:

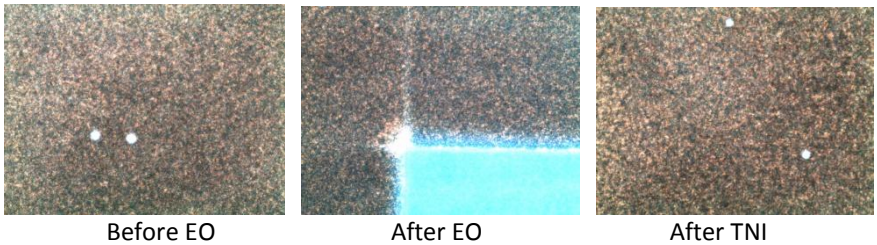

Figure 3.13 - POM micrograph for polymer POLYEGMDA$_{875}$ (1%AIBN) and LC in the proportion 30/70% (w/w) with 10% of TX100 of the total solution

As shown in figure 3.13 the sample is homogeneous in its totality, the area where the voltage is applied is in a brighter tonality, not visible before applying the voltage. After reaching the TNI the sample becomes an homogeneous matrix like in the beginning.

The analysis of the morphology by SEM is shown in Figure 3.14.

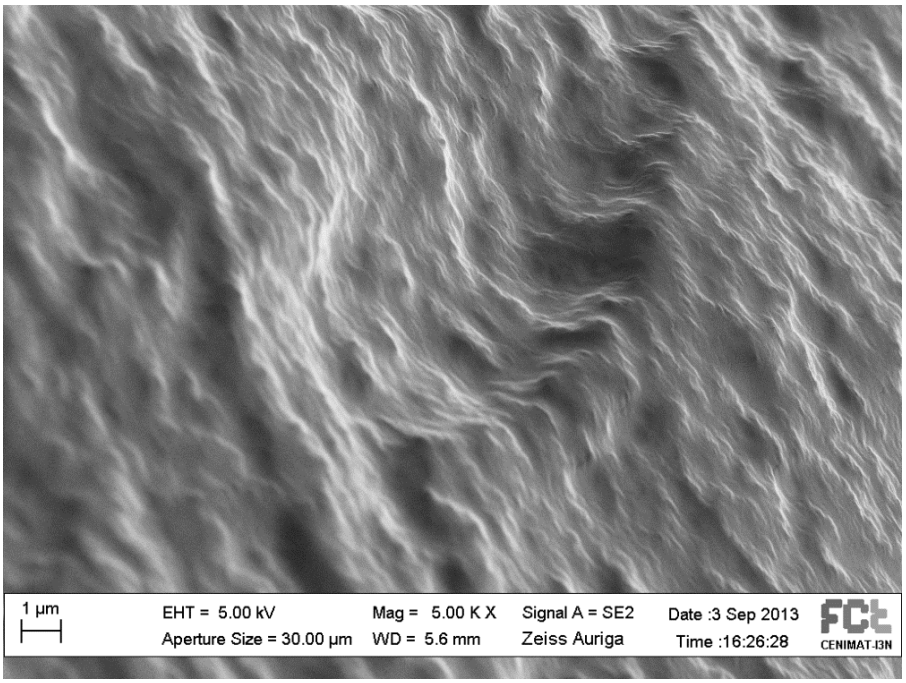

Figure 3.14 - SEM analysis for polymer POLYEGDMA$_{875}$ (1%AIBN) and LC in the proportion 30/70% (w/w) with 10%TX100 of the total solution

The FTIR spectra obtained for this PDLC composition is shown in Graph 3.31. As refered before it is possible to identify three bands: the C=C double bond band, the band of the carbonyl group and the band correspondent to a sum of the band of liquid crystal with the band of TX100.

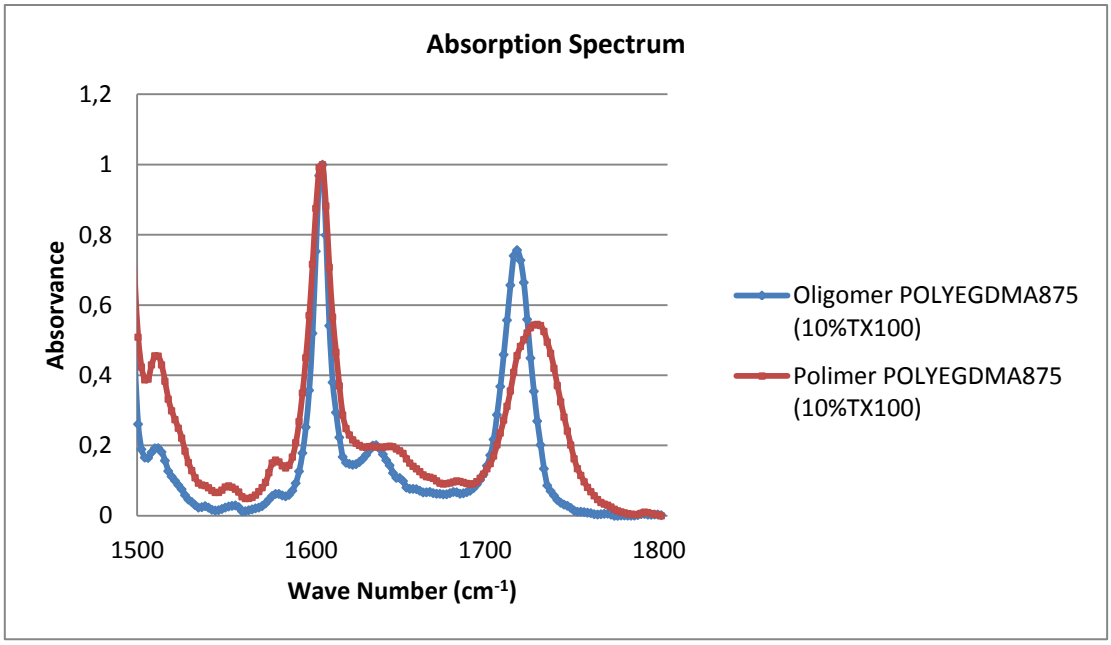

Graph 3.31 - FTIR spectra variation for the PDLC film with polymer POLYEGDMA$_{875}$ and LC in the proportion of 30/70% (w/w) and 10%TX100 of the total solution

The following results show the DSC study for the mixture of POLYEGDMA$_{875}$ and LC in the proportion of 30/70% (w/w) and 5% of TX100 of the total solution for the first and second heating stage.

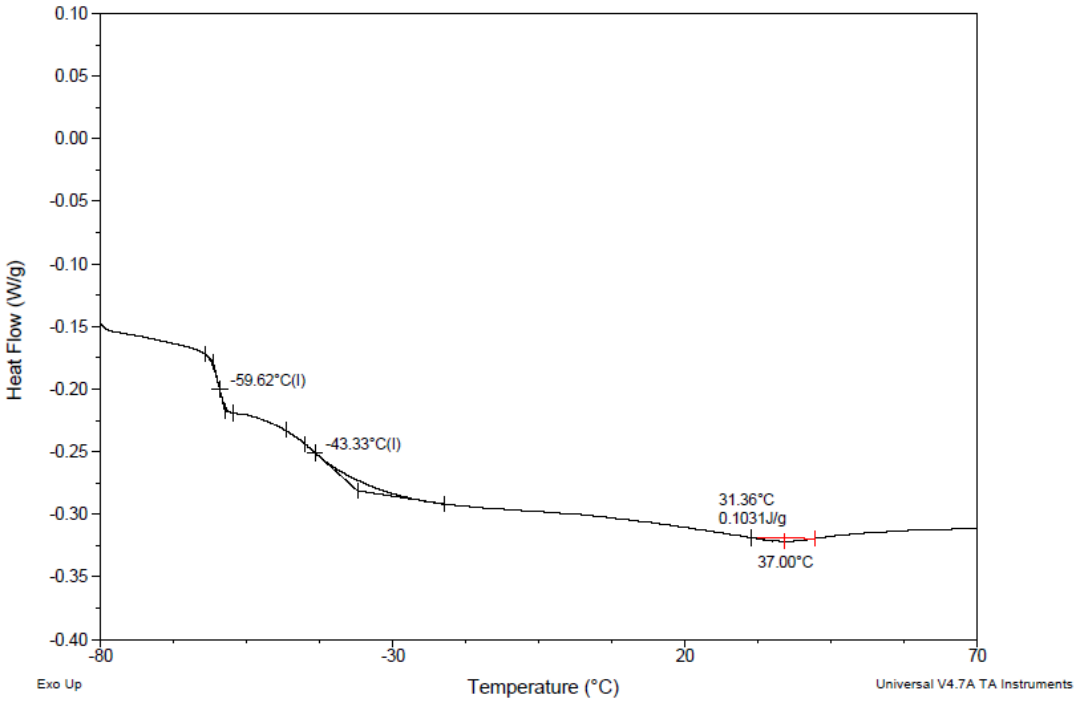

Graph 3.32 - First heating stage of the mixture of polymer POLYEGDMA$_{875}$ and LC in the proportion of 30/70% (w/w) and 10% of TX100 of the total solution

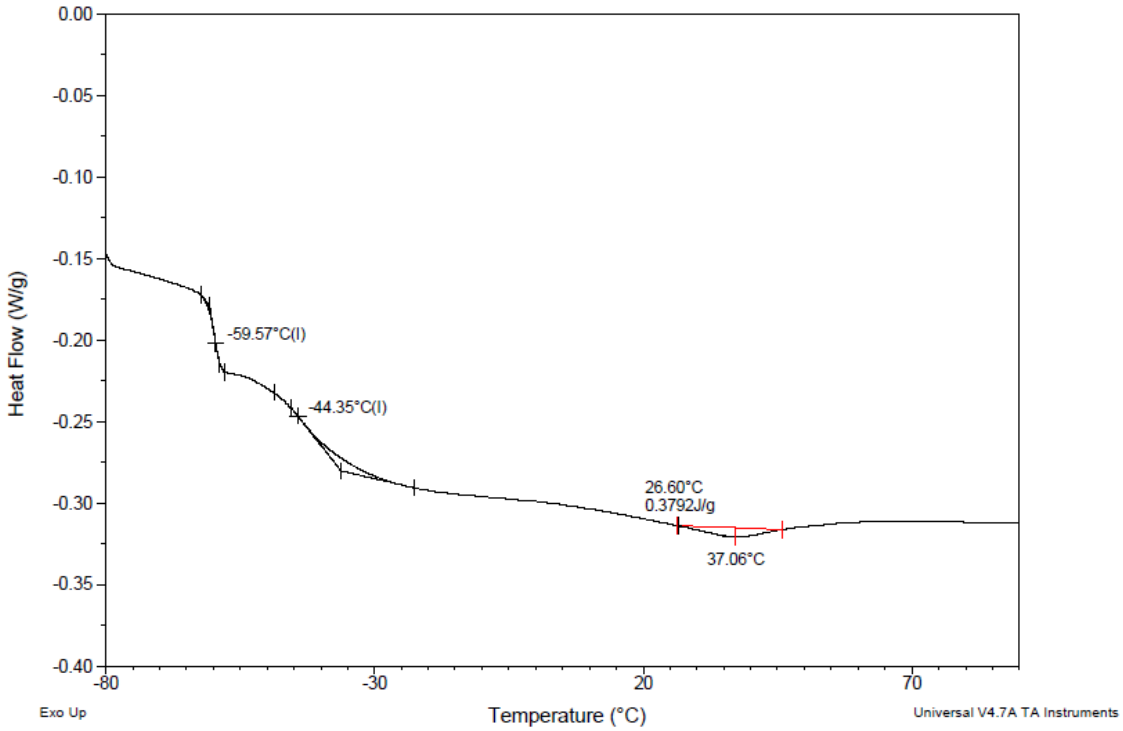

Graph 3.33 - Second heating stage of the mixture of POLYEGDMA$_{875}$ and LC in the proportion of 30/70% (w/w) and 10% of TX100 of the total solution

From the DSC study is possible to identify the following temperature transitions:

Table 3.10 - DSC study of polymer POLYEGDMA$_{875}$ and LC, 30/70 (%w/w) and 10% of TX100 of the total solution

Temperature Transitions	Temperature (ºC)	
	First Heating Cycle	Second Heating Cycle
$T_{g,1}$	-59,63	-59,58
$T_{g,2}$	-59,63	-59,58
Pick 3	37,70	37,06

The $T_{g,1}$ is characteristic of the glass transition of the nematic liquid crystal E7; the $T_{g,2}$ is characteristic of the glass transition of the polymer POLYEGDMA$_{875}$; the pick is probably the one that shows the nematic isotropic transition of liquid crystal E7, although it occurs at a lower temperature than the one presented on the DSC study for the liquid crystal without been mixed with the polymer and the additive, showed Graph 3.2.

3.1.3 Conclusions

In the next table there is a resume of all the values obtained for PME, E90 and contrast of all the PDLC films studied for both polymers, TRIEGDMA e POLYEGDMA$_{875}$.

Table 3.11 - Resume of EO response of all the PDLC films syntetized

E7/Monomer %(w/w)	TX100 (%total solution)	Polymer	PME (%)	E90 (V/µm)	Contrast (%)
50/50	0	TRIEGDMA	NO EO RESPONSE		
		POLYEGDMA$_{875}$			
60/40	0	TRIEGDMA	NO EO RESPONSE		
		POLYEGDMA$_{875}$			
70/30	0	TRIEGDMA	20	7	13
		POLYEGDMA$_{875}$	58	5	45
	0,2	TRIEGDMA	6	14	4
		POLYEGDMA$_{875}$	60	4	41
	1	TRIEGDMA	9	14	6
		POLYEGDMA$_{875}$	54	5	42
	2	TRIEGDMA	4	13	3
		POLYEGDMA$_{875}$	47	5	40
	3	TRIEGDMA	15	12	10
		POLYEGDMA$_{875}$	50	4	41
	5	TRIEGDMA	29	2	23
		POLYEGDMA$_{875}$	60	2	46
	10	TRIEGDMA	96	2	68
		POLYEGDMA$_{875}$	78	2	64
	20	POLYEGDMA$_{875}$	92	1	74
80/20	0	TRIEGDMA	19	11	11
		POLYEGDMA$_{875}$	66	4	54
90/10	0	TRIEGDMA	NO EO RESPONSE		
		POLYEGDMA$_{875}$	65	5	51

For the ratio of monomer/LC of 30/70% (w/w) it is showed on the Graphs 3.34, 3.35, 3.36 and 3.37 the variation of PME, contrast and E90 with the increasing amount of TX100.

- **EO response for TRIEGDMA**

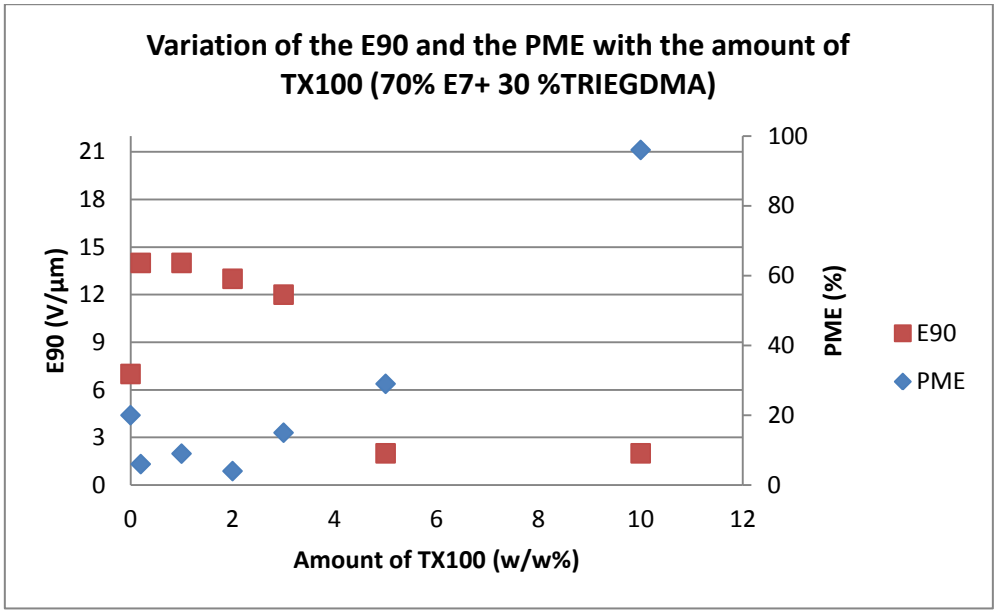

Graph 3.34- Variation of the E90 and the PME with the amount of TX100 for TRIEGDMA

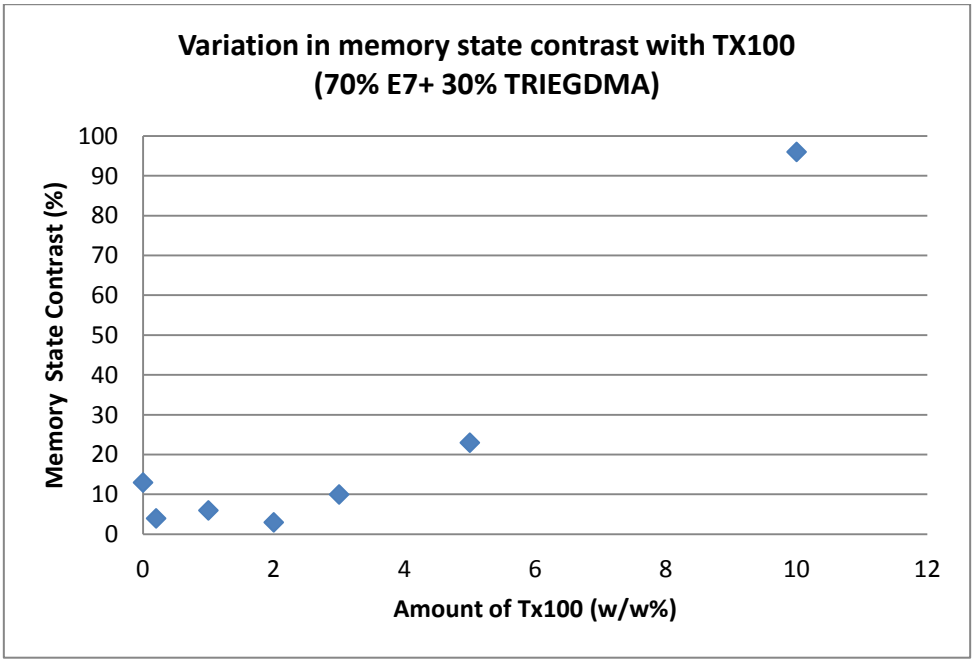

Graph 3.35 - Variation in the constrast with the amount of TX100 for TRIEGDMA

- **EO response for POLYEGDMA$_{875}$**

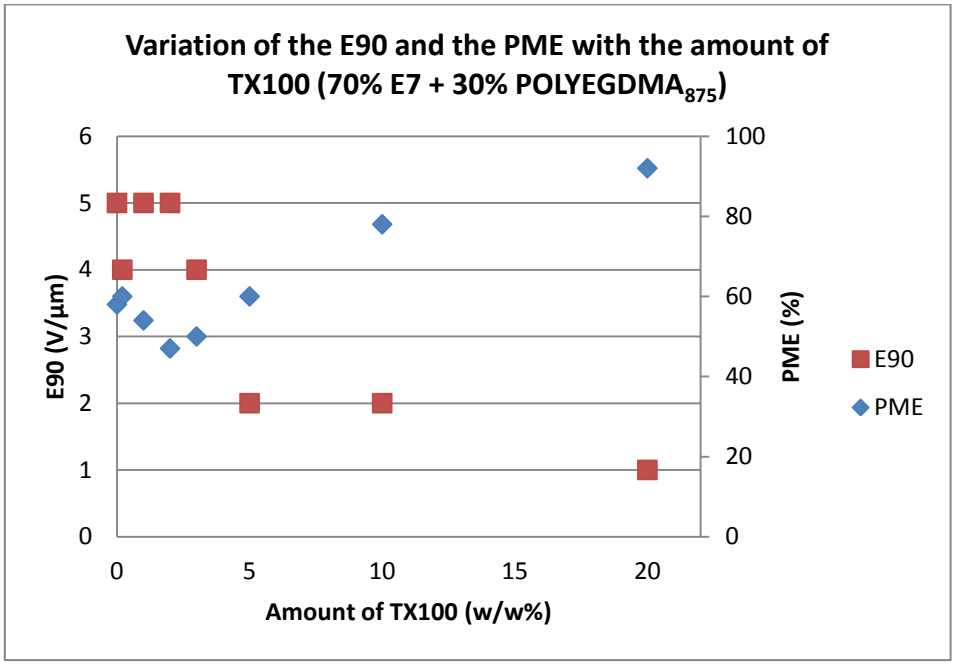

Graph 3.36 - Variation of the E90 and the PME with the amount of TX100 for POLYEGDMA$_{875}$

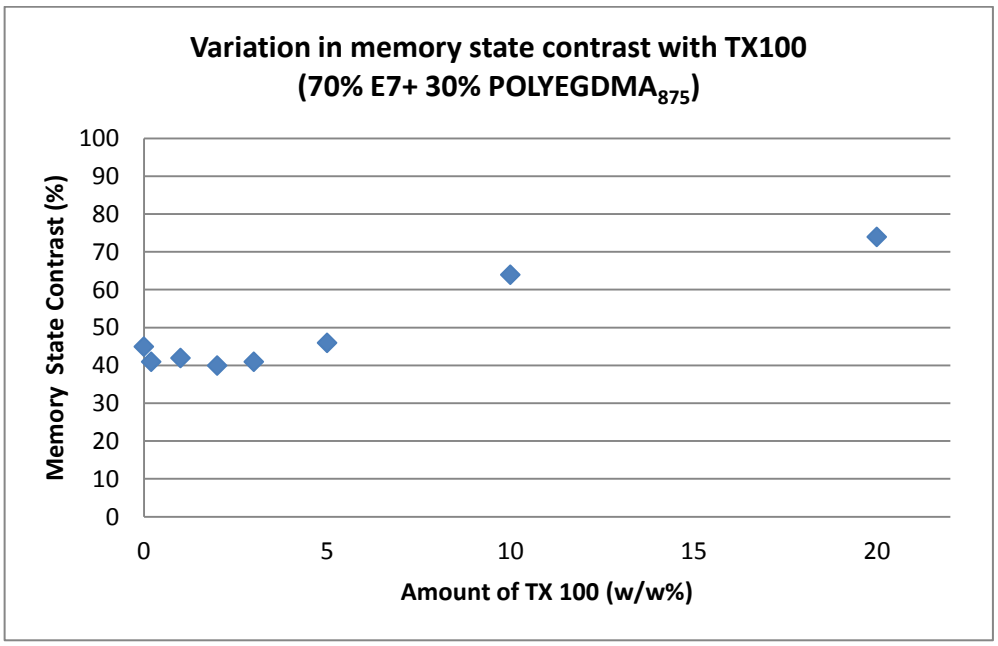

Graph 3.37 - Variation in contrast with the amount of TX100

From the EO study it is possible to conclude that the PDLC formed by TRIEGDMA does not show a significant PME unlike the PDLC formed by POLYEGDMA$_{875}$ that exhibits a strong

permanent memory effect. We can also observe that PDLC films containing a surfactant (TX100) up to 20% (w/w) (in the case of $POLYEGDMA_{875}$) showed a lower E90 and a higher PME.

Bookeun Oh et al.[26] estimated the network structure of PEGDMA polymers and presented the following structure :

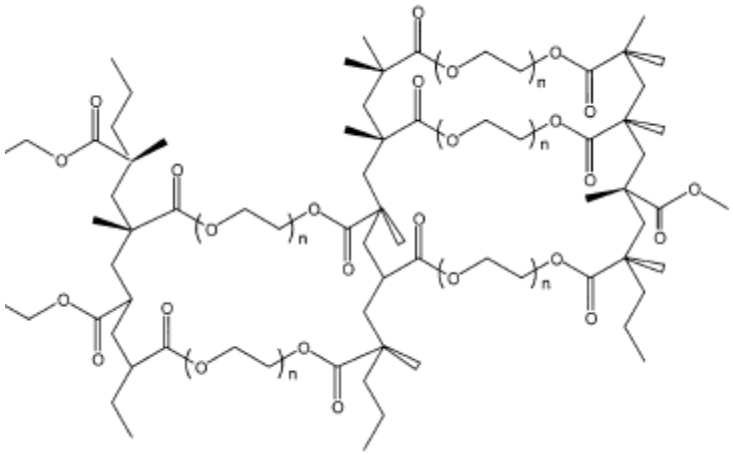

Figure 3.15 - Estimated network structure of PEGDMA polymers [26]

This author concluded the chain length of ethylene oxide determines the inter chain length between two PEGDMA polymers, and the mobility of the network polymer is decided by ethylene oxide chain length [24]. Then $POLYEGDMA_{875}$ has a longer ethylene oxide chain when compared to TRIEGDMA, forming larger microdomains. On average, the anchoring force of the liquid crystal molecules in TRIEGDMA is higher than in the $POLYEGDMA_{875}$. When a certain voltage is applied to PDLC films all the LC molecules are oriented in the direction of applied voltage. When this voltage is removed, the liquid crystal molecules in the case of TRIEGDMA, feel the anchoring force of the polymer and disorient again. In the case of $POLYEGDMA_{875}$, since the LC microdomains are larger, this disorientation of the molecules is not complete, and there are some LC molecules that remain oriented. This can explain why the PDLC film formed with this polymer, without TX100, presents a higher PME and a lower E90 than the PDLC film formed with TRIEGDMA.

Increasing the amount of TX100, in both polymers, there is a progressive increase in the permanent memory effect and a decrease of the E90. As referred before (on section 1.2.6), the addition of TX100 will reduce the original anchorage force between the LC molecules and the polymer matrix. Therefore, the LC molecules are more mobile and tend to orientate with a

lower applied voltage; when the applied voltage is removed some LC molecules dont' feel the anchorage force with the same strenght and remain with some orientation.

In the next graphs there is a DSC study comparing both polymers, TRIEGDMA and POLYEGDMA$_{875}$, (with increasing amounts of TX100 of the total solution) with E7 in the proportion of 30/70 (%w/w) and 1%AIBN, for the second heating stage, and a table summarizing all the temperatures measure by DSC for both polymers without TX100 and with increasing amounts of TX100.

- **DSC study for polymer TRIEGDMA**

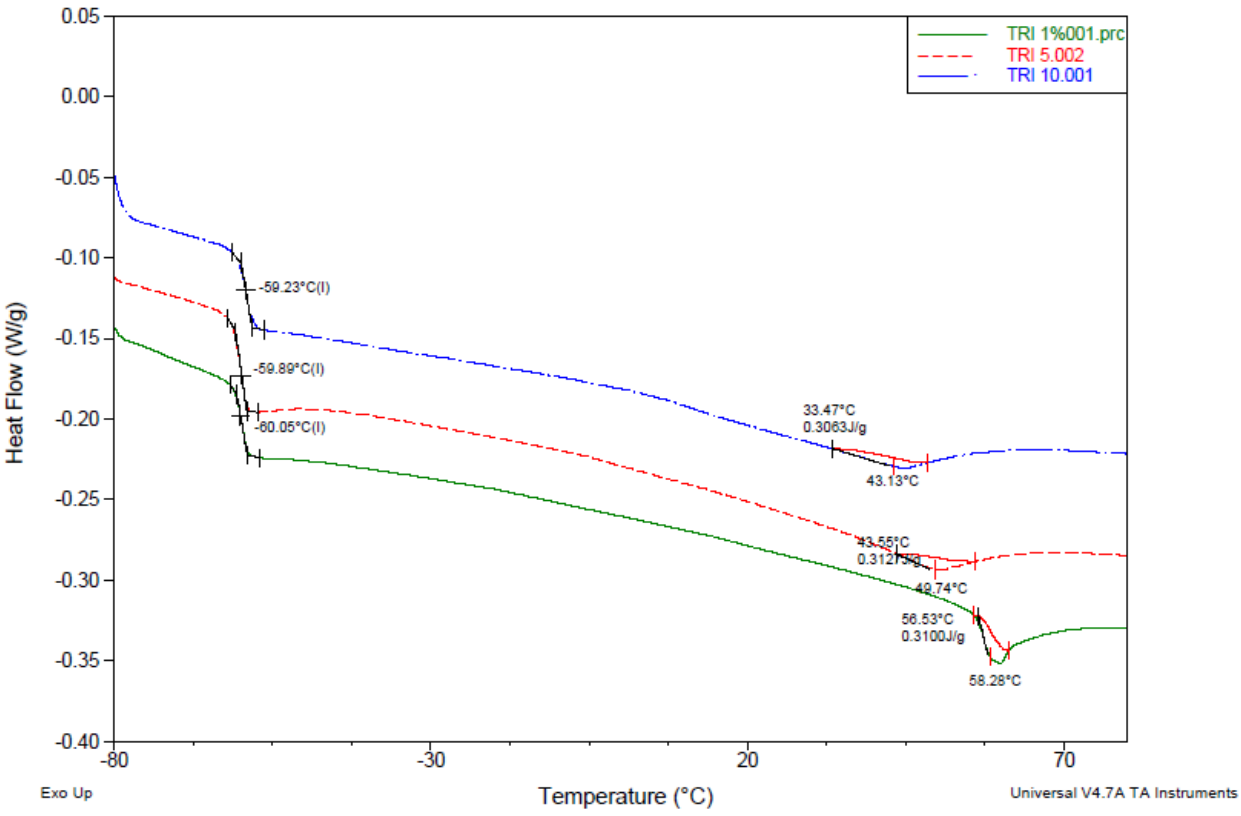

Graph 3.38 - Second heating cycle for polymer TRIEGDMA with increasing amounts of TX100

- **DSC study for polymer POLYEGMDA$_{875}$**

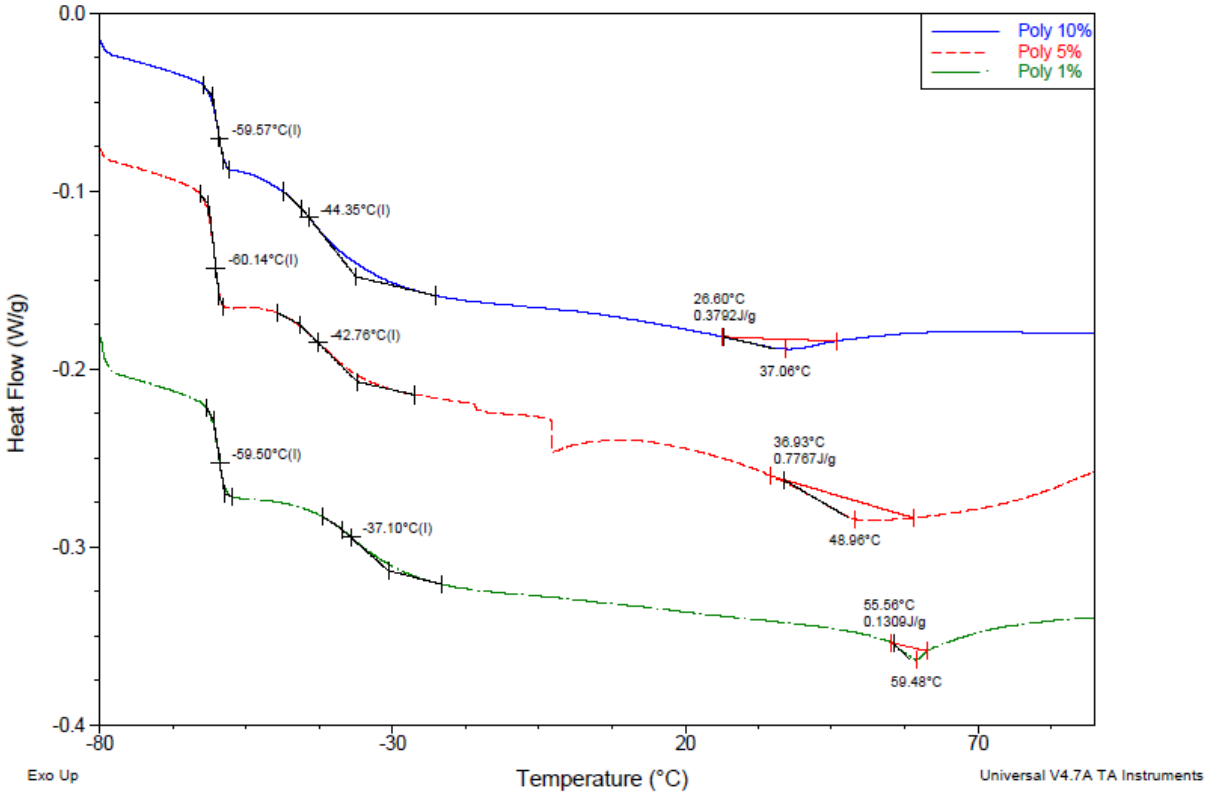

Graph 3.39 -Second heating cycle for polymer POLYEGDMA$_{875}$ with increasing amounts of TX100

In the next table is summarized all the temperatures measured by DSC for the two polymers, TRIEGDMA and POLYEGDMA$_{875}$, for increasing amounts of TX100, and the values of the nematic isotropic temperature and the glass transtion temperature of the nematic liquid crystal.

Table 3.12 - DSC study for polymers TRIEGDMA and POLYEGDMA$_{875}$ with increasing amounts of TX100

	$T_{g,E7}$ (ºC)	TNI (ºC)	
		Onset	Midpoint
Nematic Liquid Crystal, E7	-64,03	56,50	58,74

	Polymer (30% w/w)	TX100 (%w/w of total solution)	$T_{g,mixture}$ (ºC)	$T_{g,polymer}$ (ºC)	Clarification Temperature (ºC)	
					Onset	Midpoint
E7 (70%w/w)	**TRIEGDMA**	0[(1)]	-63,60	-	55,32	57,51
		1	-60,05	na	49,74	56,53
		5	-59,80	na	43,55	49,74
		10	-59,23	na	22,47	43,13
	POLYEGDMA$_{875}$	0[(1)]	-63,55	-41,59	53,94	57,92
		1	-59,50	-37,10	55,56	59,48
		5	-60,14	-42,76	36,93	48,96
		10	-59,57	-44,35	26,60	37,06

[(1)] - The values for the glass transition and clarification temperatures are presented on the DSC studies on appendix 4

From the DSC study it is possible to conclude that the $T_{g,POLYEGMDA_{875}}$ does not vary greatly, although the $T_{g,E7}$ and TNI vary with increasing amount of TX100. Considering that the polymer matrix is homogeneous and all the TX100 is entrapped inside the microdomainds, then the variation on the $T_{g,E7}$ occurs because the nematic liquid crystal glass transition is very close to the glass transition of the TX100 (graphs 3.2 and 3.7). Therefore, the T_g value observed, when TX100 is added to the mixture, is correspondent to the glass transition of the mixture of LC and TX100 and not the T_g when considering the compounds in separate.

Table 3.12 also allows to conclude that the nematic isotropic temperature of LC decreases with the amount of TX100. From the DSC study presented on graph 3.8, the melting temperature of TX100 is around 3 ºC which means that, when this additive is trapped inside the microdomains of LC, at the TNI, it behaves as an isotropic liquid increasing the entropy of the system LC-TX100, and acting as an impurity. Therefore, the nematic liquid temperature of the LC observed with the increase of TX100 represents the clarification temperature of the LC-TX100 mixture.

The influence of the addition of TX100 in T_g and TNI can be confirmed if, instead of considering the compounds polymerized, we consider the DSC of the mixture of E7 with TX100 with increasing amount of additive, as shown in the graph 3.4.0

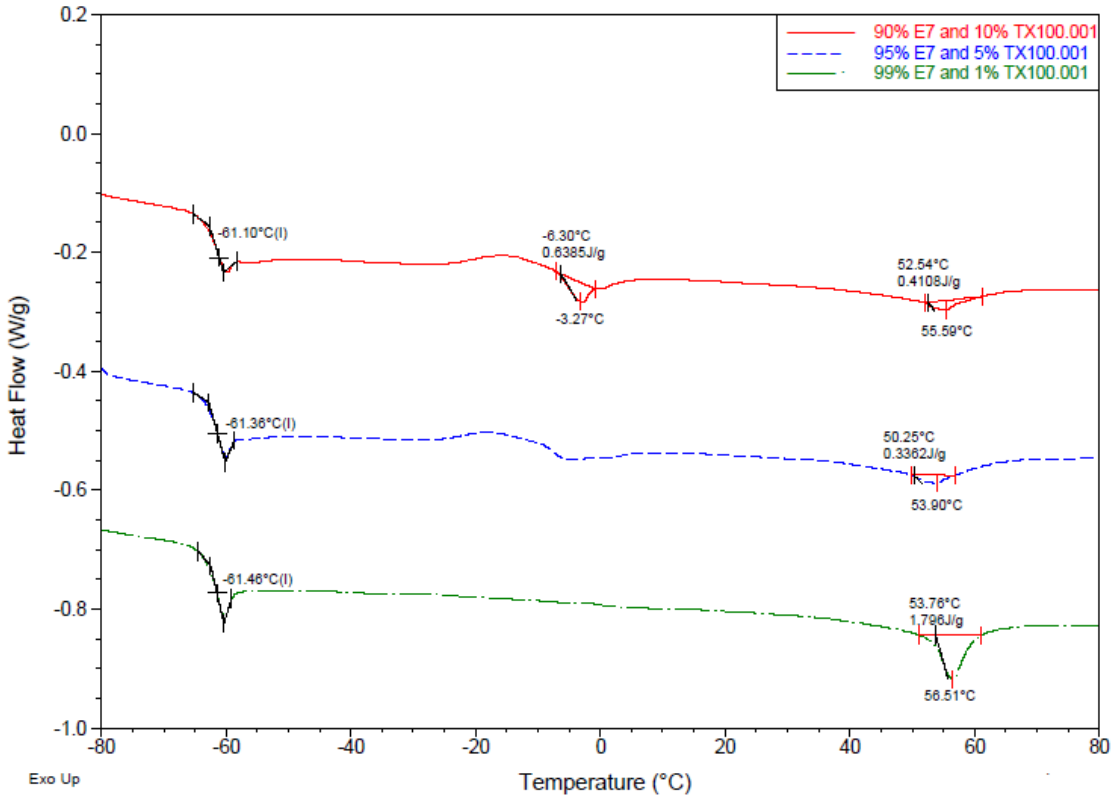

Graph 3.40 - DSC study for the mixture of LC and TX100, with increasing amounts of TX100

Graph 3.40 shows that with 1% and 5% of TX100, the TX100 is partially miscible on the liquid crytal. Therefore, the DSC study shows the results for the mixture, meaning that it is possible to see the tendency to decrease the TNI with the increase of the amount of TX100. However, with higher percentages of TX100 (10%) there is a phase separation and the DSC study shows the characteristic temperatures of the compounds when considered in separate. Thus, the nematic isotropic transition temperature increases, approaching again the temperature of the liquid crystal.

These values are in agreement with the values obtained using the technique of polarized light which are summarized in the table below for both polymers.

Table 3.13 - Values for the clarification temperature obtained from POM technique

Monomer	**Monomer/E7** **%(w/w)**	**TX100** **(%total solution)**	**Clarification Temperature (ºC)**
TRIEGDMA	30/70	1	56,0
		5	47,5
		10	43,4
$POLYEGDMA_{875}$	30/70	1	56,7
		5	45,1
		10	36,2

Furthermore, from the POM study, it is possible to conclude that in the case of the TRIEGDMA PDLC films, the TNI is not enough to disorientate all the LC molecules - it is necessary to heat the cell above the TNI temperature. On the other hand, on the PDLC films with $POLYEGDMA_{875}$ the TNI is enough to disorientate all the molecules. This demonstrates that the process is reversible, that is, it is possible, by applying a tension in the PDLC film, to obtain a permanent memory effect that is maintained until the cell is heated to TNI, and back to being a homogeneous matrix again.

From the SEM analysis, for an amplification of 5000 times, the increase amount of TX100 does not seem to influence the structure of the polymer matrix, since the scanning electron microscope images do not show a significant difference.

From the FTIR spectra it can be seen that before and after polymerization there is a decrease on the 1638 cm^{-1} band related to the disappearance of the $C = C$ double bond of the vinyl group of the methacrylate in both polymers. This fact can be justified once the polymerization of the monomers occurs, through the free radicals attack to the double bound, which breaks, originating a single bound $C - C$.

3.2 Kinetic Analysis

The kinetic analysis was done with the goal of having a general understanding of the kinetic PDLC behavior with increasing amounts of TX100 in solution and voltage. For this part of the work the kinetic behavior of the PDLC films composed from the monomers were studied, POLYEGDMA$_{875}$ and TRIEGDMA, and the liquid crystal in the proportion of 30/70 (%w/w) without and with TX100 in the percentages of 1, 5 and 10% w/w of the total solution.

Essentially, t_{90}, defined as the necessary time to reach 90% of the maximum transmittance, and t_{10}, the necessary time to reach 10% of the PDLC final transmittance after removing the applied field were determined. First T_{90} and T_{10}, were calculated, using the following two equations:

$$T_{10} = T_{min} + 0{,}1\Delta T \quad with \quad \Delta T = T_{max} - T_{min}$$

$$T_{90} = T_{min} + 0{,}9\Delta T \quad with \quad \Delta T = T_{max} - T_{min}$$

Beyond this understanding, in a second part of the work, we tried to implement a theoretical model to the experimental data, as described in appendix 2. For this final part it was only considered the best experimental curve for each PDLC film.
This model[27] [28] was formulated considering the following assumptions:

1. The system CL + polymer consists of LC-rich regions surrounded by regions rich in polymer;

2. LC-rich regions are regarded as spherical, in which the director $\vec{n}$ assumes the value of $\overrightarrow{n_o}$ at rest, (see figure).

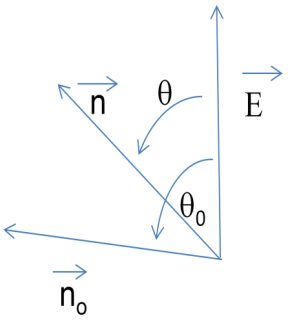

3. The application of an electric field $\vec{E}$ causes $\vec{n}$ to reorient towards the orientation of $\vec{E}$ according to an equation of equilibrium of moments of forces (NOTE: The director $\vec{n}$ is defined by the average orientation of the liquid crystal molecules).

The general equation which describes the kinetic model is the following one:

$$\frac{\gamma}{\mathrm{K}}\frac{d\theta}{dt}+\frac{\Delta\varepsilon}{2\mathrm{K}}E^2\sin 2\,\theta+\sin 2(\theta-\theta_0)=0 \quad (\mathbf{1})$$

Essentially and to apply the equation (1) to the experimental points it was considered the following approximate solutions:

I. Stationary Solution $\left(\frac{d\theta}{dt}=0\right)$

$$\mathrm{K}\sin 2(\Theta-\Theta_0)=-\frac{\Delta\varepsilon E^2}{2}\sin 2\Theta$$

$$\frac{\sin 2(\Theta-\Theta_0)}{\sin 2\Theta\,\theta}=\frac{\Delta\varepsilon E^2}{2\mathrm{K}}$$

$$\Theta=\frac{1}{2}\mathrm{artg}\frac{\sin 2\theta_0}{\cos 2\theta_0+\frac{\Delta\varepsilon E^2}{2\mathrm{K}}} \quad (2)$$

II. Solution for equation (6) with an applied field (rise)

Defining:

$$\frac{\gamma}{\mathrm{K}}=\frac{1}{b_o}$$

$$\frac{\Delta\varepsilon}{2\mathrm{K}}\mathrm{E}^2=\mathrm{a}_0$$

The equation for θ is:

$$\Theta(t)=arctg\left\{\frac{1}{\sin 2\theta_0}\left[\frac{a_0+1+\sqrt{c}\,\tanh\left(t\,b_0\sqrt{c}\right)}{1+(a_0+1)\frac{\tan h\left(t\,b_0\sqrt{c}\right)}{\sqrt{c}}}\right]-\frac{a_0-1+2\cos^2\theta_0}{\sin 2\theta_0}\right\} \quad (3)$$

$$c=(a_o-1)^2+4a_0\cos^2\Theta_0$$

NOTE: Calculus for E:

$$E = \frac{\frac{\Delta V}{d}(1+r)}{r + \frac{1}{3}\left(2 + \frac{\overline{\varepsilon_{zz}}}{\varepsilon_p}\right)}$$

$$r = \frac{V_{LC}}{V_{polymer}}$$

$$d - thickness\ of\ the\ liquid\ crystal$$

$$\Delta V - RMS\ Applied\ Voltage$$

$$\overline{\varepsilon_{zz}} = \varepsilon_{perpendicular} + \left(\varepsilon_{paralel} - \varepsilon_{perpendicular}\right)\overline{\cos^2\Theta_0}$$

$$\overline{\cos^2\Theta_0} = \frac{1}{3}(1 + \cos\Theta_0 + \cos^2\Theta_0)$$

$$\overline{cos^2\Theta_0} = \frac{\int_0^{\Theta_{\theta 0}} \cos^2\Theta \sin\Theta \ d\Theta}{\int_0^{\Theta_{\theta 0}} \sin\Theta \, d\Theta}$$

III. Solution for equation without an applied field (fall) ($\boldsymbol{E = 0}$)

$$\frac{d\Theta}{dt} + \frac{\mathrm{K}}{\gamma}\sin 2(\Theta - \Theta_0) = 0$$

$$\frac{d\theta\Theta}{\sin 2(\Theta - \Theta_0)} = -\frac{\mathrm{K}}{\gamma}dt$$

$$\Theta = \Theta_0 + arctg\Theta = \Theta_0 + arctg\left[tg(\Theta_i - \Theta_0)e^{-\frac{K}{\gamma}\Delta t}\right]$$

Considering $b = \frac{K}{\gamma}$ the previous equation can be rewrite as:

$$\Theta = \theta_0 + arctg[tg(\theta_i - \theta_0)e^{-b\Delta t}] \quad (\mathbf{4})$$

$$\Theta_i - \ angle\ between\ the\ director\ and\ \overrightarrow{E}\ for\ \Delta t = 0$$

Table 3.14 lists the parameters used in the model. The fitting parameters are painted red:

Table 3.14 - Parameters used in the model

Parameter	Unit	Name of the Parameter
t_{is}	ms	Initial time of rising
t_{fs}	ms	End time of rising
t_{id}	ms	Initial time of descent
t_{fd}	ms	End time of descent
n_v	-	Refractive Index of the glass
n_p	-	Refractive Index of the polymer
n_o	-	Ordinary index of LC
n_e	-	Extraordinary Index of LC
e_{po}	-	Relative Dielectric Constant of Polymer
e_{no}	-	Relative Ordinary Dielectric Constant of LC
e_{pa}	-	Relative Extraordinary Dielectric Constant of LC
K	Pa	Average Elastic Constant
d_K	Pa	Width of K distribution
n_K	-	Number of different values considered in K distribution
γ	Pa s	Rotational Viscosity of the director
d_{CL}	μm	Thickness of the LC
r	-	Ratio between LC Volume and polymer Volume
a_1 (regarding the model)	-	$\alpha\, d\, \frac{1}{2}\frac{8\pi}{3}\left(\frac{2\pi}{\lambda}\right)^4 R^6$
te_0	-	Θ_0
dte	-	Width of Θ_0 distribution
nte	-	Number of different values considered in Θ_0 distribution
vef	V	Root mean square voltage

3.2.1 PDLC behavior with voltage

3.2.1.1 PDLC film with TRIEGDMA

TRIEGDMA without TX100

The following graphs show the kinetic behavior of the PDLC film of TRIEGDMA and LC in the proportion of 30/70 (%w/w) without TX100. The first graph corresponds to the orientation of the LC molecules in PDLC film and the second to his disorientation.

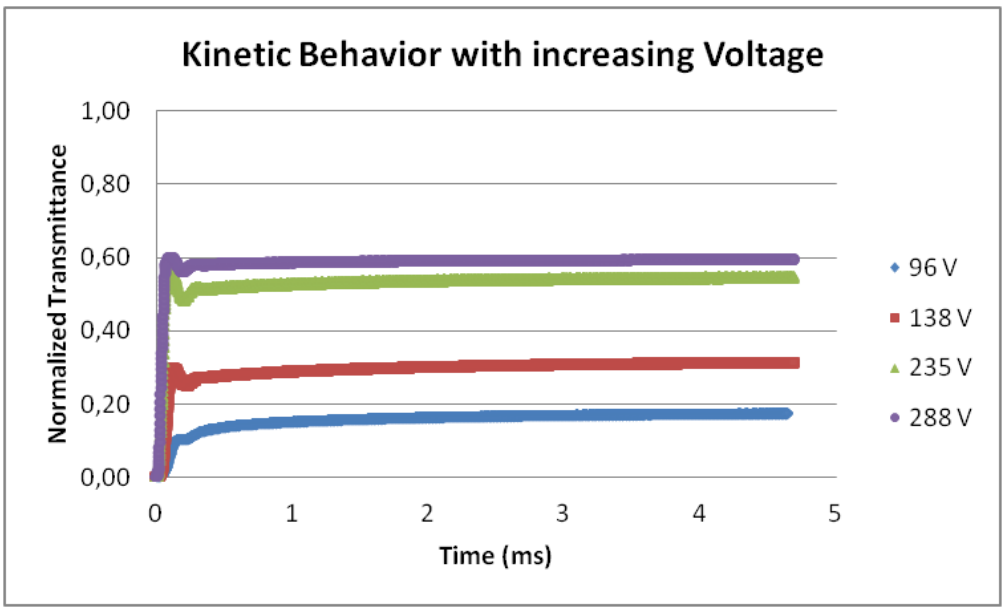

Graph 3.41 - Orientation Behavior with Increasing Voltage (30% TRIEGDMA/70% LC (%w/w) without TX100)

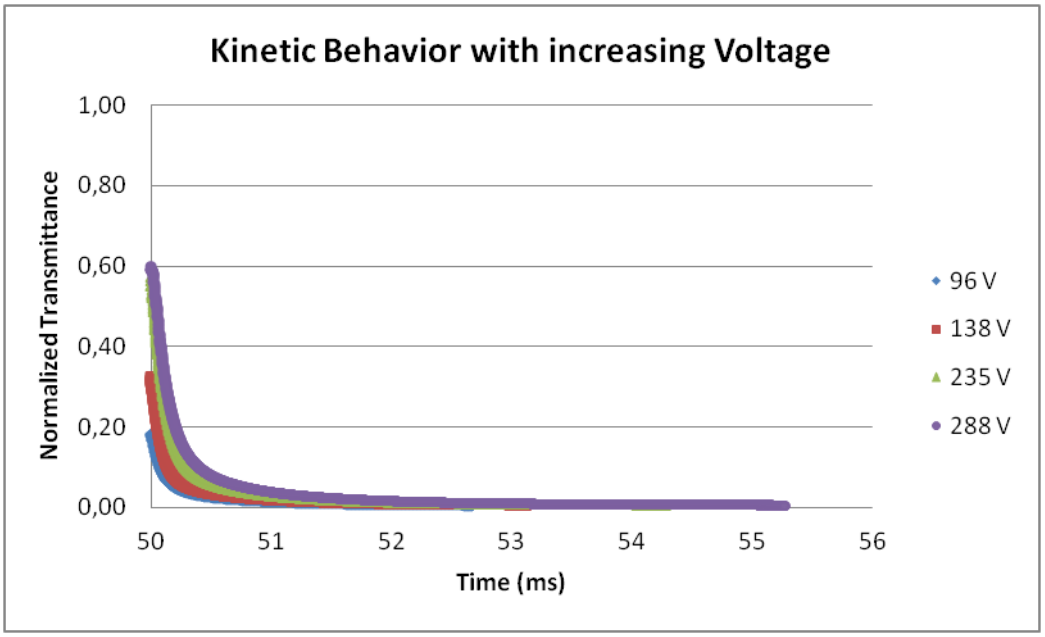

Graph 3.42 - Disorientation Behavior with Increasing Voltage (30% TRIEGDMA/70% LC (%w/w) without TX100)

TRIEGDMA with TX100

- **TRIEGDMA (1%AIBN) + E7 with 30/70% (w/w) and 1%TX100 of the total solution**

The following graphs show the kinetic behavior of the PDLC film of TRIEGDMA and LC in the proportion of 30/70 (%w/w) with 1% TX100 of the total solution. The first graph corresponds to the orientation of the LC molecules in PDLC film and the second to his disorientation.

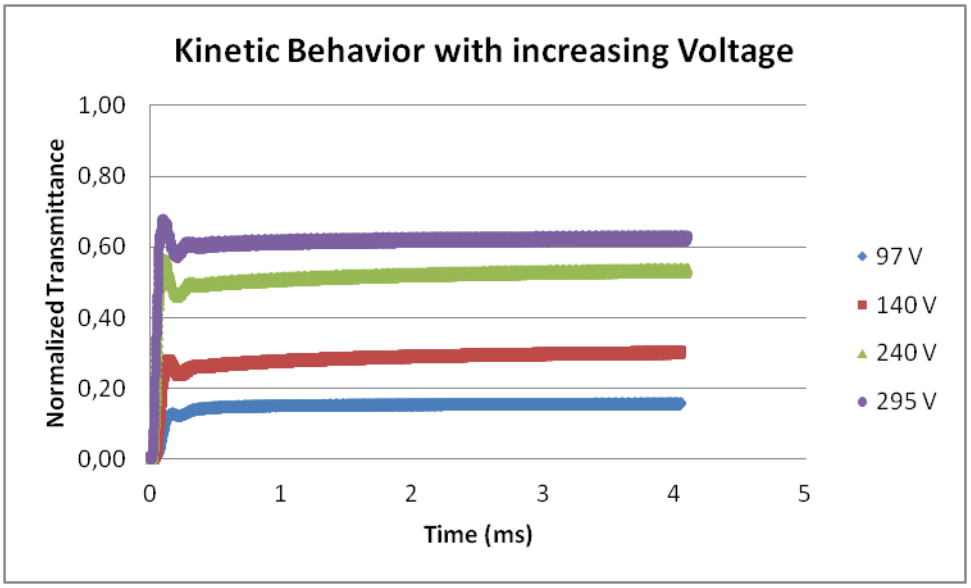

Graph 3.43 - Orientation Behavior with Increasing Voltage (30% TRIEGDMA/70% LC (%w/w) with 1%TX100)

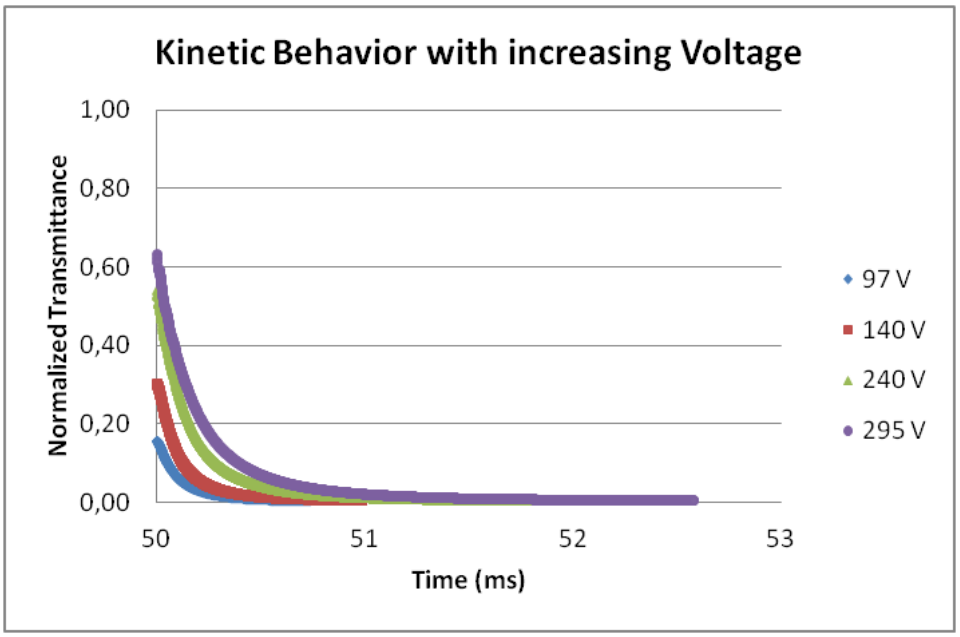

Graph 3.44 - Desorientation Behavior with Increasing Voltage (30% TRIEGDMA/70% LC (%w/w) with 1%TX100)

- **TRIEGDMA (1%AIBN) + E7 with 30/70% (w/w) and 5%TX100 of the total solution**

The following graphs show the kinetic behavior of the PDLC film of TRIEGDMA and LC in the proportion of 30/70 (%w/w) with 5% TX100 of the total solution. The first graph corresponds to the orientation of the LC molecules in PDLC film and the second to his disorientation.

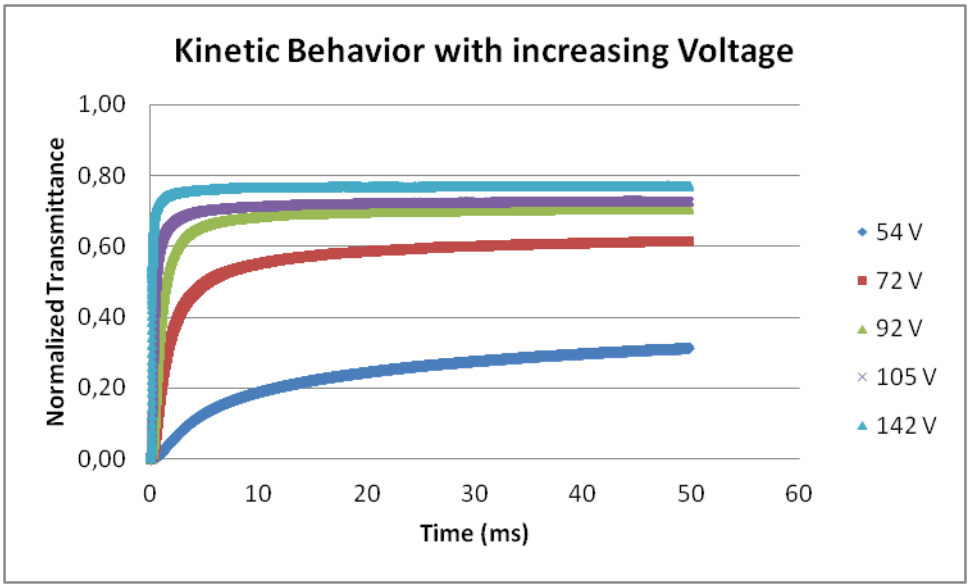

Graph 3.45 - Orientation Behavior with Increasing Voltage (30% TRIEGDMA/70% LC (%w/w) with 5%TX100)

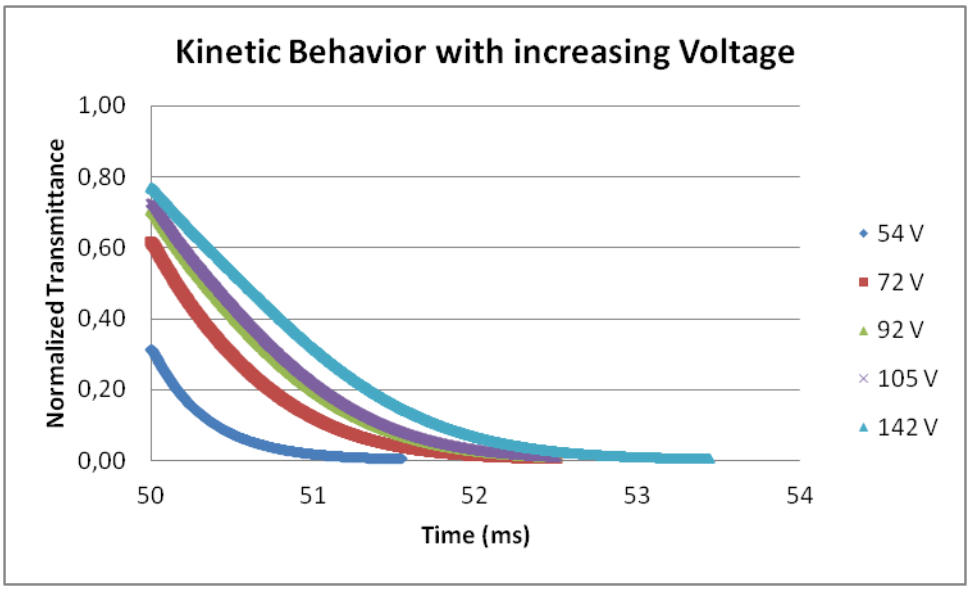

Graph 3.46- Desorientation Behavior with Increasing Voltage (30% TRIEGDMA/70% LC (%w/w) with 5%TX100)

- **TRIEGDMA (1%AIBN) + E7 with 30/70% (w/w) and 10%TX100 of the total solution**

The following graphs show the kinetic behavior of the PDLC film of TRIEGDMA and LC in the proportion of 30/70 (%w/w) with 10% TX100 of the total solution. The first graph corresponds to the orientation of the LC molecules in PDLC film and the second to his disorientation.

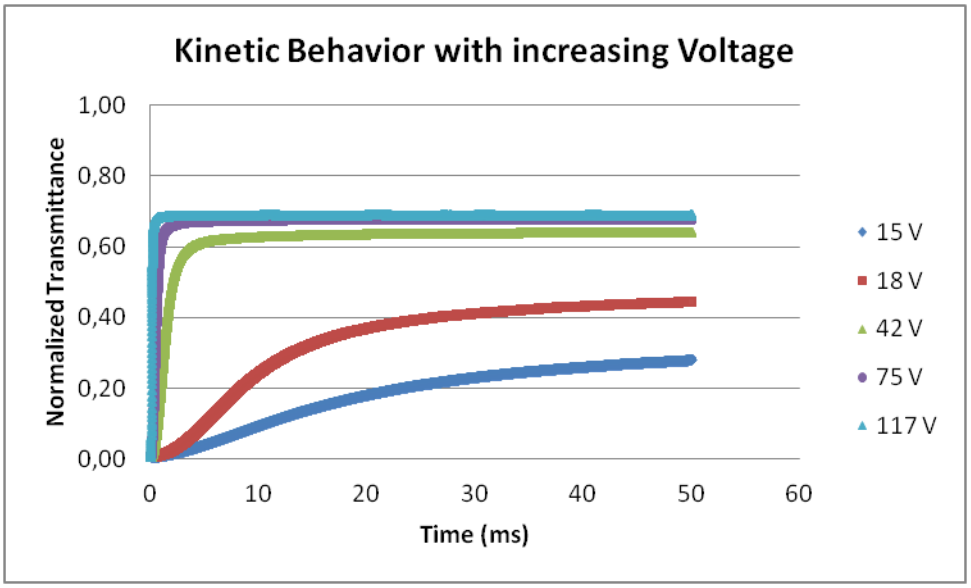

Graph 3.47 - Orientation Behavior with Increasing Voltage (30% TRIEGDMA/70% LC (%w/w) with 10%TX100)

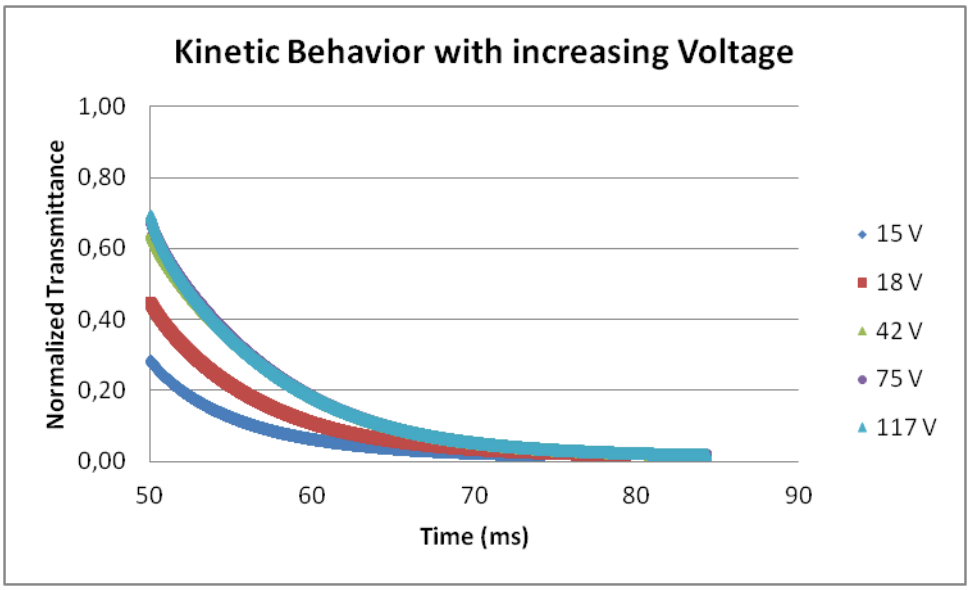

Graph 3.48- Desorientation Behavior with Increasing Voltage (30% TRIEGDMA/70% LC (%w/w) with 10%TX100

3.2.1.2 PDCL with POLYEGDMA$_{875}$

POLYEGDMA$_{875}$ without TX100

The following graphs show the kinetic behavior of the PDLC film of POLYEGDMA$_{875}$ and LC in the proportion of 30/70 (%w/w) without TX100. The first graph corresponds to the orientation of the LC molecules in PDLC film and the second to his disorientation.

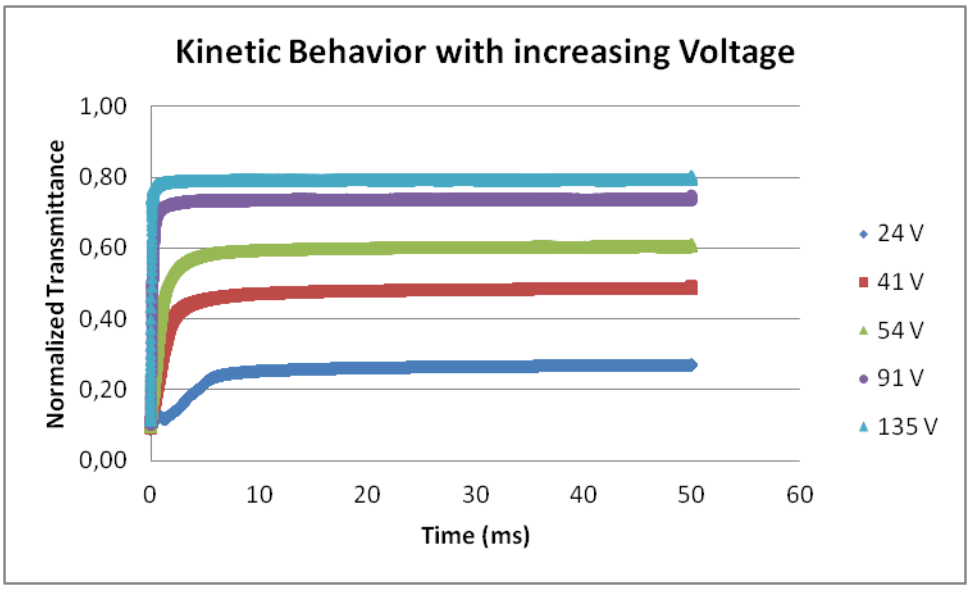

Graph 3.49 - Orientation Behavior with Increasing Voltage (30% POLYEGDMA$_{875}$/70% LC (%w/w) without TX100)

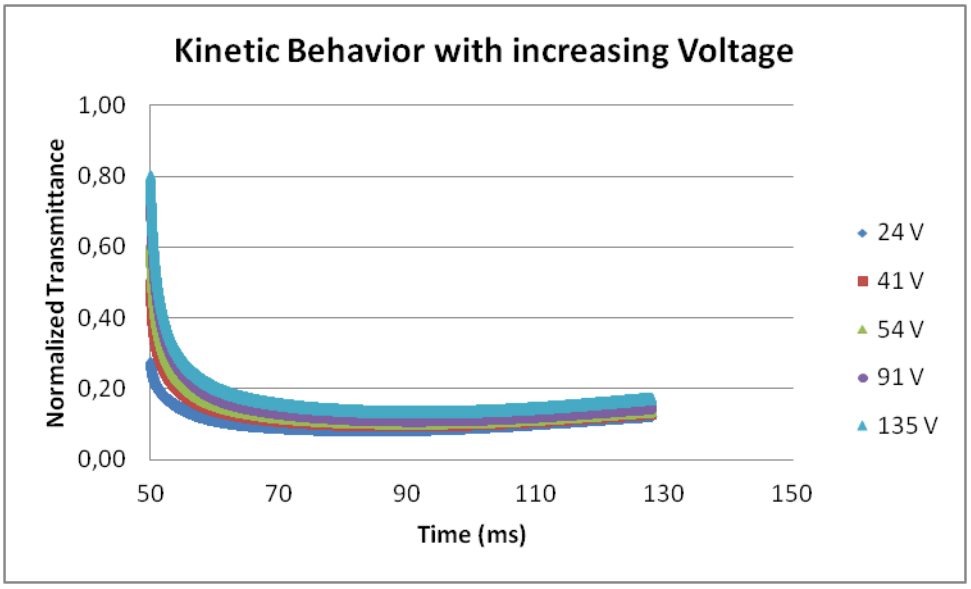

Graph 3.50 - Desorientation Behavior with Increasing Voltage (30% POLYEGDMA$_{875}$/70% LC (%w/w) without TX100)

POLYEGDMA$_{875}$ with TX100

- **POLYEGDMA$_{875}$ (1%AIBN) + E7 with 30/70% (w/w) and 1%TX100 of the total solution**

The following graphs show the kinetic behavior of the PDLC film of POLYEGDMA$_{875}$ and LC in the proportion of 30/70 (%w/w) with 1% TX100 of the total solution. The first graph corresponds to the orientation of the LC molecules in PDLC film and the second to his disorientation.

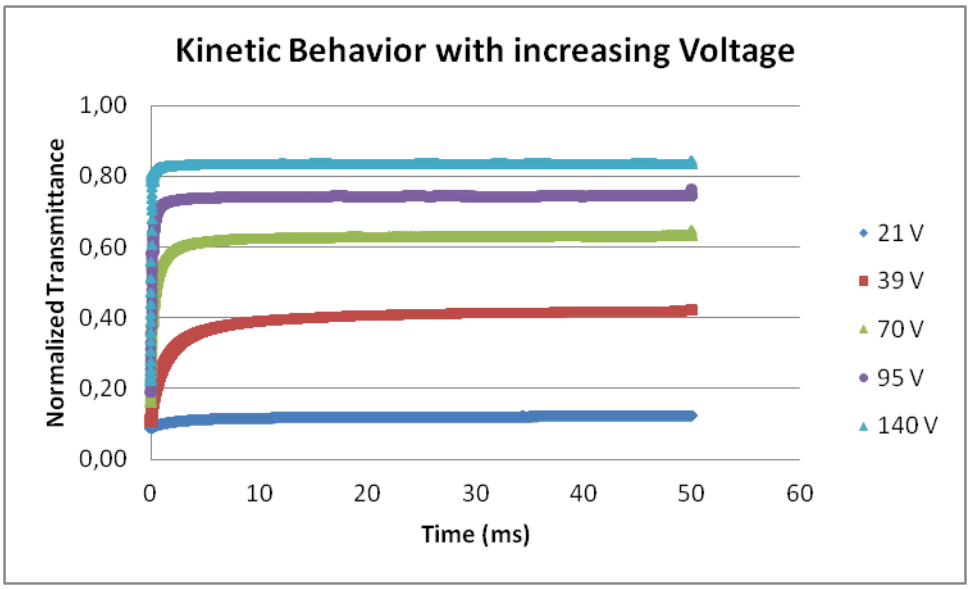

Graph 3.51 - Orientation Behavior with Increasing Voltage (30% POLYEGDMA$_{875}$/70% LC (%w/w) with 1%TX100)

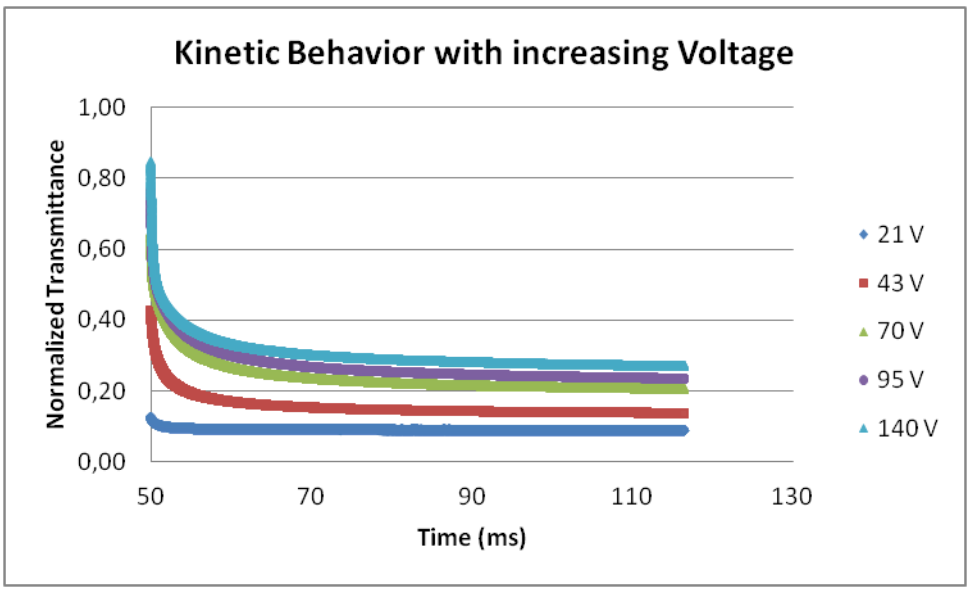

Graph 3.52 - Desorientation Behavior with Increasing Voltage (30% POLYEGDMA$_{875}$/70% LC (%w/w) with 1%TX100)

- **POLYEGDMA$_{875}$ (1%AIBN) + E7 with 30/70% (w/w) and 5%TX100 of the total solution**

The following graphs show the kinetic behavior of the PDLC film of POLYEGDMA$_{875}$ and LC in the proportion of 30/70 (%w/w) with 5% TX100 of the total solution. The first graph corresponds to the orientation of the LC molecules in PDLC film and the second to his disorientation.

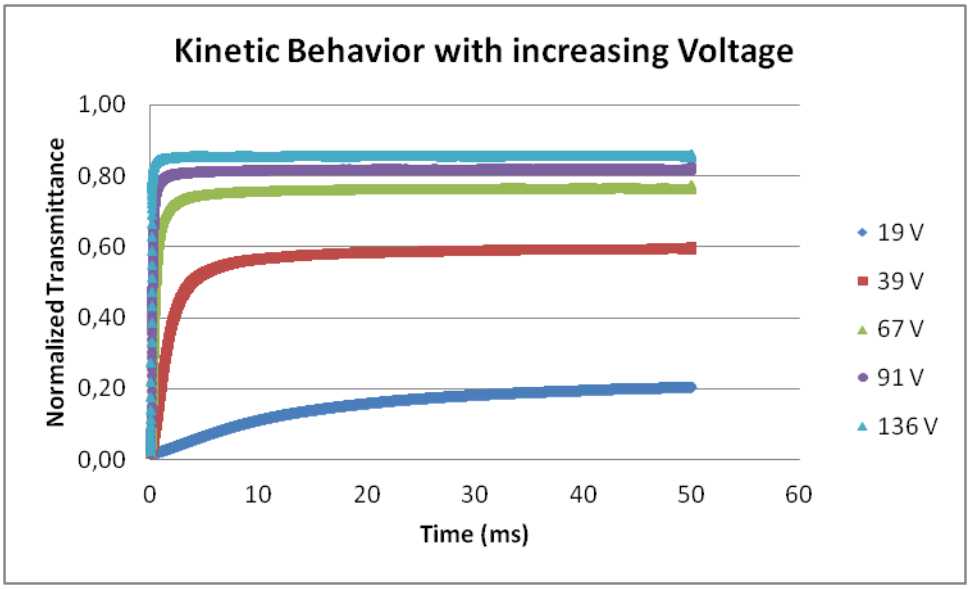

Graph 3.53- Orientation Behavior with Increasing Voltage (30% POLYEGDMA$_{875}$/70% LC (%w/w) with 5%TX100)

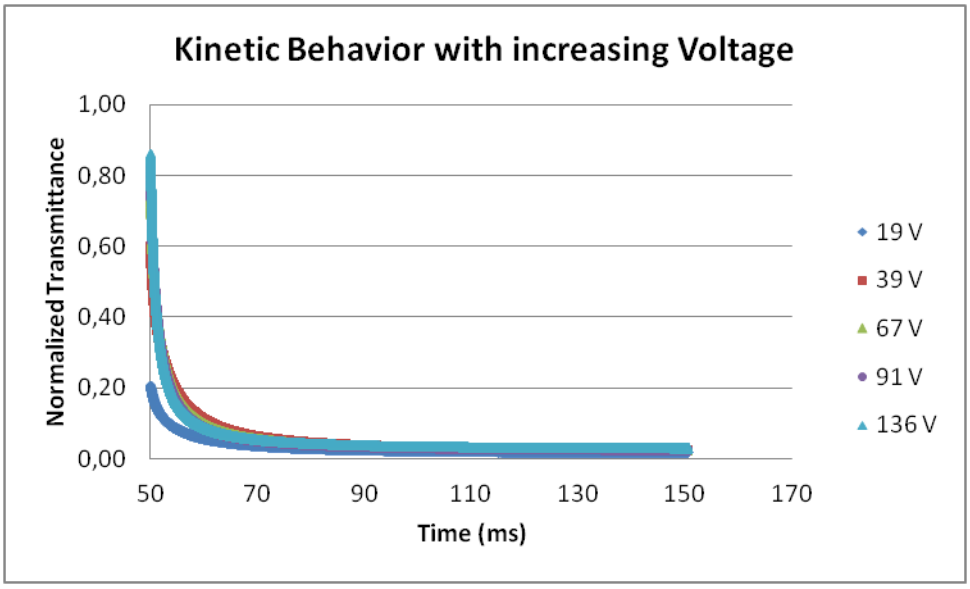

Graph 3.54 - Desorientation Behavior with Increasing Voltage (30% POLYEGDMA$_{875}$/70% LC (%w/w) with 5%TX100)

- **$POLYEGDMA_{875}$ (1%AIBN) + E7 with 30/70% (w/w) and 10%TX100 of the total solution**

The following graphs show the kinetic behavior of the PDLC film of $POLYEGDMA_{875}$ and LC in the proportion of 30/70 (%w/w) with 10% TX100 of the total solution. The first graph corresponds to the orientation of the LC molecules in PDLC film and the second to his disorientation.

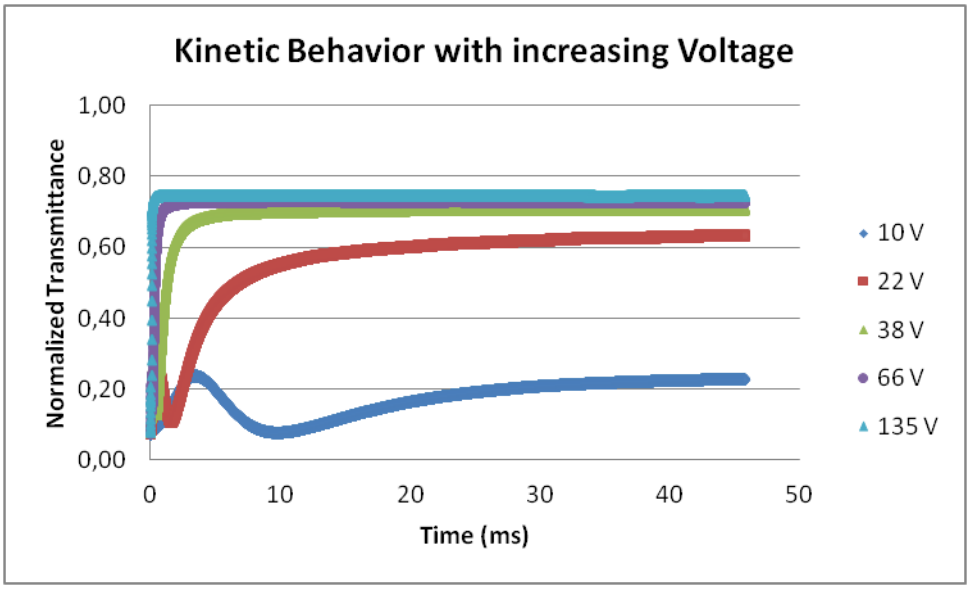

Graph 3.55 - Orientation Behavior with Increasing Voltage (30% $POLYEGDMA_{875}$/70% LC (%w/w) with 10%TX100)

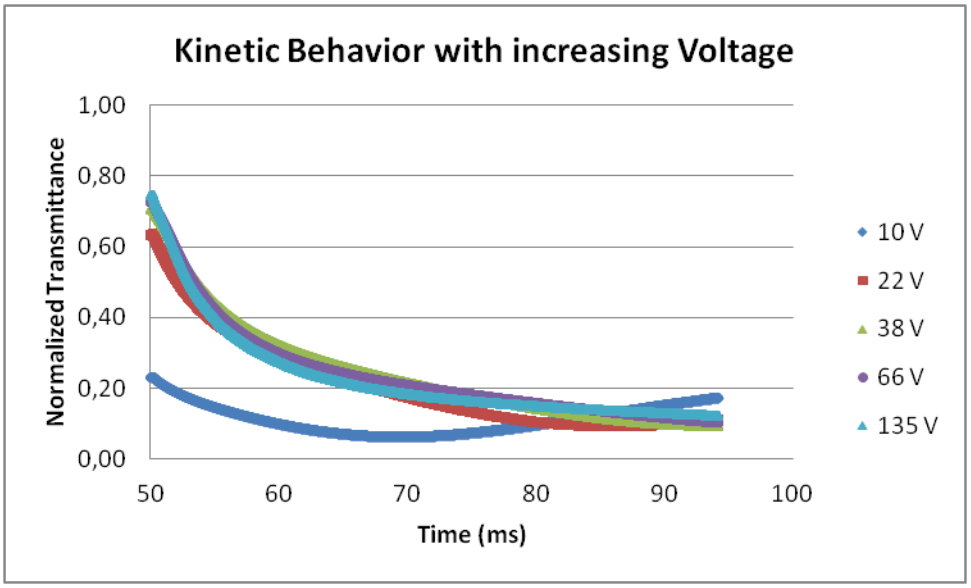

Graph 3.56 - Desorientation Behavior with Increasing Voltage (30% $POLYEGDMA_{875}$/70% LC (%w/w) with 10%TX100)

3.2.2. Fitting Model

In the next table it is summarized the experimental curves, according to the voltages, that were used to implement the theoretical model.

Table 3.15 - Experimental Curves for the fitting model

Monomer	E7/Monomer %(w/w)	TX100 (%total solution)	Effective Voltage Applied (V)
TRIEGDMA	70/30	0	235
		1	240
		5	72
		10	42
POLYEGDMA$_{875}$		0	41
		1	39
		5	39
		10	38

In this part of the work it was decided to present a graph with the experimental points as well as the theoretical model. Appendix 3 shows the graphs obtained resorting to the programming software as well as the values obtained for the parameters before and after optimization.

3.2.2.1 PDLC film with TRIEGDMA

TRIEGDMA without TX100

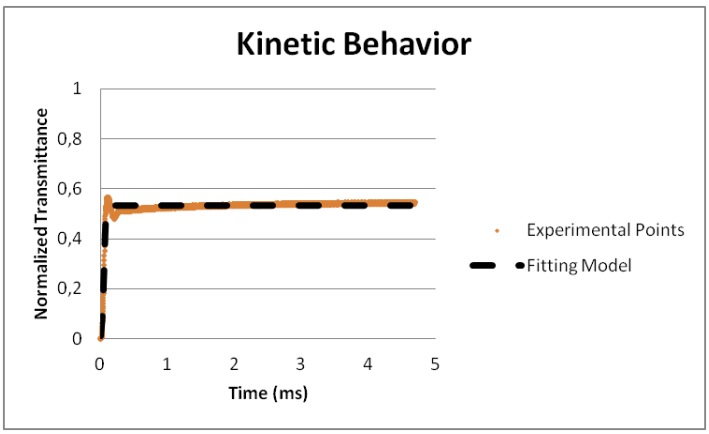

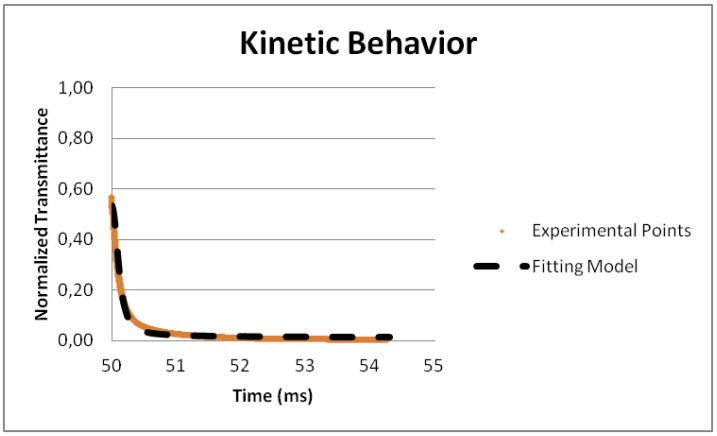

Graph 3.57 - Fitting model for the kinetic behavior of orientation and desorientation (30% TRIEGDMA/70% LC (%w/w) without TX100)

TRIEGDMA with TX100

- **TRIEGDMA (1%AIBN) + E7 with 30/70% (w/w) and 1%TX100 of the total solution**

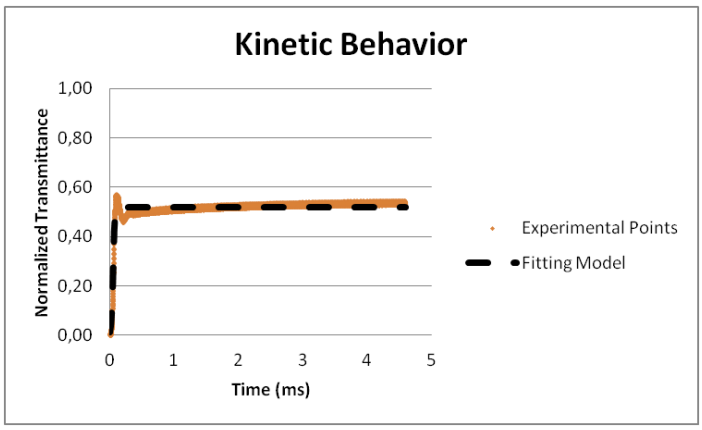

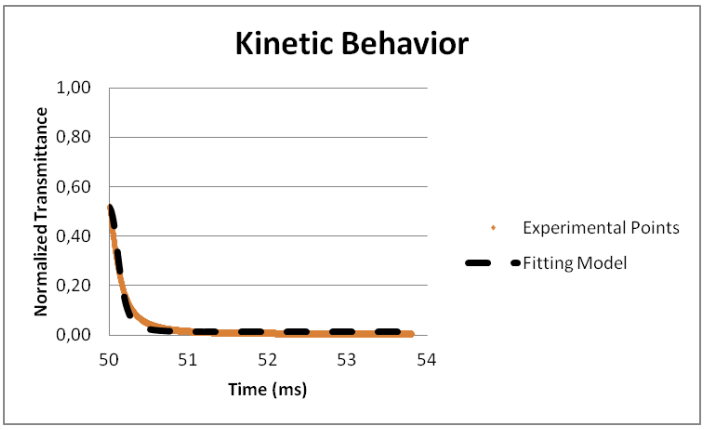

Graph 3.58- Fitting model for the kinetic behavior of orientation and desorientation (30% TRIEGDMA/70% LC (%w/w) with 1%TX100 of the total solution)

- **TRIEGDMA (1%AIBN) + E7 with 30/70% (w/w) and 5%TX100 of the total solution**

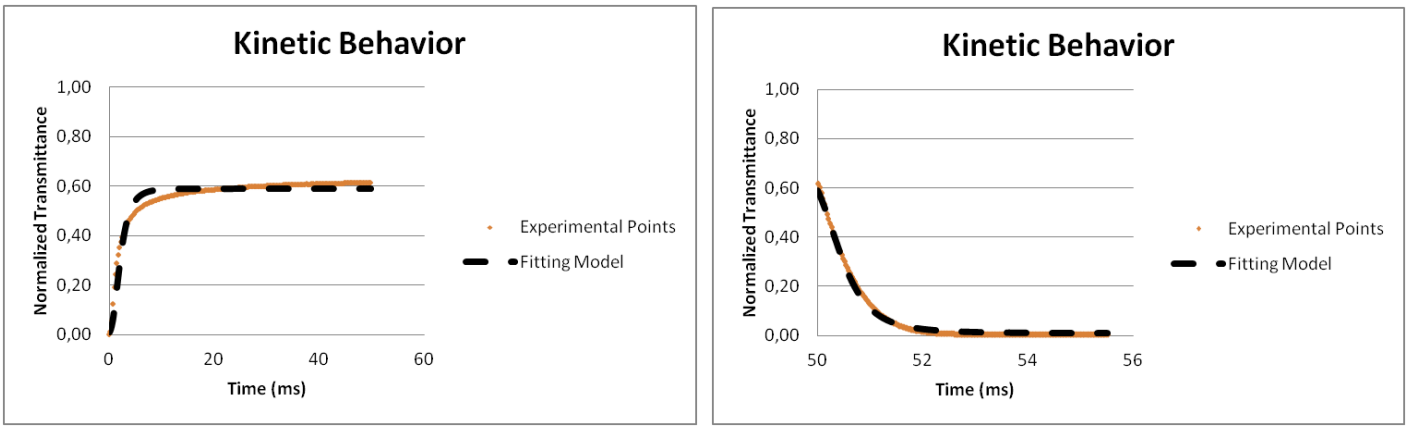

Graph 3.59 - Fitting model for the kinetic behavior of orientation and desorientation (30% TRIEGDMA/70% LC (%w/w) with 5%TX100 of the total solution)

- **TRIEGDMA (1%AIBN) + E7 with 30/70% (w/w) and 10%TX100 of the total solution**

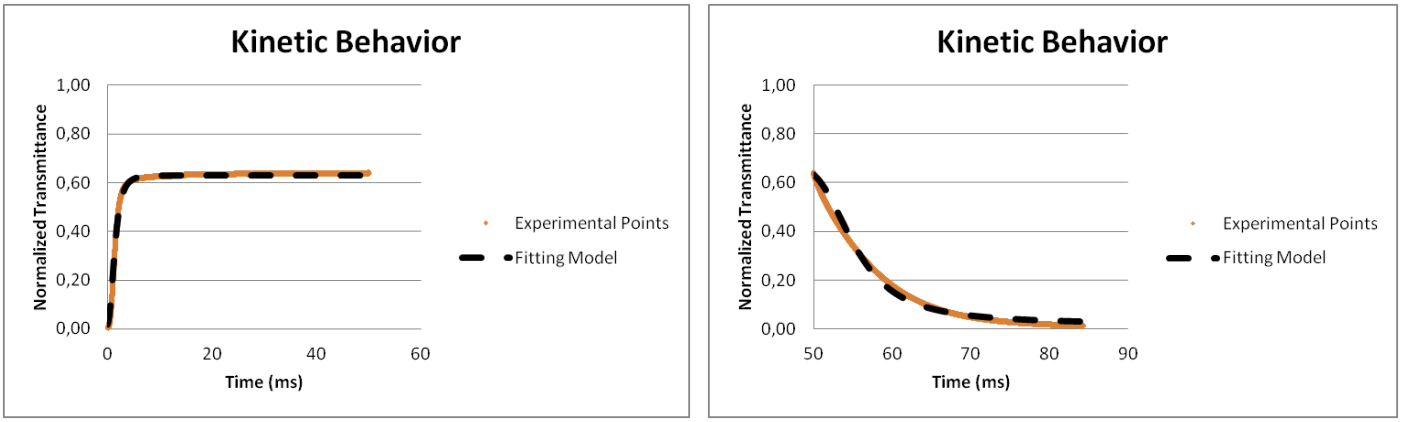

Graph 3.60 - Fitting model for the kinetic behavior of orientation and desorientation (30% TRIEGDMA/70% LC (%w/w) with 10%TX100 of the total solution)

3.2.2.2 PDLC film with $POLYEGDMA_{875}$

$POLYEGDMA_{875}$ without TX100

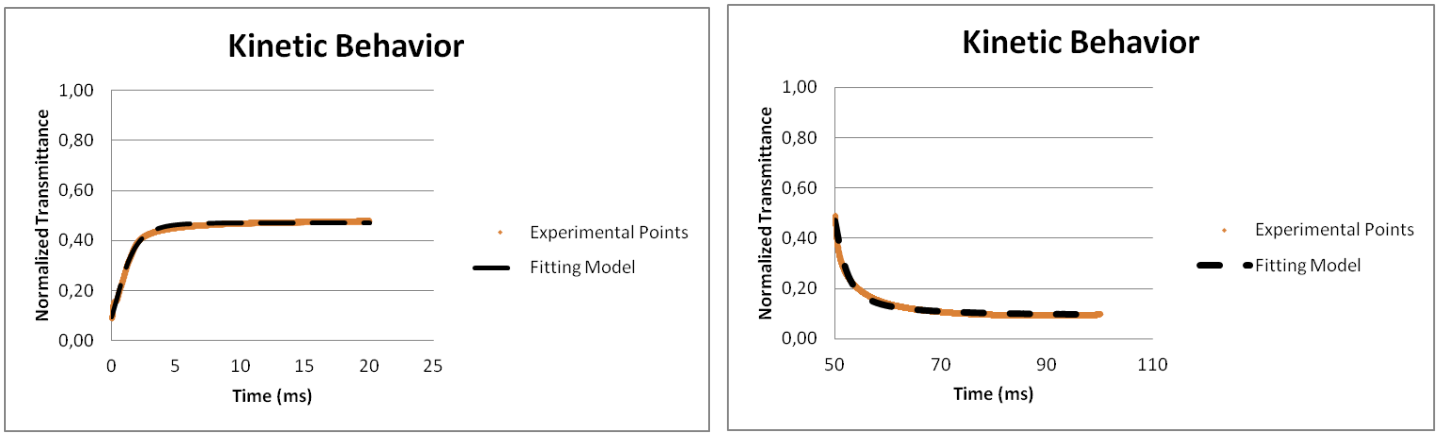

Graph 3.61 - Fitting model for the kinetic behavior of orientation and desorientation (30% $POLYEGDMA_{875}$/70% LC (%w/w) without TX100)

$POLYEGDMA_{875}$ with TX100

- **$POLYEGDMA_{875}$(1%AIBN) + E7 with 30/70% (w/w) and 1%TX100 of the total solution**

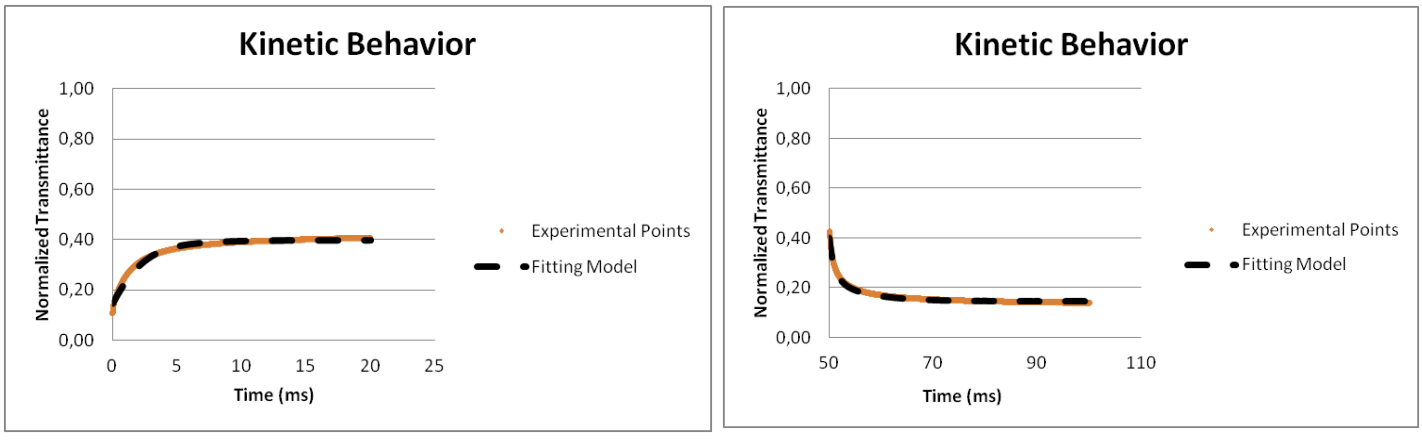

Graph 3.62- Fitting model for the kinetic behavior of orientation and desorientation (30% $POLYEGDMA_{875}$/70% LC (%w/w) with 1%TX100 of the total solution)

- **POLYEGDMA$_{875}$(1%AIBN) + E7 with 30/70% (w/w) and 5%TX100 of the total solution**

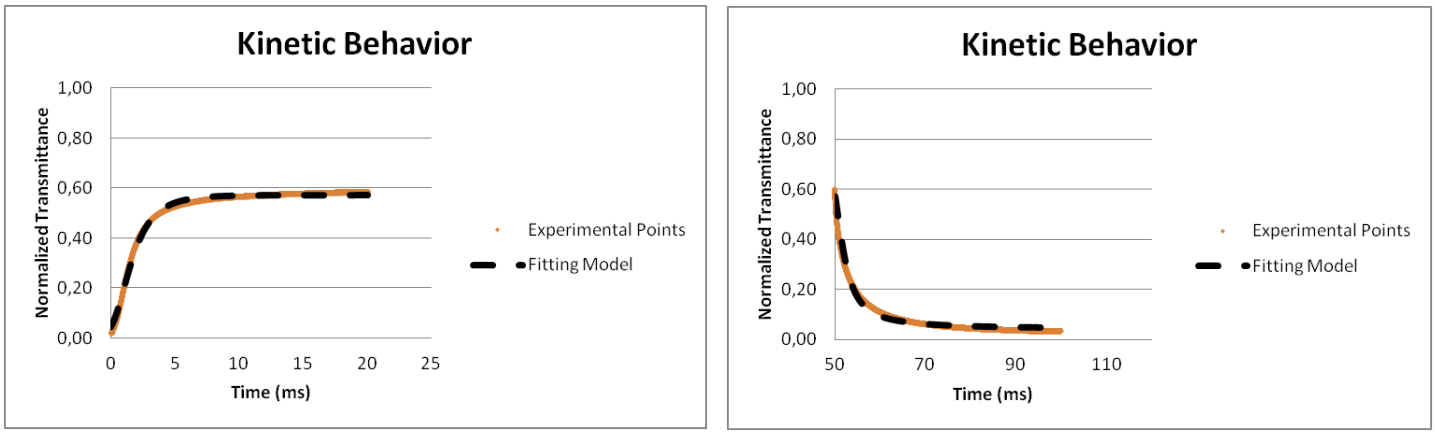

Graph 3.63 - Fitting model for the kinetic behavior of orientation and desorientation (30% POLYEGDMA$_{875}$/70% LC (%w/w) with 5%TX100 of the total solution)

- **POLYEGDMA$_{875}$(1%AIBN) + E7 with 30/70% (w/w) and 10%TX100 of the total solution**

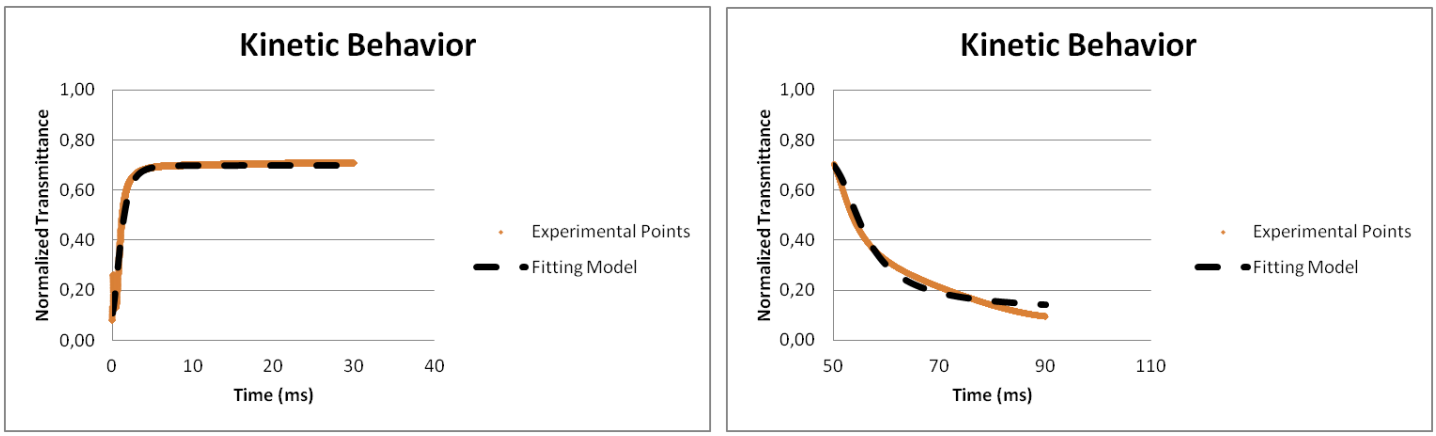

Graph 3.64- Fitting model for the kinetic behavior of orientation and desorientation (30% POLYEGDMA$_{875}$/70% LC (%w/w) with 10%TX100 of the total solution)

3.2.3 Conclusions

RESULTS FOR TRIEGDMA

- **TRIEGDMA (1%AIBN) + E7 with 30/70% (w/w) without TX100**

Table 3.16 - Determination of t_{10} and t_{90} for the PDLC film of 30 % TRIEGDMA/70% LC (%w/w) without TX100

V_{RMS} (V)	Maximum Transmittance	t_{90} (ms)	t_{10} (ms)
96	0,18	1,39	0,60
138	0,32	0,11	0,47
235	0,55	0,22	0,50
288	0,60	0,06	0,64

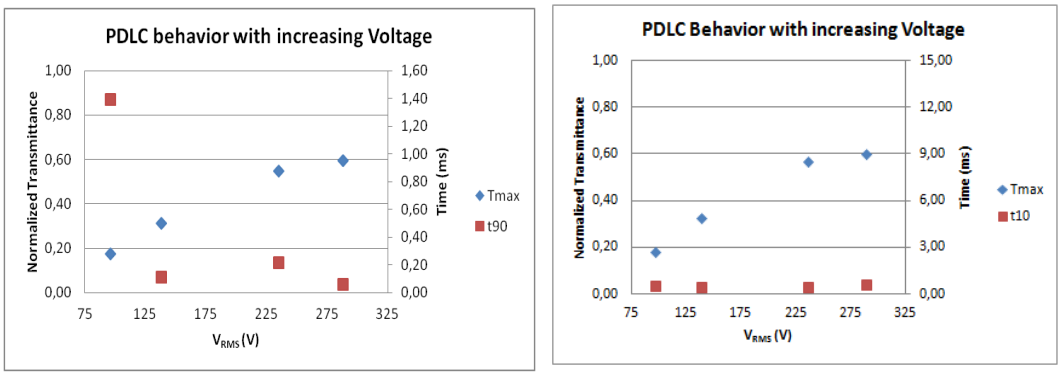

Graph 3.65 - PDLC orientation and desorientation behavior with increasing Voltage (30% TRIEGDMA/70% LC (%w/w) without TX100

- **TRIEGDMA (1%AIBN) + E7 with 30/70% (w/w) and 1%TX100 of the total solution**

Table 3.17 - Determination of t_{10} and t_{90} for the PDLC film of 70 % TRIEGDMA/30% LC (%w/w) with 1%TX100 do the total solution

V_{RMS} (V)	Maximum Transmittance	t_{90} (ms)	t_{10} (ms)
97	0,16	0,46	0,32
140	0,30	0,12	0,33
240	0,54	0,07	0,45
295	0,63	0,06	0,56

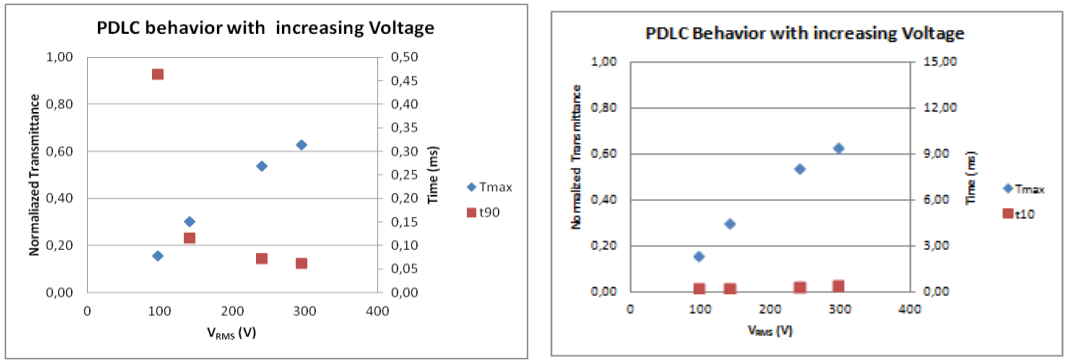

Graph 3.66 - PDLC orientation and desorientation behavior with increasing Voltage (30% TRIEGDMA/70% LC (%w/w) with 1%TX100 of the total solution

- **TRIEGDMA (1%AIBN) + E7 with 30/70% (w/w) and 5%TX100 of the total solution**

Table 3.18 - Determination of t_{10} and t_{90} for the PDLC films of 30% TRIEGDMA/ 70% LC (%w/w) with 5% TX100 of the total solutions

V_{RMS} (V)	Maximum Transmittance	t_{90} (ms)	t_{10} (ms)
54	0,31	32,43	0,81
72	0,62	10,43	1,35
92	0,71	3,56	1,55
105	0,73	0,48	1,55
142	0,77	0,47	1,95

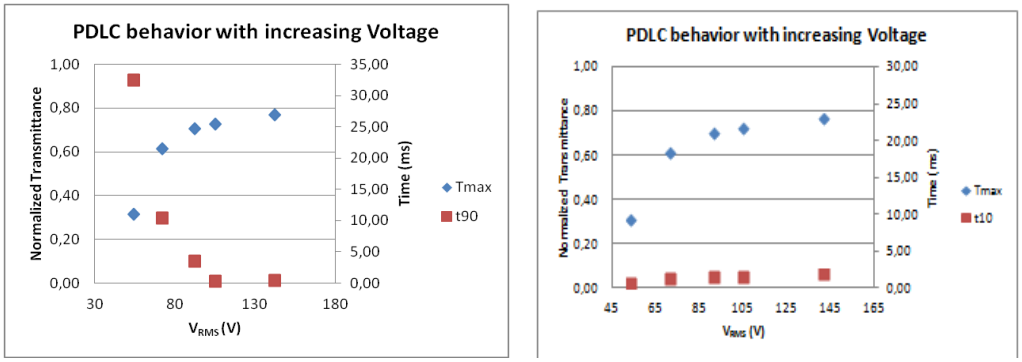

Graph 3.67 - PDLC orientation and desorientation behavior with increasing Voltage (30% TRIEGDMA/70% LC (%w/w) with 5%TX100 of the total solution

- **TRIEGDMA (1%AIBN) + E7 with 30/70% (w/w) and 10%TX100 of the total solution**

Table 3.19 Determination of t_{10} and t_{90} for the PDLC films of 30% TRIEGDMA/ 70% LC (%w/w) with 10% TX100 of the total solutions

V_{RMS} (V)	Maximum Transmittance	t_{90} (ms)	t_{10} (ms)
15	0,28	37,09	3,02
18	0,44	26,45	4,66
42	0,64	2,98	6,32
75	0,68	1,01	5,96
117	0,69	0,24	6,98

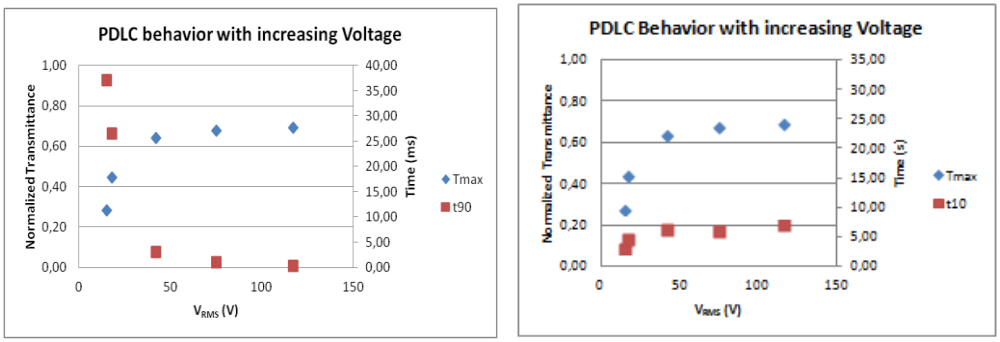

Graph 3.68- PDLC orientation and desorientation behavior with increasing Voltage (30% TRIEGDMA/70% LC (%w/w) with 10%TX100 of the total solution

RESULTS FOR POLYEGDMA$_{875}$

- **POLYEGMDA$_{875}$ (1%AIBN) + E7 with 30/70% (w/w) without TX100**

Table 3.20- Determination of t10 and t90 for the PDLC film of 30 %POLYEGDMA$_{875}$/70%LC (%w/w) without TX100

V_{RMS} (V)	Maximum Transmittance	t_{90} (ms)	t_{10} (ms)
24	0,27	10,30	12,84
41	0,49	4,95	11,23
54	0,61	3,17	10,49
91	0,75	0,52	9,98
135	0,80	0,52	10,44

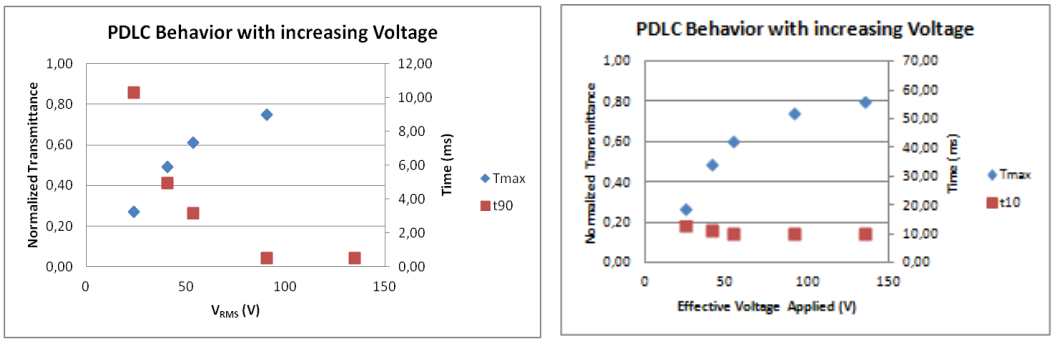

Graph 3.69 - PDLC orientation and desorientation behavior with increasing Voltage (30% POLYEGDMA$_{875}$/70% LC (%w/w) without TX100

- **POLYEGMDA$_{875}$ (1%AIBN) + E7 with 30/70% (w/w) and 1%TX100 of the total solution**

Table 3.21 - Determination of t10 and t90 for the PDLC film of 30 % POLYEGDMA$_{875}$/70% LC (%w/w) with 1%TX100 of the total solution

V_{RMS} (V)	Maximum Transmittance	t_{90} (ms)	t_{10} (ms)
21	0,12	15,74	2,72
39	0,43	10,76	11,33
70	0,65	2,52	13,91
95	0,77	0,73	12,58
140	0,85	0,73	10,90

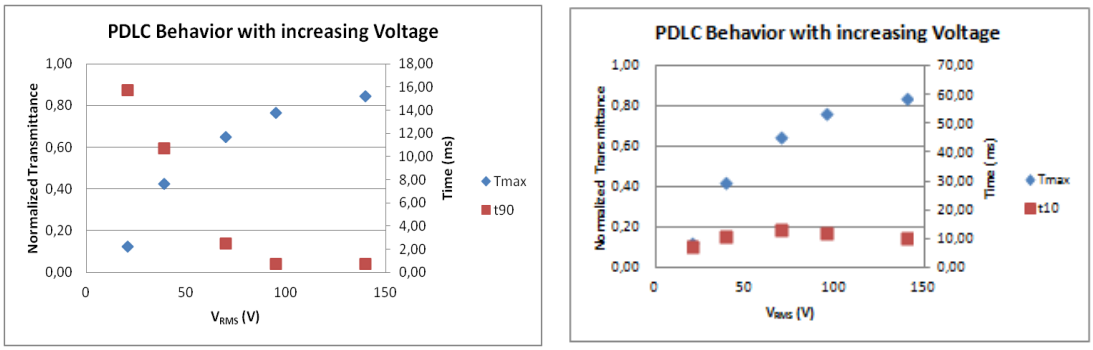

raph 3.70 - PDLC orientation and desorientation behavior with increasing Voltage (30% POLYEGDMA$_{875}$/70% LC (%w/w) with 1%TX100 of the total solution

- **POLYEGMDA$_{875}$ (1%AIBN) + E7 with 30/70% (w/w) and 5%TX100 of the total solution**

Table 3.22- Determination of t10 and t90 for the PDLC film of 30 %POLYEGMDA$_{875}$/70%LC (%w/w) without TX100

V_{RMS} (V)	Maximum Transmittance	t_{90} (ms)	t_{10} (ms)
19	0,21	32,69	20,05
39	0,60	6,30	14,21
67	0,77	1,52	9,84
91	0,83	0,52	7,95
136	0,86	0,19	7,29

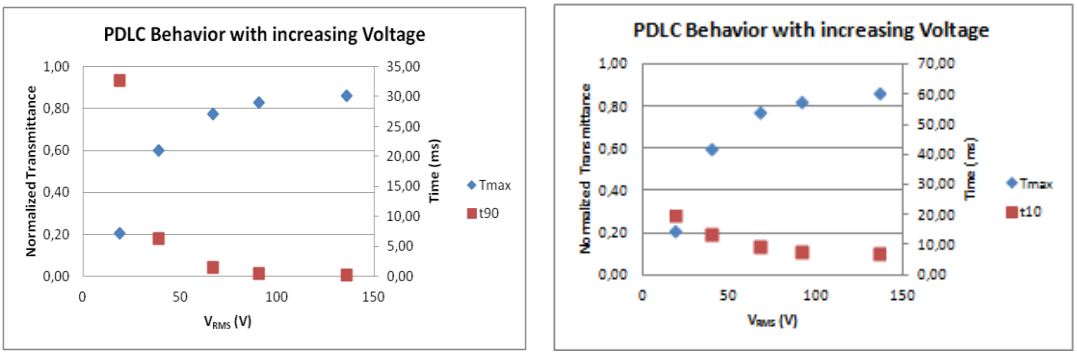

Graph 3.71 - PDLC orientation and desorientation behavior with increasing Voltage (30% POLYEGMDA$_{875}$/70% LC (%w/w) with 5%TX100 of the total solution

- **POLYEGMDA$_{875}$ (1%AIBN) + E7 with 30/70% (w/w) and 10%TX100 of the total solution**

Table 3.23 - Determination of t10 and t90 for the PDLC film of 70 % POLYEGDMA$_{875}$/30% LC (%w/w) with 10%TX100 of the total solution

V_{RMS} (V)	Maximum Transmittance	t_{90} (ms)	t_{10} (ms)
10	0,23	32,33	9,83
22	0,63	13,18	12,13
38	0,71	2,37	13,00
66	0,73	0,63	10,72
135	0,74	0,12	11,73

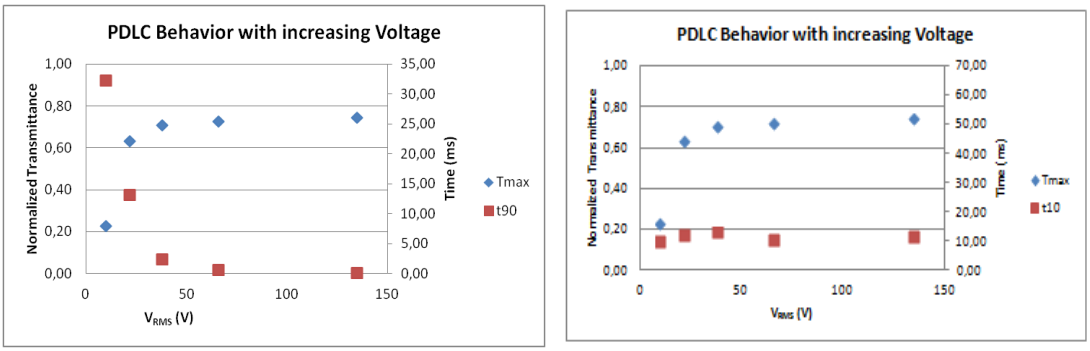

Graph 3.72 - PDLC orientation and desorientation behavior with increasing Voltage (30% POLYEGMDA$_{875}$/70% LC (%w/w) with 10%TX100 of the total solution

In order to understand if the amount of TX100 had an impact on the orientation and disorientation, an interpolation of the obtained values was performed to the same applied voltage of 100 V. The obtained values are on table 3.24 and 3.25.

Table 3.24 - Impact of the amount of TX100 on the kinetic of the PDLC film with polymer TRIEGDMA and E7 in the proportion of 30/70 (%w/w)

V_{RMS} (V)	Amount of TX100 (%w/w of total solution)	t90 (ms)	t10 (ms)	Maximum Transmittance
100	0	1,27	50,55	0,19
	1	0,44	50,42	0,17
	5	1,67	51,44	0,72
	10	0,55	55,39	0,70

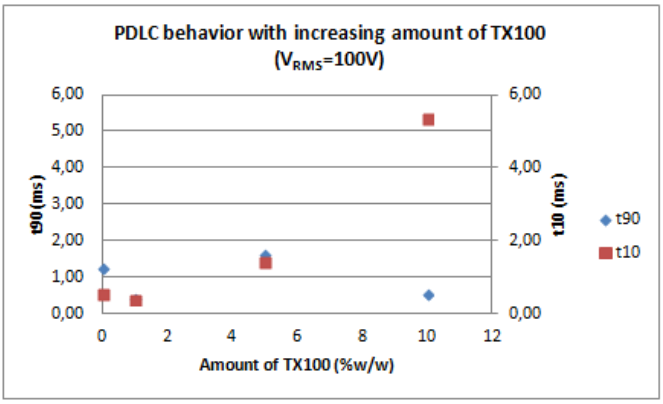

Graph 3.73 - PDLC behavior with increasing amount of TX100 for PDLC film with TRIEGDMA and E7 in the proportion of 30/70 (%w/w)

Table 3.25 - Impact of the amount of TX100 on the kinetic of the PDLC film with polymer $POLYEGDMA_{875}$ and E7 in the proportion of 30/70 (%w/w)

V_{RMS} (V)	Amount of TX100 (%w/w of total solution)	t90 (ms)	t10 (ms)	Maximum Transmittance
100	0	0,52	61,00	0,76
	1	0,73	61,29	0,78
	5	0,46	61,87	0,84
	10	0,38	61,48	0,73

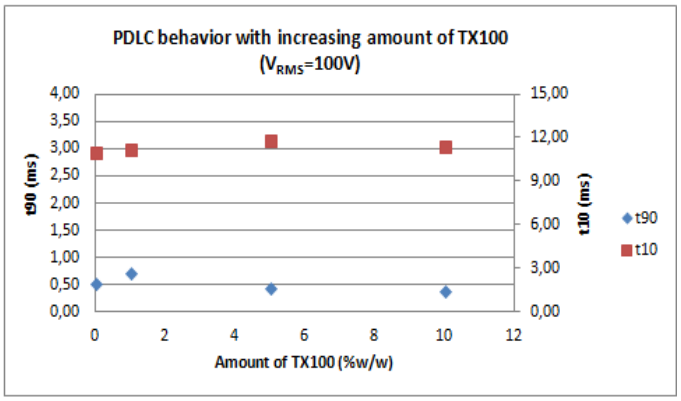

Graph 3.74 - PDLC behavior with increasing amount of TX100 for PDLC film with polymer $POLEGDMA_{875}$ and E7 in the proportion of 30/70 (%w/w)

From the analysis of the dynamic results it is possible to conclude that with increasing applied field the maximum transmittance of the film increases until saturation is reached, which means that from a certain applied voltage the nematic director in the sample is totally orientated. Also, with increasing applied voltage the orientation time (t_{90}) decreaes. On one hand, considering a constant applied voltage of 100 V it is possible to conclude that the orientation time is independent on the amount of TX100 in both polymers. On the ohter hand, the disorientation time does not change with the increase of the applied voltage but increases with the amount of TX100, in the case of polymer TRIEGDMA.These observations lead us to consider that the orientation process it dominated by the applied electric field, as also shown by t_{90} which decreases with the increase of the applied voltage, but is insensitive to the presence of the surfactant. The disorientation time, in the case of polymer POLYEGDMA$_{875}$, is independent of the amount of TX100, unlike the polymer TRIEGDMA where the addition of a surfactant causes an increase on this time. It is possible to understand these results considering that the addition of TX100 causes a weakening of the forces responsable to bring the director back to its original orientation. In the case of TRIEGDMA the addition of the surfactant produces a more evident effect than in POLYEGDMA$_{875}$. We assign this difference in behavior to the characteristic polymeric matrix of each polymer. The network of TRIEGDMA, being tighter, gives rise to a stronger influence of the LC-polymer interface over the bulk LC in the LC rich regions. In average, the LC molecules in the POLYEGDMA$_{875}$ network, do not feel the anchorage force of the polymer wall as strongly as the LC molecules in the TRIEGDMA network. Therefore, the previous results suggest that the presence of TX100, in the case of TRIEGDMA, decreases the anchorage force while in the case of POLYEGDMA$_{875}$ the addition of TX100 is less significant. In order to quantify the dynamic behavior of the system, the fitting model previously described was used, yielding the following values for the most significant parameters.

Table 3.26 - Parameter values from the Fitting Model

E7 (%w/w)	Polymer (%w/w)	%TX100 (%w/w) of the total solution	V_{RMS} (V)	K (Pa)	γ (Pa.s)	a1
70	TRIEGDMA (30)	1	240	652	0,13	318
		5	72	268	0,20	1011
		10	42	26	0,39	1374
	POLYEGDMA$_{875}$ (30)	1	39	103	0,24	423
		5	39	35	0,25	832
		10	38	18	0,24	540

It is possible to conclude that K has a tendency to decrease with the increasing amount of TX100, with a bigger impact on the case of TRIEGDMA. Since this parameter translates the interaction between the LC and the polymer matrix, it is possible to conclude that with the increase of amount of surfactant, the anchoring force between the LC and the polymer matrix is

reduced. Nevertheless, the value of K is always lower for polymer POLYEGDMA$_{875}$ than for TRIEGDMA; this demonstrates that the anchorage force between the LC molecules and the polymeric matrix is always lower in polymer POLYEGDMA$_{875}$ than in polymer TRIEGDMA, possibly due to the fact that this polymer presents a tighter polymeric matrix. In the case of TRIEGDMA, the presence of surfactant acts also as an impurity in the LC probably decreasing its order and in that way increasing its effective viscosity. In the case of POLYEGMDA$_{875}$, the network is larger, meaning that the presence of the surfactant on the boundary regions has a smaller influence on the dynamic behaviour of the microdomains.

Considering αR^6 and $\alpha = \frac{N_T}{V_T}$ with N_T total number of diffusers and V_T total system volume then:

$$\alpha R^6 = \frac{N_T}{V_T} R^6 = \frac{N_T}{V_T} (R^3)^2$$

As the microdomain were assumed to be spherical then $V = \frac{4}{3}\pi R^3 \Leftrightarrow R^3 = \frac{V}{\frac{4}{3}\pi}$,where V represents the total volume of each liquid crystal microdomain the previous equation can be rewritten as:

$$\alpha R^6 = \frac{N_T}{V_T} \left(\frac{V}{\frac{4}{3}\pi} \right)^2$$

The total volume of all the LC region is given by $V_{LC} = N_T V \Rightarrow V = \frac{V_{LC}}{N_T}$ then:

$$\alpha R^6 = \frac{N_T}{V_T} \left(\frac{V}{\frac{4}{3}\pi} \right)^2 = \frac{N_T}{V_T} \frac{1}{\left(\frac{4}{3}\pi\right)^2} \left(\frac{V_{LC}}{N_T} \right)^2$$

$$\alpha R^6 = \frac{{V_{LC}}^2}{V_T \left(\frac{4}{3}\pi\right)^2} \frac{1}{N_T}$$

Once $a_1 = \alpha d \frac{1}{2} \frac{8\pi}{3} \left(\frac{2\pi}{\lambda}\right)^4 R^6 \Rightarrow \alpha R^6 = \frac{a_1}{d \frac{1}{2} \frac{8\pi}{3} \left(\frac{2\pi}{\lambda}\right)^4} = A' a_1$, then

$$A' a_1 = \frac{{V_{LC}}^2}{V_T \left(\frac{4}{3}\pi\right)^2} \frac{1}{N_T}$$

Therefore, it is possible to conclude that with the increasing amount of TX100, the value of a_1 in the case of TRIEGDMA increases which means that the number of diffusers decrease and consequently, their volume increases. In particularly from 1% TX100 to 10%TX100, the value increases substantially, which is in concordance with the sudden increase on the PME. In the case of POLYEGMDA$_{875}$ significative fluctuations are found in the values, indicating they are affected by a significative error, within this error the parameter a_1 seems to be constant.

4. Final Remarks

In the present work, several PDLC films were studied focusing the study on the PDLC films with 30% monomer (having 1% of AIBN as initiator), 70% liquid crystal, without TX100 and with increasing amounts of TX100.

The addition of TX100 will reduce the anchorage force between the liquid crystal and the polymeric matrix, and so,with the increase of the amount of TX100, there is an increase on the permanent memory effect and a decrease on the E90. This is also proved through the kinetic analysis, since the elastic constant, K, that translates the interaction between the LC and the polymer matrix, also decreases with the increase amount of TX100.

Also the increase on the permanent memory effect, on the case of TRIEGDMA, can be justified by the value of the parameter a_1 from the kinetic model that increases substantially. This parameter is inversely proportional to the number of microdomains but directly proportional to its volume, meaning that the number of microdomains decreases and consequently its volume increases. Therefore, as referred above, the size of microdomains is an important factor for the PDLC performance. Higher microdomains have, in theory, higher permanent memory effects. Particularly, increasing the amount of TX100 from 1% to 10%TX100, the value of a_1 increases considerably, which is in concordance with the sudden increase on the PME.

The increase of this additive also decreases the original TNI of the nematic liquid crystal. This can be explained considering that, not only at this temperature, TX100 behaves as an isotropic liquid, but also that its addition will increase the viscosity of the mixture. This is justified through DSC and POM techniques, where this decrease can be seen, and also through the kinetic analysis. Through the kinetic study there is an increase on the value of the rotational viscosity, γ, with the increase of TX100, which can mean that the TX100 is not only found in the interface between the LC and the polymeric matrix, but also mixed with the LC in the case of TRIEGDMA. Therefore, TX100 will increase the entropy of the mixture and its viscosity, decreasing the nematic isotropic original temperature of the LC.

From the SEM analysis, for an amplification of 5000 times, the increase amount of TX100 does not seem to influence significantly the structure of the polymer matrix.

5. References

[1] Seynuk, B. (2006), *Liquid Crystals: a Simple View on a Complex Matter*. Retrieved from Kent State University SPIE Student Chapter: http://dept.kent.edu/spie/liquidcrystals/

[2] Andrienko, Denis (2006), *Introduction to liquid crystals*, International Max Planck Research School.

[3] Nunes, A.M. (2001), *Estudo por DRS de um cristal líquido sobre uma matrix polimérica*. Internship report, Lisboa.

[4] Collings, P.J.(2002), *Liquid Crystals: Nature's Delicate Phase of Matter*, 2 ed, Princeton University.

[5] Neto, A. M. F. S. R. A., *The Physics of Lyotropic Liquid Crystals: Phase Transitions and Structural*, Oxford University Press: 2005.

[6] Drzaic, P.S (1998), *Liquid Crystal Dispersions*. Singapore: World Scientific.

[7] Justice, R.S. (2006). *Interface morphology and phase separation in polymer dispersed liquid crystal (PDLC) composites*. Master Thesis, University of Cincinnati.

[8] Han, J. (2006), *Study of Memory Effects in Polymer Dispersed Liquid Crystal Films*. Journal of the Korean Physical Society, 49, 1482-1487.

[9] Coates, D. (1995), *Polymer-Dispersed Liquid Crystals, Journal of Materials Chemistry*, 5, 2063-2072.

[10] Yokoyama, H. (1988) , *Surface Anchoring of Nematic Liquid Crystals.* Mol. Cryst. liq. Cryst. 165, 265-316.

[11] Andy, F. Y. G.; Tsung, C. K.; Mo, H. L. (1992) , *Polymer Dispersed Liquid crystal Films with memory characteristics.* J. Appl.Phys. 31, 3366-3369.

[12] Rumiko, Y.; Susumu, S. (1992) , *Highly transparent memory states by phase transition with a field in polymer dispersed liquid crystal films*. J. Appl. Phys., 31, 254-256.

[13] Brás, A.R.E, et al. (2008), *Characterization of a Nematic Mixture by Reversed-Phase HPLC and UV Spectroscopy: Application to Phase Behavior Studies in Liquid Crystal-CO_2 Systems*. Liquid Crystal, 35, 429-441.

[14] Chung, David B.; Tsuda, Hideaki; Chida, Hideo, Mochizuki, Akihiro (1997) ; *Effects and Structural Model of Surfactants on the Hysteresis Behavior of Polymer Dispersed Liquid Crystals*, 81-87.

[15] Barros M.T; Mouquinho A; Petrova K.; Saavedra M.; Sotomayor J. (2001), Cent. Eur. J. Chem., 9, 557-566.

[16] Mouquinho, A.; Saavedra M.; Maiau, A.; Petrova, K.; Barros, M. T.; Figuerinhas, J.L.; Sotomayor, J- (2011), *Mol. Cryst. Liq. Crystal*, 542,132 / [654]-140[662].

[17] Melo, Carlos Alberto da Silva Ribeiro (2009). *The additive effects in Matrix Dispersed Liquid Crystals*. Dissertação para obtenção de grau de Mestre em Engenharia Química e Bioquímica (Universidade Nova de Lisboa - Faculdade de Ciências e Tecnologias).

[18] Instec Inc. http://www.instec.com/, 2011

[19] Colombani, D. (1997). *Chain-growth control in free radical polymerization*. Prog. Polym. Sci. , 22, 1649-1720.

[20] http://cnx.org/content/m38343/latest/?collection=col10699/latest.

[21] Nunes, D.; *Cenimat.* Private Communication.

[22] César, Ana Sofia Reboredo César(2011). *Liquid Crystal and PDLC memory effect*. Dissertação para a obenção do grau de Mestre em Engenharia Química e Bioquímica (Universidade Nova de Lisboa - Faculdade de Ciências e Tecnologias).

[23] http://plc.cwru.edu/tutorial/enhanced/files/lc/phase/phase.htm.

[24] Plaza, Maria Teresa Viciosa (2007). *Molecular mobility of n-ethylene glycol dimethacrylate glass formers upon free radical polymerization*. Dissertation presented to obtain a PhD. Degree in Chemical Physics (Universidade Nova de Lisboa - Faculdade de Ciências e Tecnologias).

[25] Yakacki, C.M.; Shandas R.; Safranski, D.; Ortega A. M.; Sassaman K.; Gall K.; (2008). *Biocompatible Shape-Memory Polymer Networks*. 2429.

[26] Bookeun, O.; Jung, W. I.; Kim D.; Rhee, H.; (2002). *Preparation of UV Curable Gel Polymer Electrolytes and Their Electrochemical Properties*, 23, 684-685.

[27**]** Doane, J. W.; Wu, B.; Erdmann, J.H.; Doane W.; (2006). *PDLC shutters: where has this technology gone?,* Kent State University, Liquid Crystal Institute Department of Physics, 33, 1313-1314.

[28] Wu, B.; Erdmann, J.H.; Doane, J.W.; (2006). Response times and voltages for PDLC light shutter, Kent State University, Liquid Crystal Institute Department of Physics, 33, 1315-1322.

[29] Melo, Carlos Alberto da Silva Ribeiro (2009). *The additive effects in Matrix Dispersed Liquid Crystals*. Dissertação para obtenção de grau de Mestre em Engenharia Química e Bioquímica (Universidade Nova de Lisboa - Faculdade de Ciências e Tecnologias).

[30] Silva, Cátia João Borges (2011). *Efeito da velocidade de polimerização na eficiência de PDLCs*. Dissertação para obtenção de grau de Mestre em Engenharia Química e Bioquímica (Universidade Nova de Lisboa - Faculdade de Ciências e Tecnologias).

[31] Vicari, L (2003). *Optical Applications of Liquid Crystals*, Institute of Physics - Series in Optics and Optoelectronics.

[32] Ferreira, José Carlos de Gouveia (2004), *Estudo da degradabilidade de poliestireno modificado quimicamente*, Dissertação para obtenção de grau de Mestre em Química (Universidade do Minho).

[33] Martis, A. F. (1991);. *Os Cristais Líquidos*. Colóquio/Ciências, FCG, 7, 253.

[34] Yokoyama, H. (1988) , Surface *Anchoring of Nematic Liquid Crystals.* Mol. Cryst. liq. Cryst. 165, 265-316.

[35] Andy, F. Y. G.; Tsung, C. K.; Mo, H. L. (1992) , *Polymer Dispersed Liquid crystal Films with memory characteristics.* J. Appl.Phys. 31, 3366-3369.

[36] Rumiko, Y.; Susumu, S. (1992) , *Highly transparent memory states by phase transition with a field in polymer dispersed liquid crystal films*. J. Appl. Phys., 31, 254-256.

[35] Maiau, Alexandre Miguel Duque Martins (2009), *Preparation and Characterization of New PDLCs*, Dissertação para obtenção de grau de Mestre em Engenharia Química e Bioquímica (Universidade Nova de Lisboa - Faculdade de Ciências e Tecnologias).

[37] Andrienko, D.(2006), *Introduction to liquid crystals*, International Max Planck Reserach Scool, Modeeling of soft matter.

[38] Kashima, M.; Cao, H.; Liu, H.; Meng, Q.; Wang, D.; Li, F.; Yang, H. (2001), *Effects of chain length of crosslinking agents on the electro-optical properties of polymer-dispersed liquid crystal films,* Deparment of Materials Physics and Chemistry.

[39] Jeong,E.H.; Sun, K. R.; Kang, M. C., Jeong, H. M.; Kim, B. H. (2009), *Memory effect of polymer dispersed liquid crystal by hybridization with nanoclay*, National Core Research Center for Hybrid Materials Solutions; Department of Polymer Science and Engineering, Pusan National University; Department of Chemistry, University of Ulsan.

[40] Tsai, T.; Leem C.; Lin, M.; Lee, W. (2012), *Polymer-dispersed liquid crystal nanocomposites comprising montmorillonite clay modified by conducting pentamerous oligoaniline,* Journal of Materials Chemistry, 22, 13050.

[41] Hoppe, C. E., Galante, M. J., Oyanguren, P. A., & Williams, R. J. (2004). *Optical Properties of novel thermally switched PDLC films composed of a liquid crystal distributed in a thermoplastic/thermoset polymer blend*. Materials Science & Engineering C , 24, 591-594.

[42] Kremer, F., & Schönhals, A. (2003). *Broadband Dielectric Spectroscopy. Springer*

[43] Madhusudana, N. V. (2001). *Recent advances in thermotropic liquid crystals.* Current Science - Special section: soft condensed matter , 80, 1018-1025.

[44] Malik, P., & Raina, K. K. (2004). *Droplet orientation and optical properties of polymer dispersed liquid crystal composite films.* Optical Materials , 27, 613.

[45] Kim, B., & Woo, J. (2007). *Surfactant Effects on Morphology and Switching of Holographic PDLCs Based on Polyurethane Acrylates*. ChemPhysChem 8 , 175-180.

[46] Chênevert, R.; Pelchat, N.; Morin, P. (2009), *Lipase-mediated enantioselective acylation of alcohols with functionalized vinyl esters: acyl donor tolerance and applications.* Tetrahedron: Asymmetry, 20, 1191-1196.

[47] Lal, J.; Green, R. (1995), *The Preparation of Some Esters of Methacrylic Acid*. J. Org. Chem 1955, 20, 1030-1033.

[48] Slugovc, C.; Demel, S.; Riegler, S.; Hobisch, J.; Stelzer, F (2004)., *Influence of functional groups on ring opening metathesis polymerisation and polymer properties*. J. Mol. Cat. A, 213, 107-113.

6. Appendices

Appendix 1 - EO and POM studies

1. Polymer TRIEGDMA and LC in the proportion of 50/50 (%w/w) without TX100

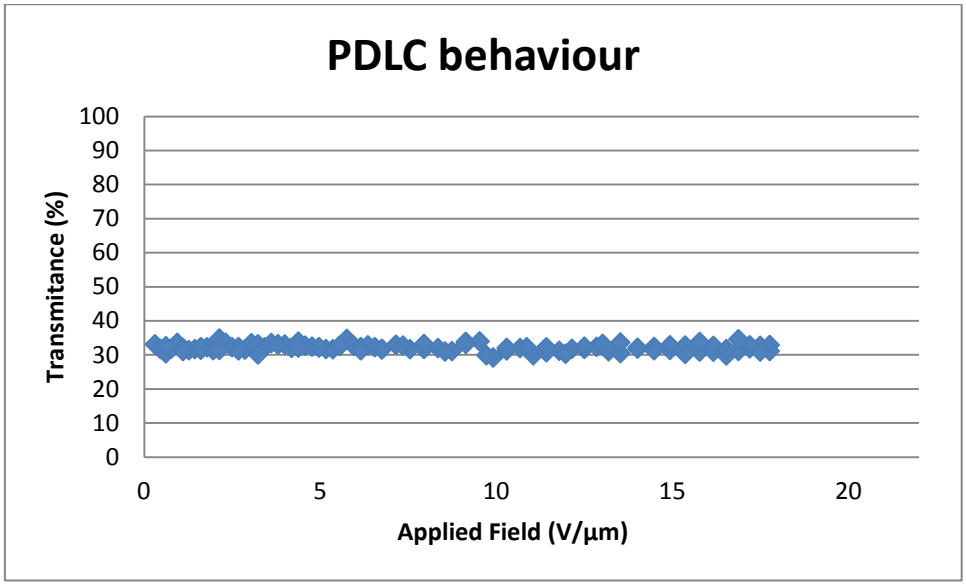

Graph 6.1 - EO response of the system polymer TRIEGDMA (1%AIBN) and LC in the proportion 50/50% (w/w) without TX100

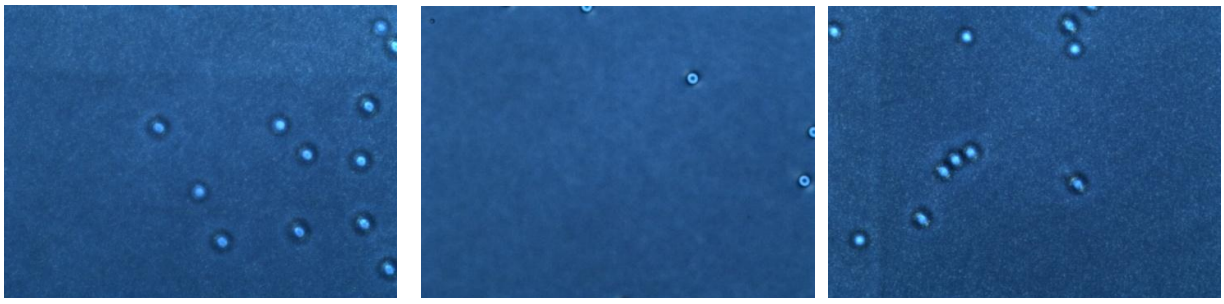

Before EO | After EO | After TNI

Figure 6.1 - POM micrograph for polymer TRIEGDMA (1%AIBN) and LC in the proportion 50/50% (w/w) without TX100

2. Polymer TRIEGDMA and LC in the proportion of 40/60 (%w/w) without TX100

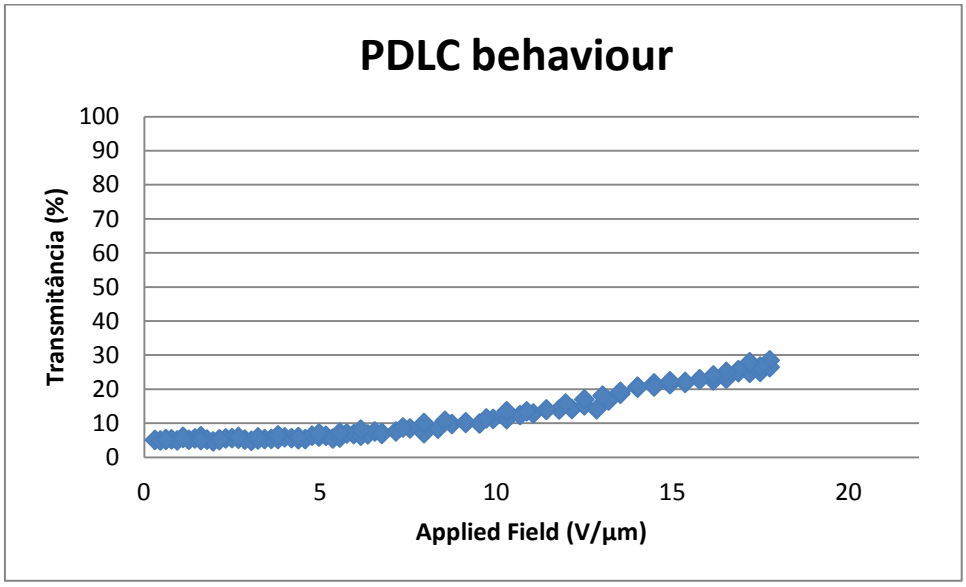

Graph 6.2- EO response of the system polymer TRIEGDMA (1%AIBN) and LC in the proportion 40/60% (w/w) without TX100

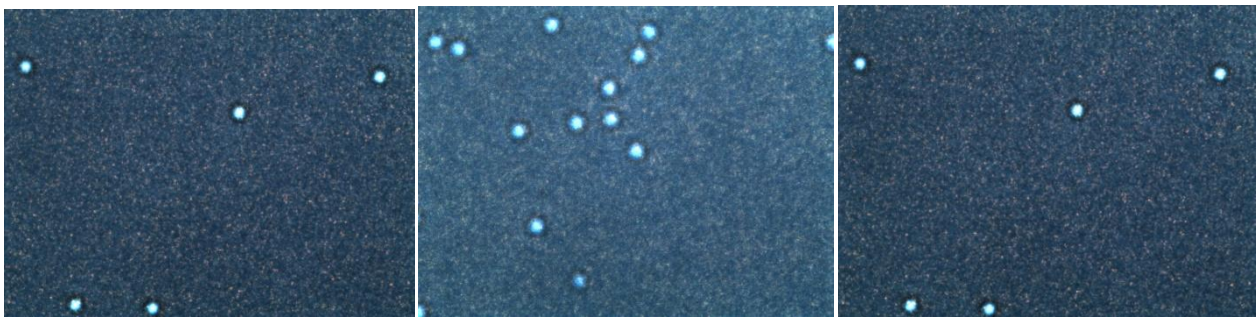

Before EO After EO After TNI

Figure 6.2 - POM micrograph for polymer TRIEGDMA (1%AIBN) and LC in the proportion 40/60% (w/w) without TX100

3. TRIEGDMA and LC in the proportion of 30/70 (%w/w) with 0,2% of TX100 of the total solution

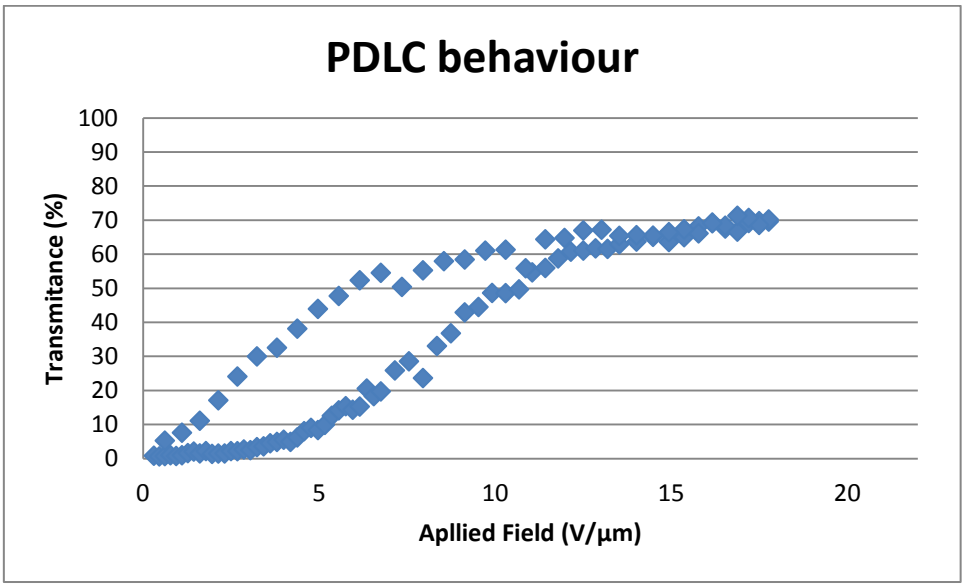

Graph 6.3 - EO response of the system polymer TRIEGDMA (1%AIBN) and LC in the proportion 30/70% (w/w) with 0,2% TX100 of the total solution

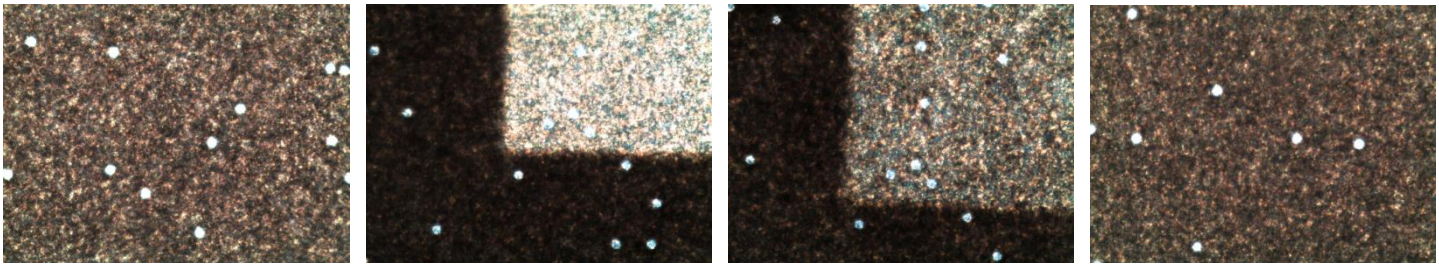

Figure 6.3 - POM micrograph for polymer TRIEGDMA (1%AIBN) and LC in the proportion 30/70% (w/w) with 0,2 TX100 of the total solution

4. TRIEGDMA and LC in the proportion of 30/70 (%w/w) with 2% of TX100 of the total solution

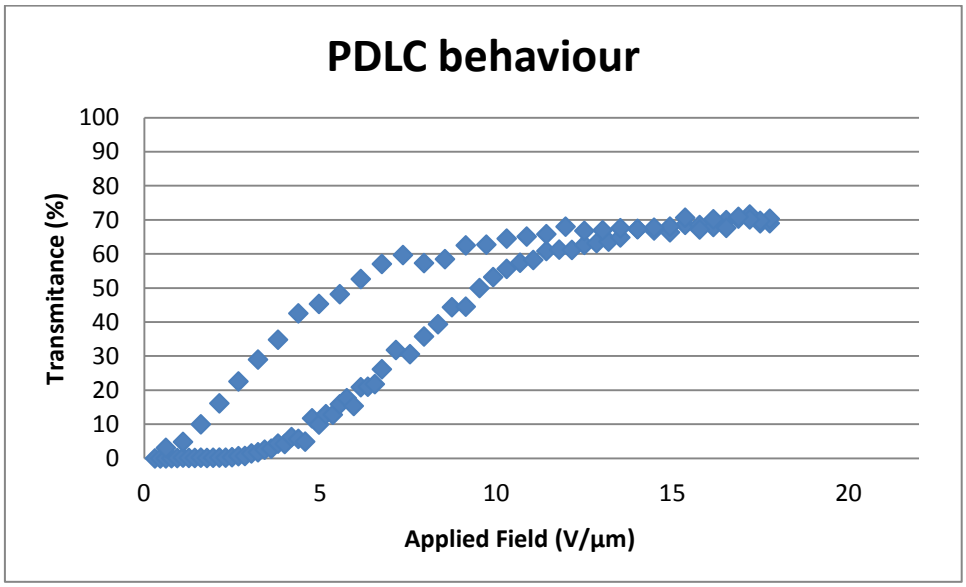

Graph 6.4 - EO response of the system polymer TRIEGDMA (1%AIBN) and LC in the proportion 30/70% (w/w) with 2% TX100 of the total solution

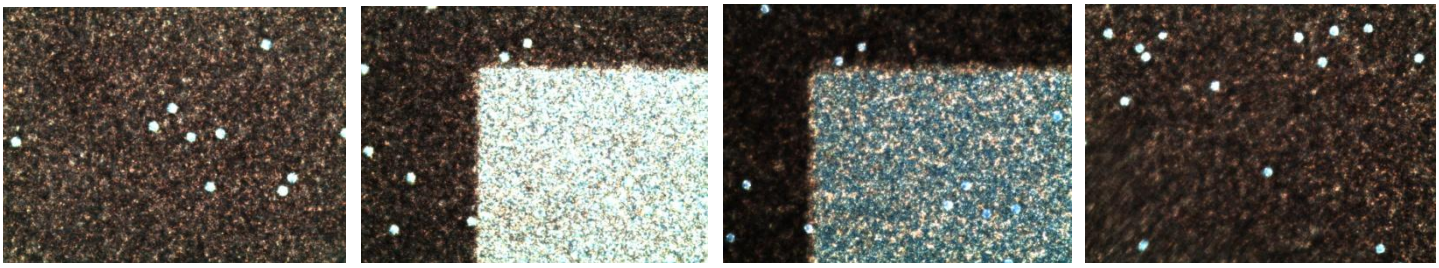

Before EO | After EO | After TNI | After TNI+stove

Figure 6.4- POM micrograph for polymer TRIEGDMA (1%AIBN) and LC in the proportion 30/70% (w/w) with 2% TX100 of the total solution

5. Polymer TRIEGDMA and LC in the proportion of 30/70 (%w/w) with 3% of TX100 of the total solution

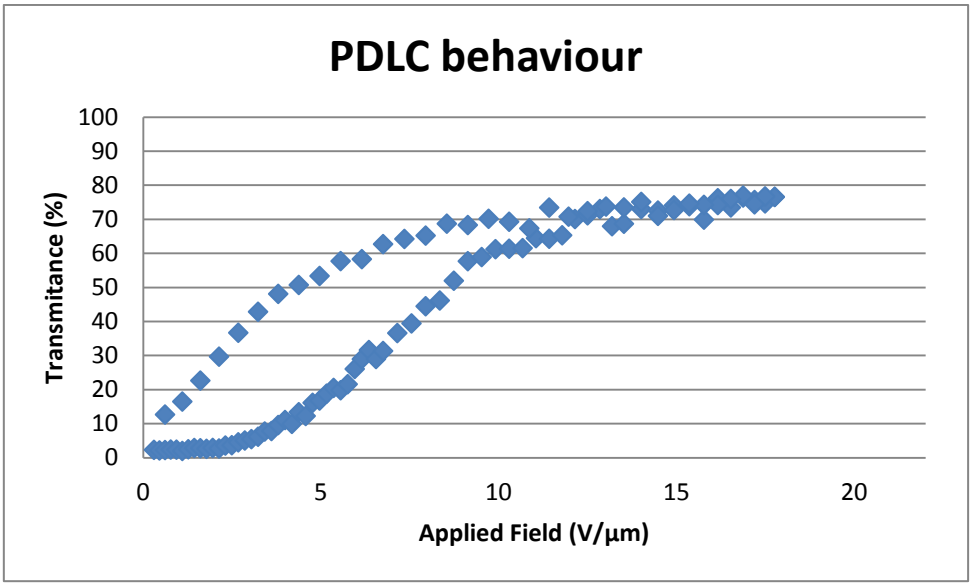

Graph 6.5- EO response of the system polymer TRIEGDMA (1%AIBN) and LC in the proportion 30/70% (w/w) with 3% TX100 of the total solution

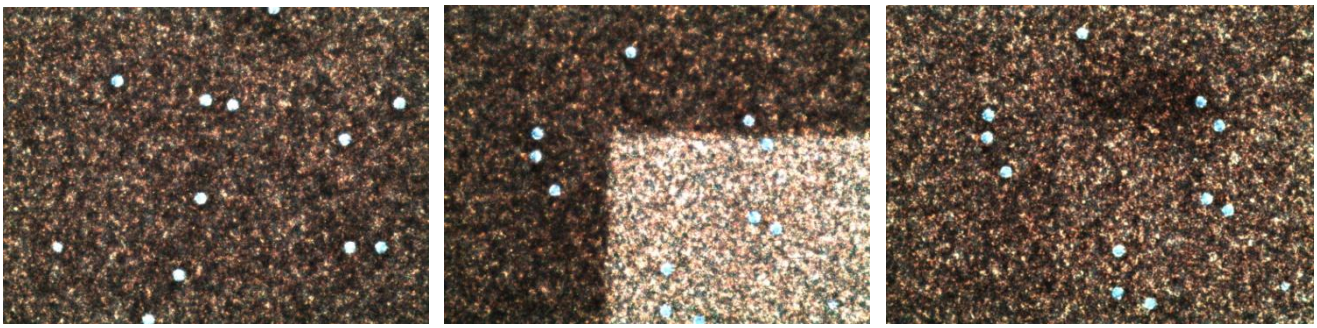

Before EO After EO After TNI

Figure 6.5 - POM micrograph for polymer TRIEGDMA (1%AIBN) and LC in the proportion 30/70% (w/w) with 3% TX100 of the total solution

6. Polymer TRIEGDMA and LC in the proportion of 20/80 (%w/w) without TX100

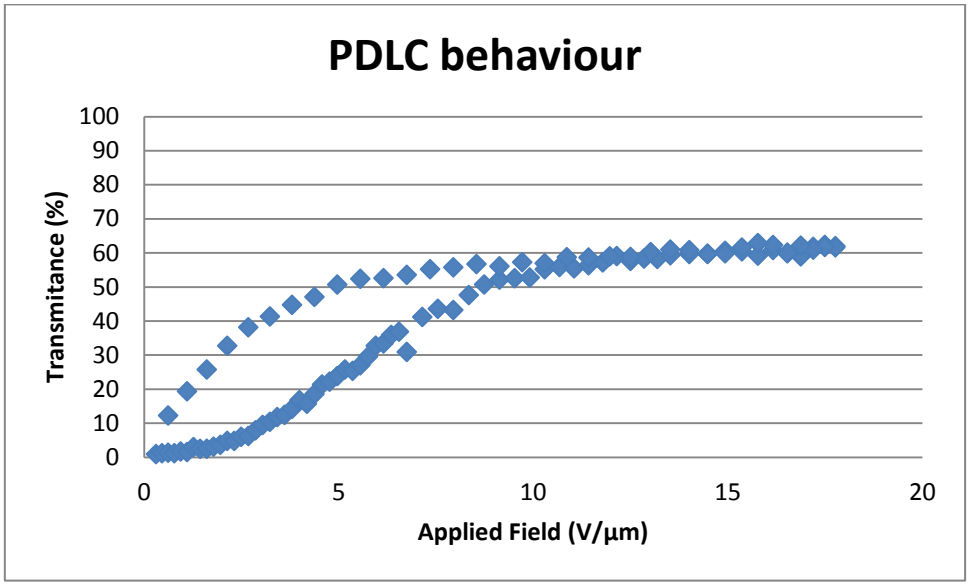

Figure 6.6 - EO response of the system polymer TRIEGDMA (1%AIBN) and LC in the proportion 20/80% (w/w) without TX100

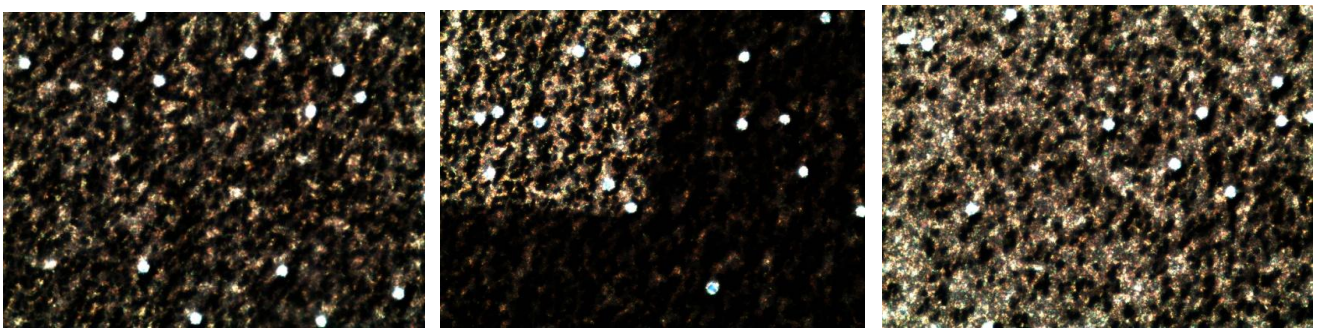

Before EO | After EO | After TNI

Figure 6.7 - POM micrograph for polymer TRIEGDMA (1%AIBN) and LC in the proportion 20/80% (w/w) without TX100

7. Polymer TRIEGDMA and LC in the proportion of 10/90 (%w/w) without TX100

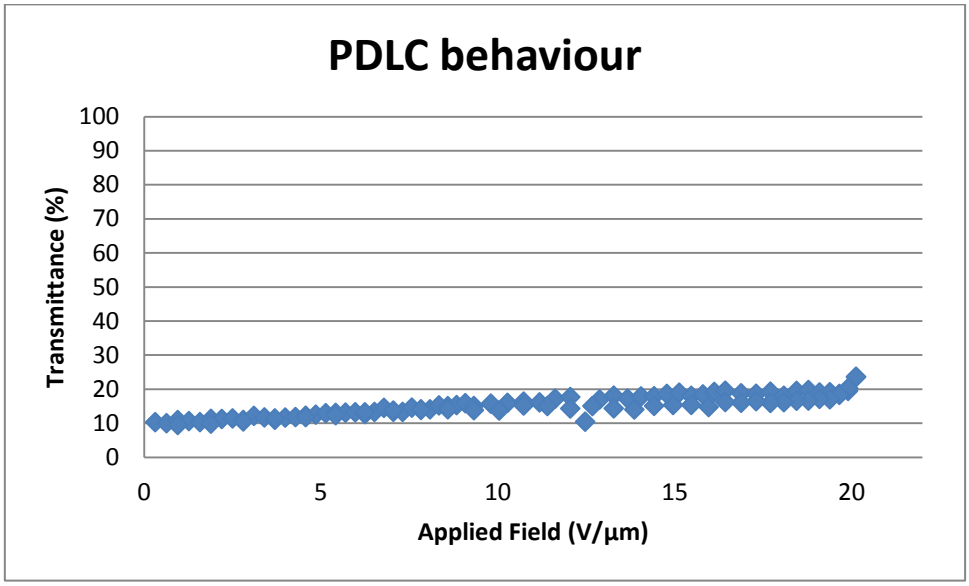

Graph 6.6 - EO response of the system polymer TRIEGDMA (1%AIBN) and LC in the proportion 10/90% (w/w) without TX100

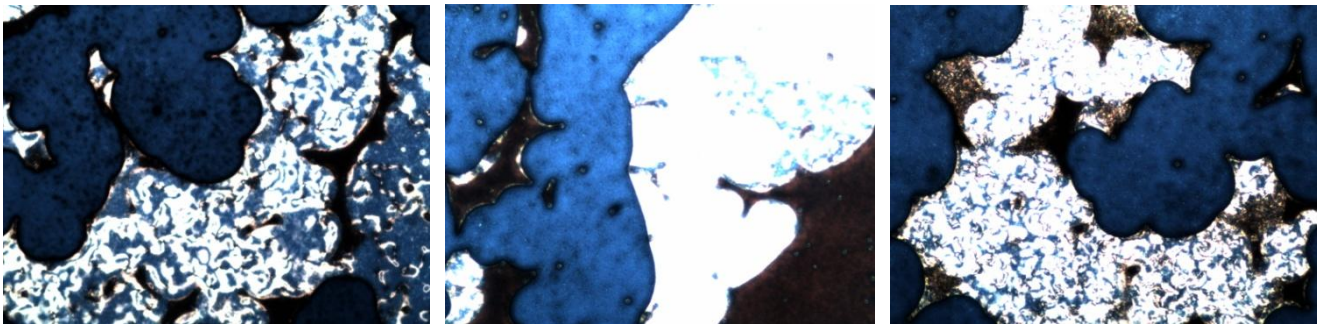

Before EO | After EO | After TNI

Figure 6.8 - POM micrograph for polymer TRIEGDMA (1%AIBN) and LC in the proportion 10/90% (w/w) without TX100

8. Polymer POLYEGDMA$_{875}$ and LC in the proportion of 50/50 (%w/w) without TX100

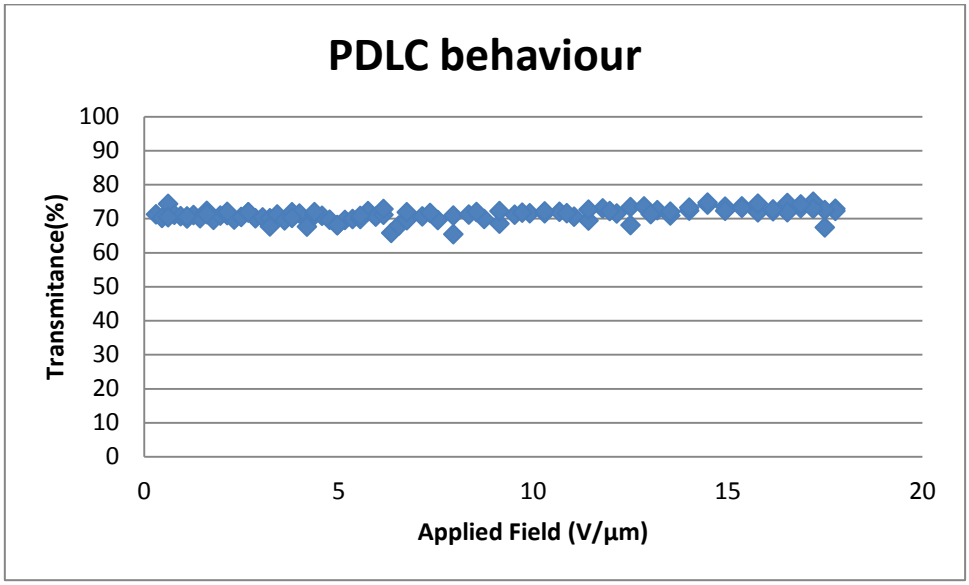

Graph 6.7 - EO response of the system polymer POLYEGMDA$_{875}$ (1%AIBN) and LC in the proportion 50/50% (w/w) without TX100

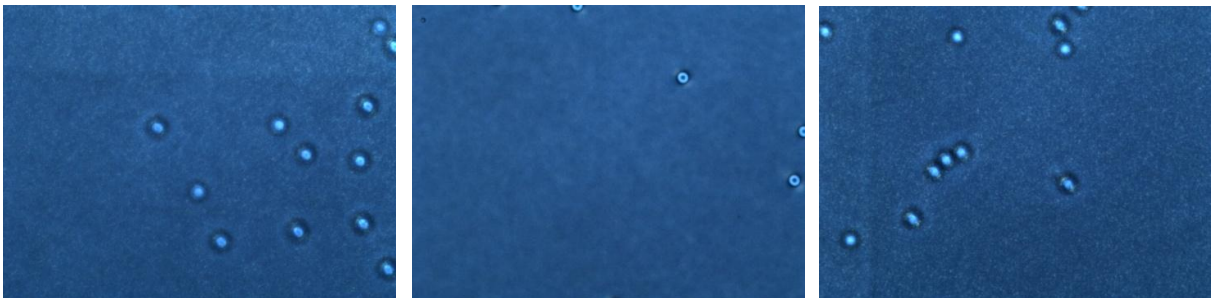

Before EO | After EO | After TNI

Figure 6.9 - POM micrograph for polymer POLYEGMDA$_{875}$ (1%AIBN) and LC in the proportion 50/50% (w/w) without TX100

9. Polymer$POLYEGDMA_{875}$ and LC in the proportion of 40/60 (%w/w) without TX100

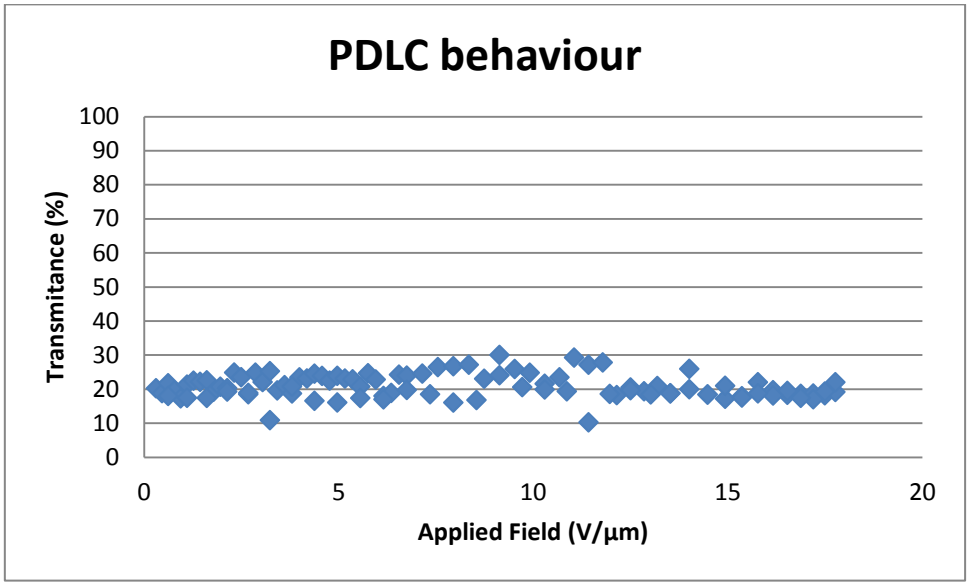

Graph 6.8 - EO response of the system polymer $POLYEGMDA_{875}$ (1%AIBN) and LC in the proportion 40/60% (w/w) without TX100

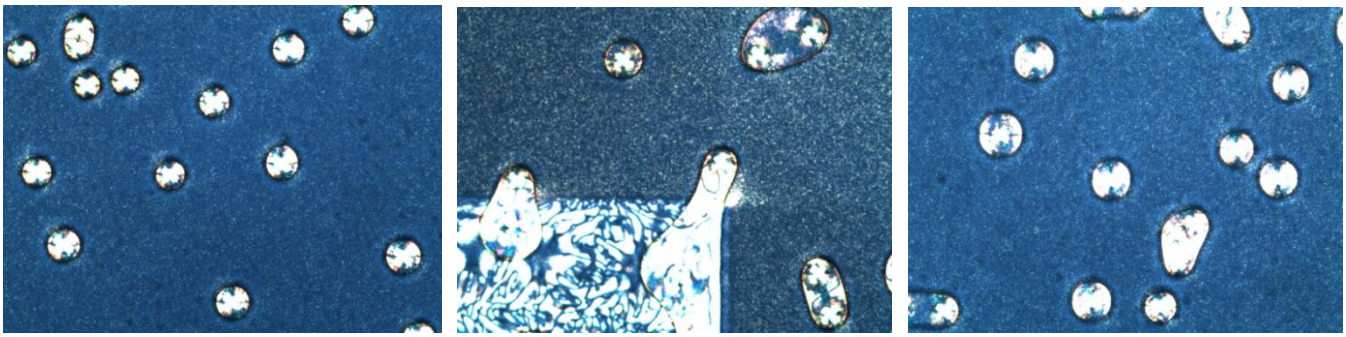

Before EO | After EO | After TNI

Graph 6.9 - POM micrograph for polymer $POLYEGDMA_{875}$ (1%AIBN) and LC in the proportion 40/60% (w/w) without TX100

10. Polymer POLYEGDMA$_{875}$ and LC in the proportion of 30/70 (%w/w) with 0,2% of TX100 of the total solution

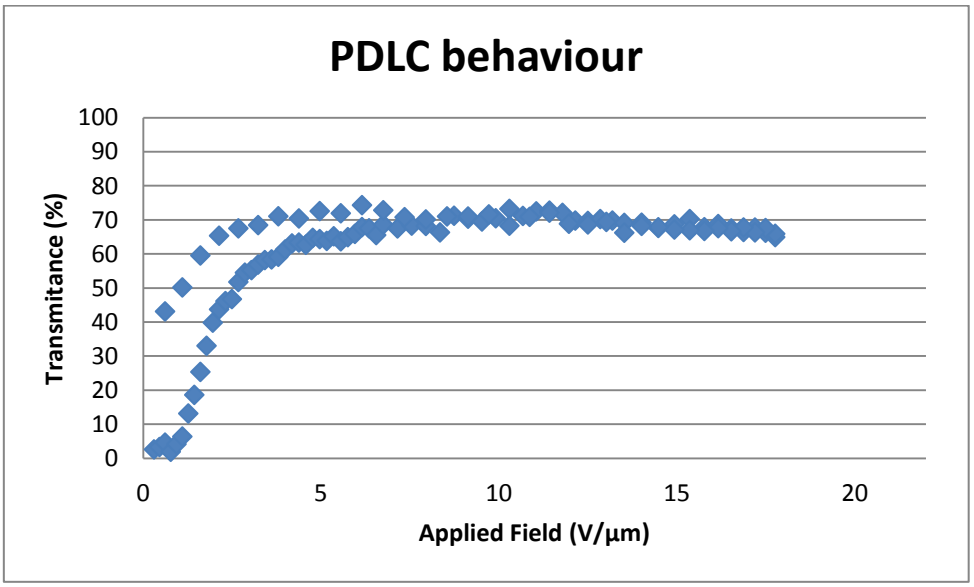

Graph 6.10 - EO response of the system polymer POLYEGMDA$_{875}$ (1%AIBN) and LC in the proportion 30/70% (w/w) with 0,2%TX100 of the total solution

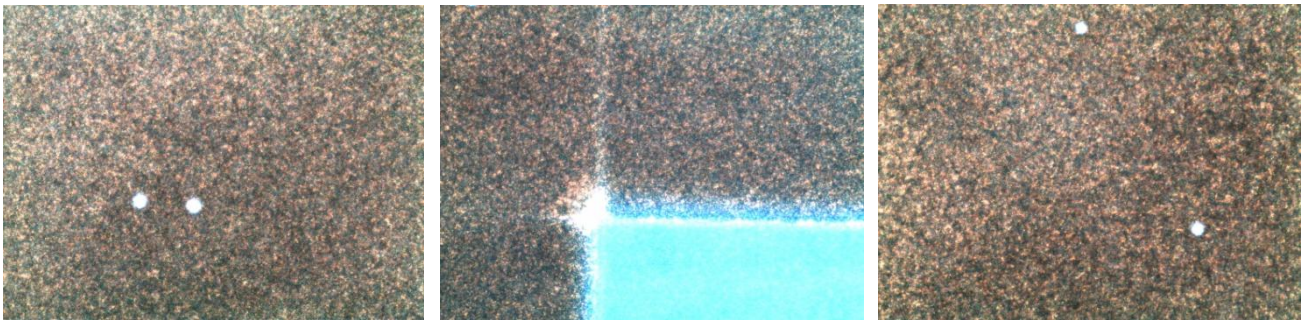

Before EO | After EO | After TNI

Figure - 6.10 POM micrograph for polymer POLYEGDMA$_{875}$ (1%AIBN) and LC in the proportion 30/70% (w/w) with 0,2%TX100 of the total solution

11. Polymer POLYEGDMA$_{875}$ and LC in the proportion of 30/70 (%w/w) with 2% of TX100 of the total solution

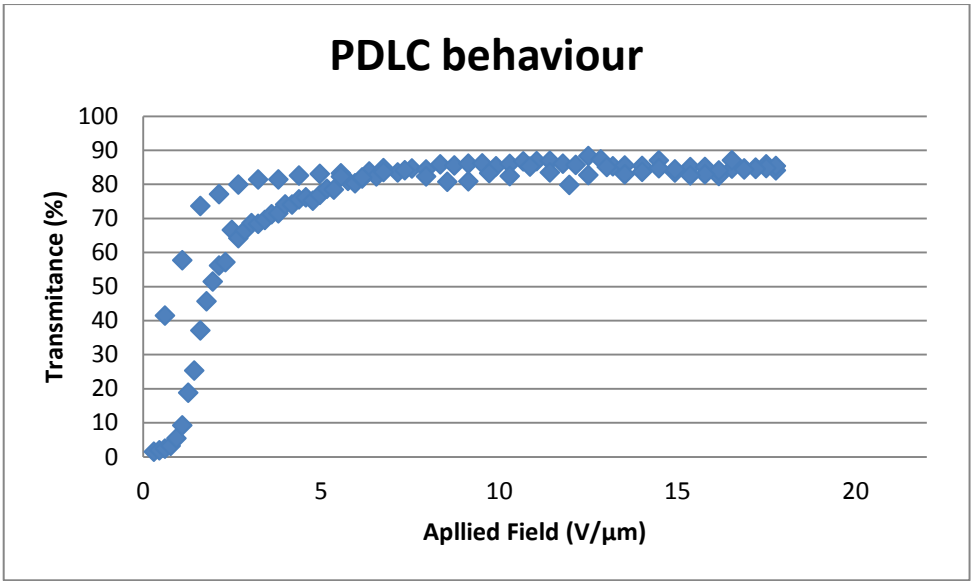

Graph 6.11 -- EO response of the system polymer POLYEGMDA$_{875}$ (1%AIBN) and LC in the proportion 30/70% (w/w) with 2%TX100 of the total solution

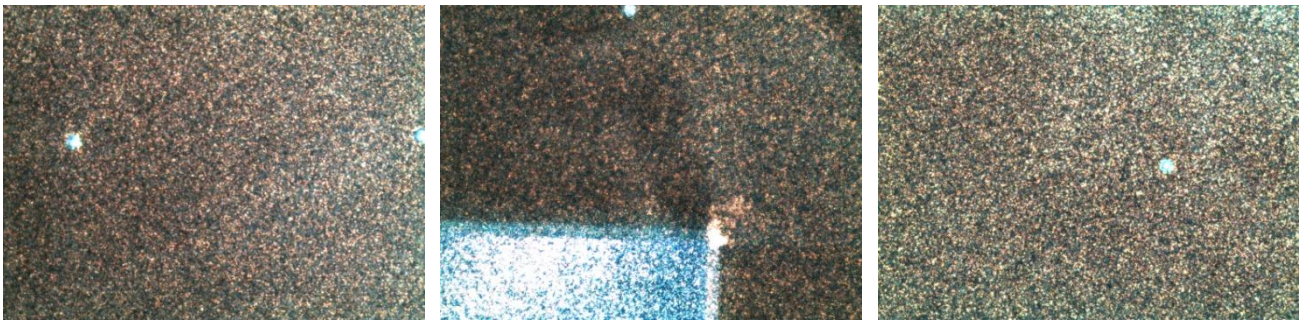

Before EO | After EO | After TNI

Figure 6.11 - POM micrograph for polymer POLYEGDMA$_{875}$ (1%AIBN) and LC in the proportion 30/70% (w/w) with 2%TX100 of the total solution

12.Polymer POLYEGDMA$_{875}$ and LC in the proportion of 30/70 (%w/w) with 3% of TX100 of the total solution

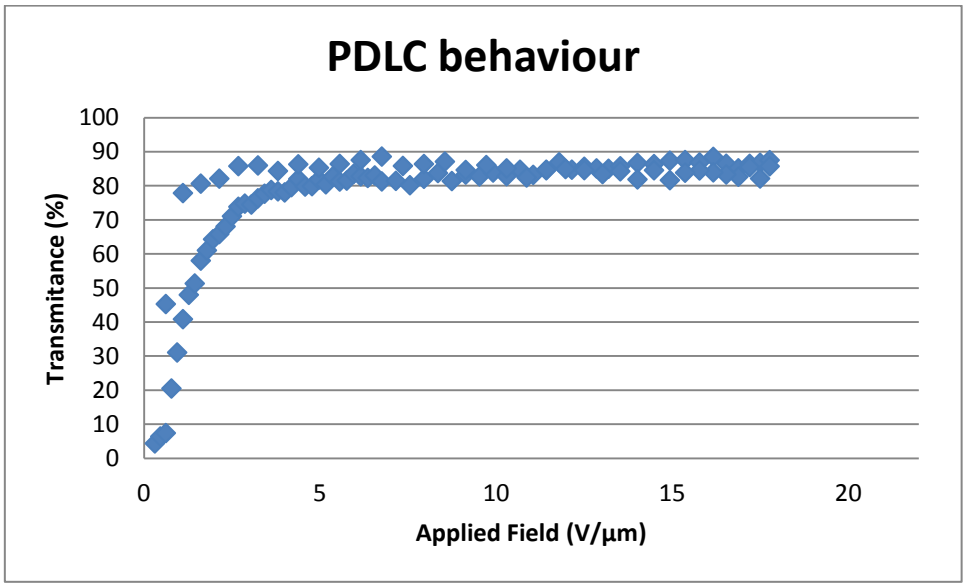

Graph 6.12 - EO response of the system polymer POLYEGMDA$_{875}$ (1%AIBN) and LC in the proportion 30/70% (w/w) with 3%TX100 of the total solution

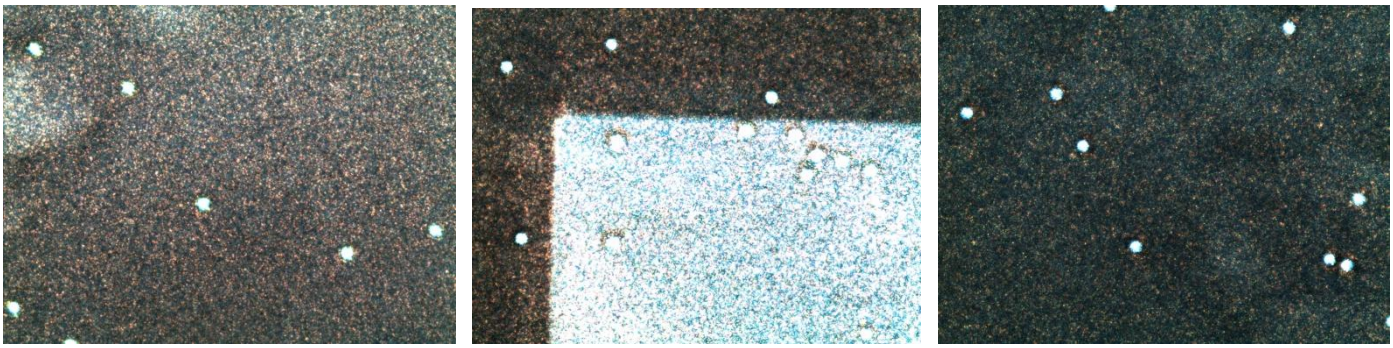

Before EO | After EO | After TNI

Figure 6.12 - POM micrograph for polymer POLYEGDMA$_{875}$ (1%AIBN) and LC in the proportion 30/70% (w/w) with 3%TX100 of the total solution

13.Polymer POLYEGDMA$_{875}$ and LC in the proportion of 20/80 (%w/w) without TX100

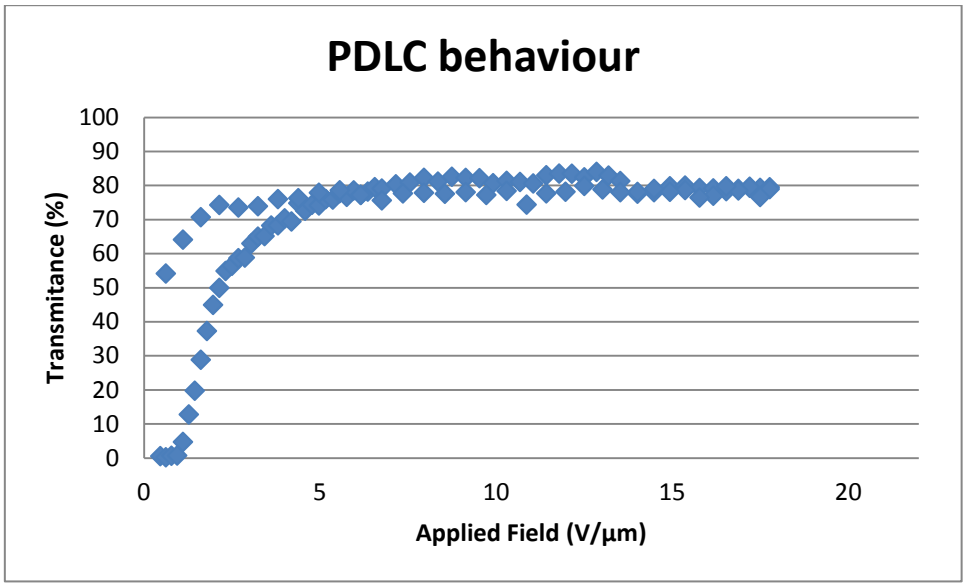

Graph 6.13 - EO response of the system polymer POLYEGMDA$_{875}$ (1%AIBN) and LC in the proportion 20/80% (w/w) without TX100

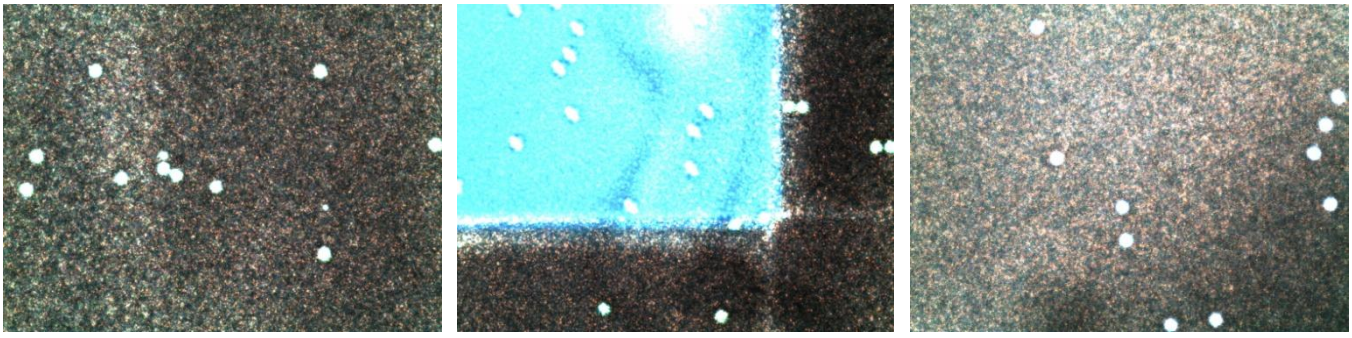

Before EO | After EO | After TNI

Figure 6.13 - POM micrograph for polymer POLYEGDMA$_{875}$ (1%AIBN) and LC in the proportion 20/80% (w/w) without TX100

14.Polymer POLYEGDMA$_{875}$ and LC in the proportion of 10/90 (%w/w) without TX100

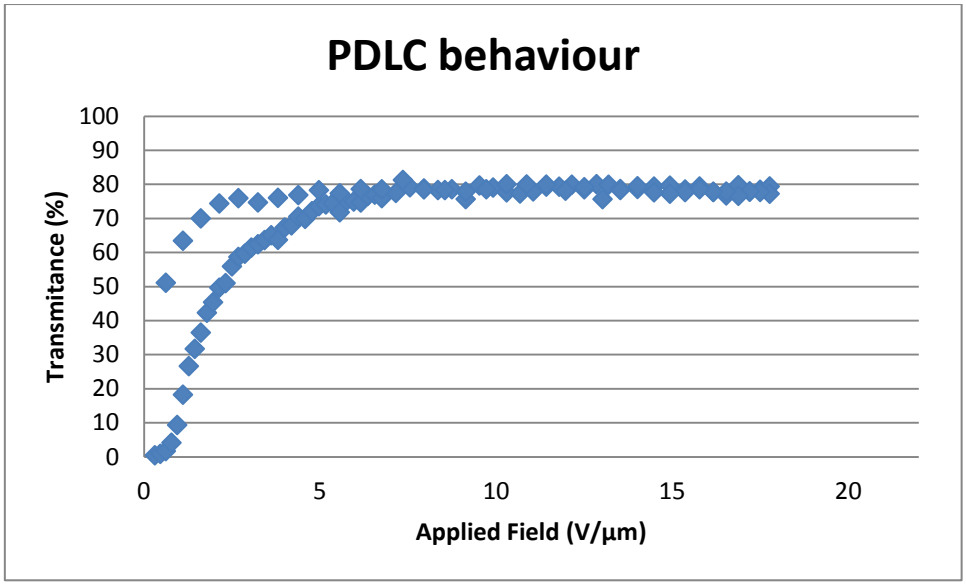

Graph 6.14 - EO response of the system polymer POLYEGMDA$_{875}$ (1%AIBN) and LC in the proportion 10/90% (w/w) without TX100

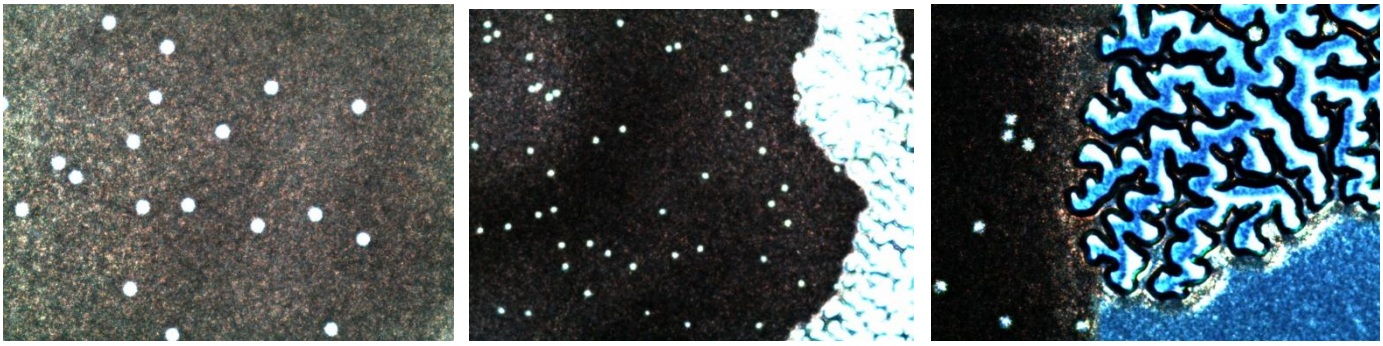

Before EO | After EO | After TNI

Figure 6.14 - POM micrograph for polymer POLYEGDMA$_{875}$ (1%AIBN) and LC in the proportion 10/90% (w/w) without TX100

Appendix 2 - Mathematical Formulation of the Fitting Model

This model was formulated considering the following assumptions:

4. The system CL + polymer consists of LC-rich regions surrounded by regions rich in polymer;

5. LC-rich regions are regarded as spherical, in which the director $\vec{n}$ assumes the value of $\overrightarrow{n_o}$ at rest, (see figure).
6.

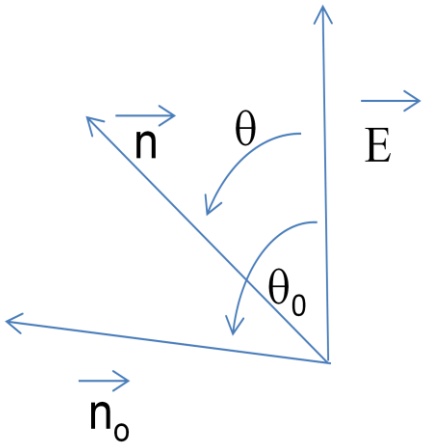

7. The application of an electric field $\vec{E}$ causes $\vec{n}$ to reorient towards the orientation of $\vec{E}$ according to an equation of equilibrium of moments of forces (NOTE: The director $\vec{n}$ is defined by the average orientation of the liquid crystal molecules).

Balance equation of moments of forces acting on the director $\vec{n}$

$$\vec{\Gamma}_{viscous} + \vec{\Gamma}_{electric} + \vec{\Gamma}_{elastic} = \vec{0} \quad (1)$$

Assuming that

$$\vec{\Gamma}_{viscous} = -\gamma \frac{d\theta}{dt} \hat{e}_x \quad (2)$$

$$[\gamma - Rotacional\ Viscosity\ of\ the\ Director]$$

$$\vec{\Gamma}_{electric} = \Delta\varepsilon\,(\vec{n}\,\vec{E})(\vec{n} \times \vec{E}) \quad [\Delta\varepsilon = \varepsilon_{paralel} - \varepsilon_{perpendicular}]$$

$$\vec{\Gamma}_{electric} = -\frac{\Delta\varepsilon}{2} E^2 \sin 2\theta \; \hat{e}_x \quad (3)$$

$$\vec{\Gamma}_{elastic} = \vec{n} \times \vec{h} \quad \left[\vec{h} - Molecular\ Field\right] \quad (4)$$

$$h_i = -\frac{\partial F}{\partial n_i} + \frac{\partial}{\partial X_\alpha}\left[\frac{\partial F}{\partial\left(\frac{\partial n_i}{\partial X_\alpha}\right)}\right] \quad [F - \ Elastic\ free\ energy\ density\ of\ the\ nematic\ LC]$$

Simplified Model for $\vec{\Gamma}_{elastic}$:

$$F = K\,[1 - \ (\vec{n}\,.\overrightarrow{n_0})^2]$$

This expression translates the energy cost for the director $\vec{n}$ to move away from $\vec{n}_0$. Using this simplified model equation (4) can be rewrite as:

$$\vec{\Gamma}_{elastic} = -K \sin 2(\theta - \theta_0)\, \hat{e}_x \quad (5)$$

Replacing the expressions (2), (3) and (5) on equation (1) we have an expression for Θ given by:

$$\gamma \frac{\mathrm{d}\theta\Theta}{\mathrm{dt}} + \frac{\Delta\varepsilon}{2}\mathrm{E}^2 \sin 2\theta\Theta + \mathrm{K} \sin 2(\Theta\theta - \theta\Theta_0) = 0$$

$$\frac{\gamma}{\mathrm{K}}\frac{d\theta}{dt} + \frac{\Delta\varepsilon}{2\mathrm{K}}E^2 \sin 2\,\theta + \sin 2(\theta - \theta_0) = 0 \quad (6)$$

Particular solutions for (6):

IV. Stationary Solution $\left(\frac{d\theta}{dt} = 0\right)$

$$\mathrm{K} \sin 2(\Theta\theta - \theta\Theta_0) = -\frac{\Delta\varepsilon E^2}{2} \sin 2\Theta\,\theta$$

$$\frac{\sin 2(\Theta\theta - \theta\Theta_0)}{\sin 2\Theta\,\theta} = \frac{\Delta\varepsilon E^2}{2K}$$

$$\Theta\theta = \frac{1}{2}\text{artg}\frac{\sin 2\theta_0}{\cos 2\theta_0 + \frac{\Delta\varepsilon E^2}{2K}} \quad (7)$$

V. Solution for equation (6) with an applied field (rise)

Defining:

$$\frac{\gamma}{K} = \frac{1}{b_o}$$

$$\frac{\Delta\varepsilon}{2K}E^2 = a_0$$

The equation for θ is:

$$\Theta\theta(t) = arctg\left\{\frac{1}{\sin 2\theta_0}\left[\frac{a_0 + 1 + \sqrt{c}\,\tanh\left(t\,b_0\sqrt{c}\right)}{1 + (a_0 + 1)\frac{\tan h\left(t\,b_0\sqrt{c}\right)}{\sqrt{c}}}\right] - \frac{a_0 - 1 + 2\cos^2\theta_0}{\sin 2\theta_0}\right\} \quad (8)$$

$$c = (a_o - 1)^2 + 4a_0\cos^2\theta\Theta_0$$

NOTE: Calculus for E:

$$E = \frac{\frac{\Delta V}{d}(1 + r)}{r + \frac{1}{3}\left(2 + \frac{\overline{\varepsilon_{zz}}}{\varepsilon_p}\right)}$$

$$r = \frac{V_{LC}}{V_{polymer}}$$

$d - thickness\ of\ the\ liquid\ crystal$

$\Delta V - RMS\ Applied\ Voltage$

$$\overline{\varepsilon_{zz}} = \varepsilon_{perpendicular} + \left(\varepsilon_{paralel} - \varepsilon_{perpendicular}\right)\overline{\cos^2\theta\Theta_0}$$

$$\overline{\cos^2\theta\Theta_0} = \frac{1}{3}(1 + \cos\theta\,\Theta_0 + \cos^2\theta\Theta_0)$$

$$\overline{cos^2\theta\Theta_0} = \frac{\int_0^{\Theta_{\theta 0}} \cos^2\theta\Theta \sin\theta\,\Theta\ d\theta\Theta}{\int_0^{\Theta_{\theta 0}} \sin\theta\,\Theta\, d\theta\Theta}$$

VI. Solution for equation (6) without an applied field (fall) ($\boldsymbol{E = 0}$)

$$\frac{d\theta\Theta}{dt} + \frac{\mathrm{K}}{\gamma}\sin 2(\Theta\theta - \theta\Theta_0) = 0$$

$$\frac{d\theta\Theta}{\sin 2(\Theta\theta - \theta\Theta_0)} = -\frac{\mathrm{K}}{\gamma}dt$$

$$\Theta = \theta\Theta_0 + arctg\left[tg(\theta\Theta_i - \theta\Theta_0)e^{-\frac{K}{\gamma}\Delta t}\right]$$

Considering $b = \frac{K}{\gamma}$ the previous equation can be rewrite as:

$$\Theta = \theta_0 + arctg[tg(\theta_i - \theta_0)e^{-b\Delta t}] \quad (9)$$

$\theta_i -$ *angle between the director and* $\overrightarrow{E}$ *for* $\Delta t = 0$

Optical Response

Considering $\boldsymbol{I}$ as transmitted light intensity and $\boldsymbol{I_0}$ as intensity of light incident on the sample and using the Lambert-Beer law:

$$\boldsymbol{I = f^2 I_0 e^{-\sigma(\theta)\alpha d}}$$

where f represents the Fresnel factors given by:

$$\boldsymbol{f = T_{1(air \rightarrow glass)} \times T_{1(glass \rightarrow LC)} = \frac{4 n_{air} n_{glass}}{(n_{air} + n_{glass})^2} \times \frac{4 n_{glass} n_p}{(n_{glass} + n_p)^2}}$$

α -Number of diffuser elements per unit volume

d - Film thickness of the LC+polymer film

σ – Scattering cross-section

T_1 - Transmittance of the medium 1 to medium 2 through normal incidence

Determination of $\sigma(\Theta)$ considering light scattering by a dielectric sphere of radius R

$$\sigma(\Theta\theta) = \frac{1}{2}\left(\sigma_{perpendicular} + \sigma_{paralel}\right)$$

$$\sigma(\theta) = \frac{1}{2}\left\{\frac{8\pi}{3}\left(\frac{2\pi}{\lambda}\right)^4 R^6 \left[\left|\frac{n_\theta^2 - n_p^2}{n_\theta^2 + 2n_p^2}\right|^2 + \left|\frac{n_o^2 - n_p^2}{n_o^2 + 2n_p^2}\right|^2\right]\right\}$$

$$n_\theta = \frac{n_o n_e}{\sqrt{n_o^2 \sin^2\theta\Theta + n_e^2 \cos^2\theta\Theta}}$$

n_p - Refractive index of the polymer

n_o - Ordinary index of LC

n_e - Extraordinary index of LC

Therefore considering all previous equations, the final expression for the transmittion coefficient is:

$$\frac{I}{I_0} = f^2 e^{-\sigma(\theta\Theta)\alpha d}, f = \frac{4n_{air}n_{glass}}{\left(n_{air}+n_{glass}\right)^2} \times \frac{4n_{glass}n_p}{\left(n_{glass}+n_p\right)^2}$$

n_{air} - Refractive Index of the air=1

n_{glass} - Refractive Index of the glass≈1,51

$n_{polymer}$ - Refractive Index of the polymer (fitting parameter)

$$\frac{I}{I_0} = f^2 e^{-\alpha d \frac{1}{2}\left\{\frac{8\pi}{3}\left(\frac{2\pi}{\lambda}\right)^4 R^6\left[\left|\frac{n_\theta^2-n_p^2}{n_\theta^2+2n_p^2}\right|^2+\left|\frac{n_o^2-n_p^2}{n_o^2+2n_p^2}\right|^2\right]\right\}}$$

Considering $\alpha\ d\ \frac{1}{2}\frac{8\pi}{3}\left(\frac{2\pi}{\lambda}\right)^4 R^6 = a_1$ **,** the previous equation can be rewrite as:

$$\boldsymbol{\frac{I}{I_0} = f^2 e^{-a_1\left\{\left[\left|\frac{n_\theta^2-n_p^2}{n_\theta^2+2n_p^2}\right|^2+\left|\frac{n_o^2-n_p^2}{n_o^2+2n_p^2}\right|^2\right]\right\}}, f = \frac{4n_{air}n_{glass}}{\left(n_{air}+n_{glass}\right)^2} \times \frac{4n_{glass}n_p}{\left(n_{glass}+n_p\right)^2}\ (10)}$$

Appendix 3 - Fitting Model Results

TRIEGDMA

- **TRIEGDMA (1%AIBN) + E7 with 30/70% (w/w) without TX100**

Table 6.1 - Value of the parameters before and after optimization

Parameter	Before Optimization	After Optimization
t_{is}	0,00	0,00
t_{fs}	4,69	4,69
t_{id}	50,04	50,04
t_{fd}	0,05	0,05
n_v	1,33	1,33
n_p	1,46	1,46
n_o	1,52	1,52
n_e	1,74	1,74
e_{po}	1,50	1,50
e_{no}	5,30	5,20
e_{pa}	19,00	19,00
K	328,29	328,08
d_K	577,46	568,54
n_K	8,00	8,00
γ	0,07	0,07
d_{CL}	25,00	25,00
r_{CL}	2,33	2,33
a_1	414,72	414,86
te_0	1,06	1,05
dte	0,97	0,99
nte	8,00	8,00
vef	235,00	235,00

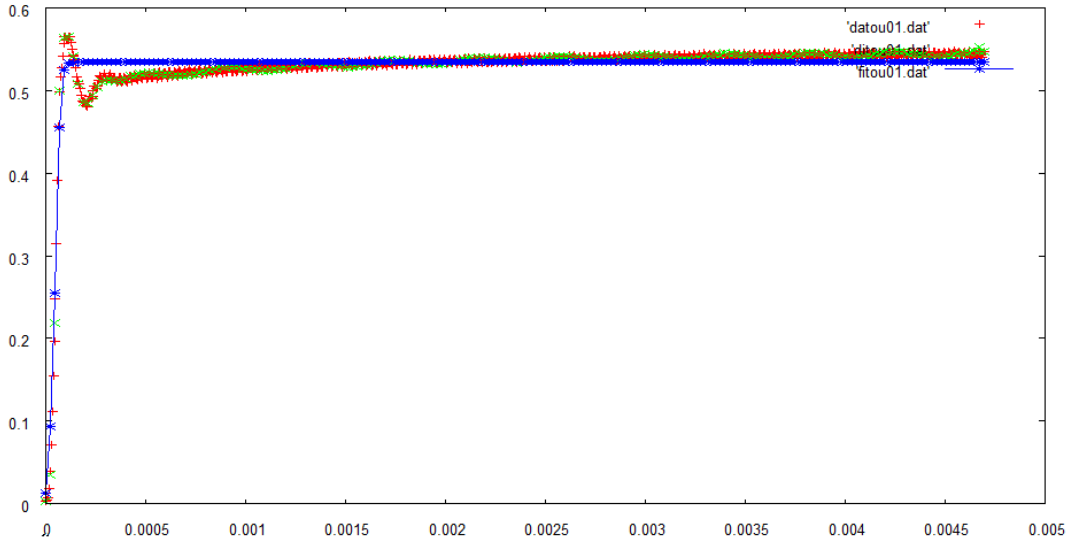

Graph 6.15 - Kinetic Behavior of orientation

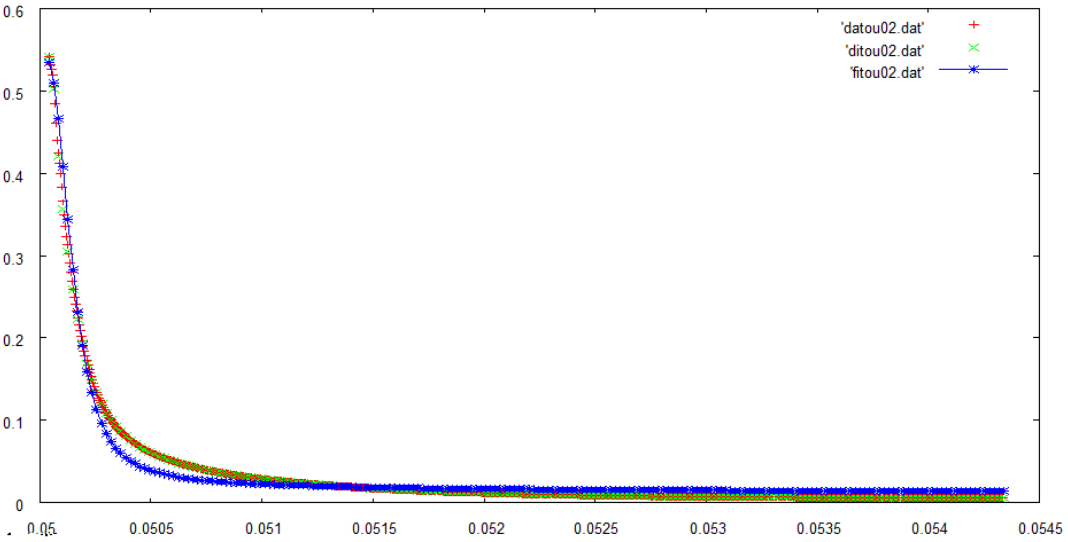

Graph 6.16 - Kinetic Behavior of Desorientation

- **TRIEGDMA (1%AIBN) + E7 with 30/70% (w/w) and 1%TX100 of the total solution**

Table 6.2 - Value of the parameters before and after optimization

Parameter	Before Optimization	After Optimization
t_{is}	0,00	0,00
t_{fs}	4,59	4,59
t_{id}	50,05	50,05
t_{fd}	53,85	53,85
n_v	1,33	1,33
n_p	1,45	1,45
n_o	1,52	1,52
n_e	1,74	1,74
e_{po}	3,44	3,12
e_{no}	5,20	5,10
e_{pa}	19,00	19,00
K	652,28	616,37
d_K	700,00	700,00
n_K	8,00	8,00
γ	0,13	0,13
d_{CL}	25,00	25,00
r_{CL}	2,33	2,33
a_1	318,34	319,57
te_0	1,25	1,25
dte	0,72	0,72
nte	8,00	8,00
vef	240,00	210,00

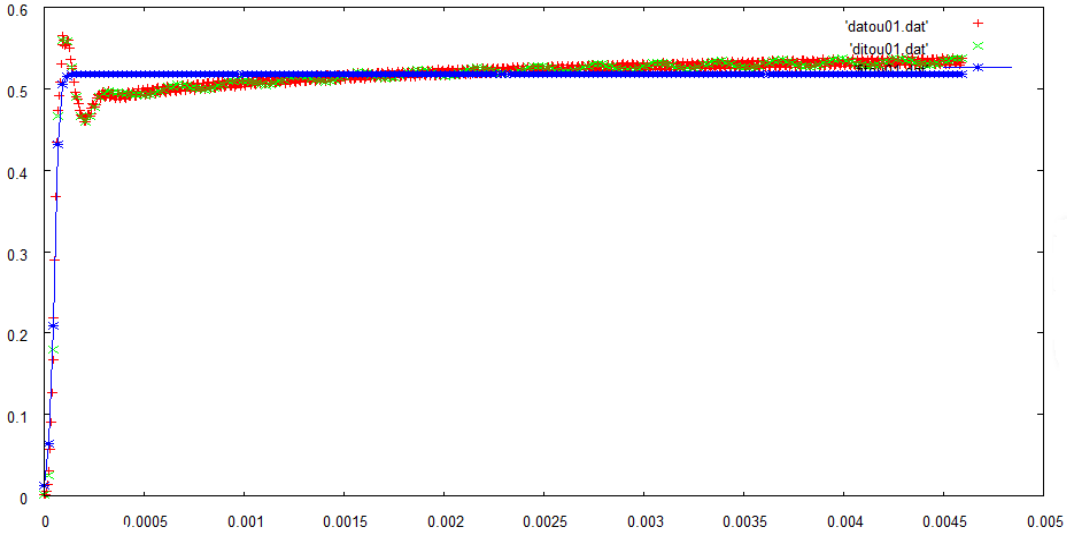

Graph 6.17- Kinetic Behavior of orientation

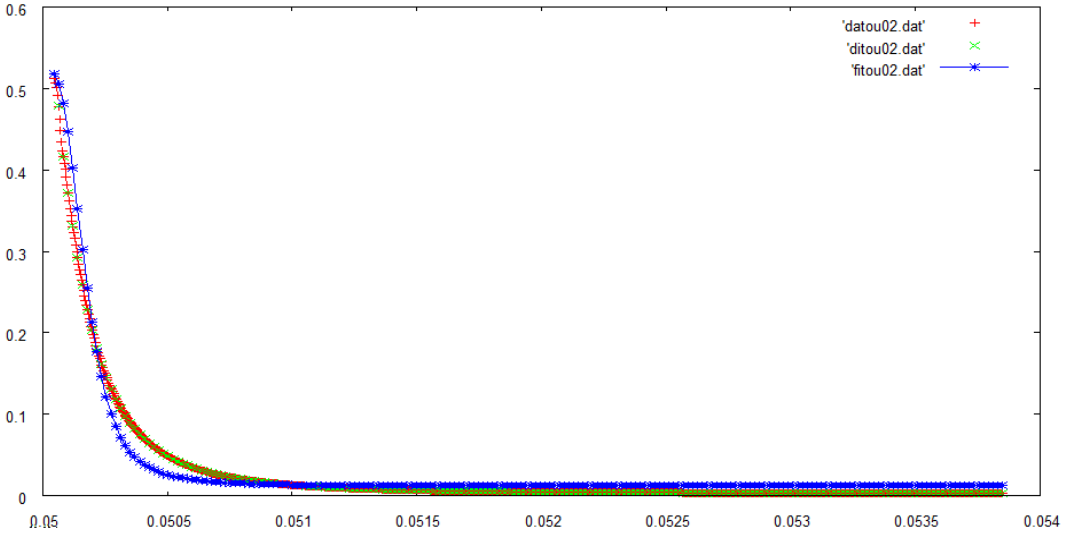

Graph 6.18 - Kinetic Behavior of desorientation

- **TRIEGDMA (1%AIBN) + E7 with 30/70% (w/w) and 5%TX100 of the total solution**

Table 6.3 - Value of the parameters before and after optimization

Parameter	Before Optimization	After Optimization
t_{is}	0,00	0,00
t_{fs}	49,78	49,78
t_{id}	50,05	50,05
t_{fd}	55,55	55,55
n_v	1,33	1,33
n_p	1,56	1,56
n_o	1,52	1,52
n_e	1,74	1,74
e_{po}	2,46	2,46
e_{no}	5,20	5,20
e_{pa}	19,00	19,00
K	268,36	268,36
d_K	0,02	0,02
n_K	8,00	8,00
γ	0,20	0,20
d_{CL}	25,00	25,00
r_{CL}	2,33	2,33
a_1	1011,31	1011,31
te_0	1,08	1,08
dte	0,052	0,0052
nte	8,00	8,00
vef	72,00	72,00

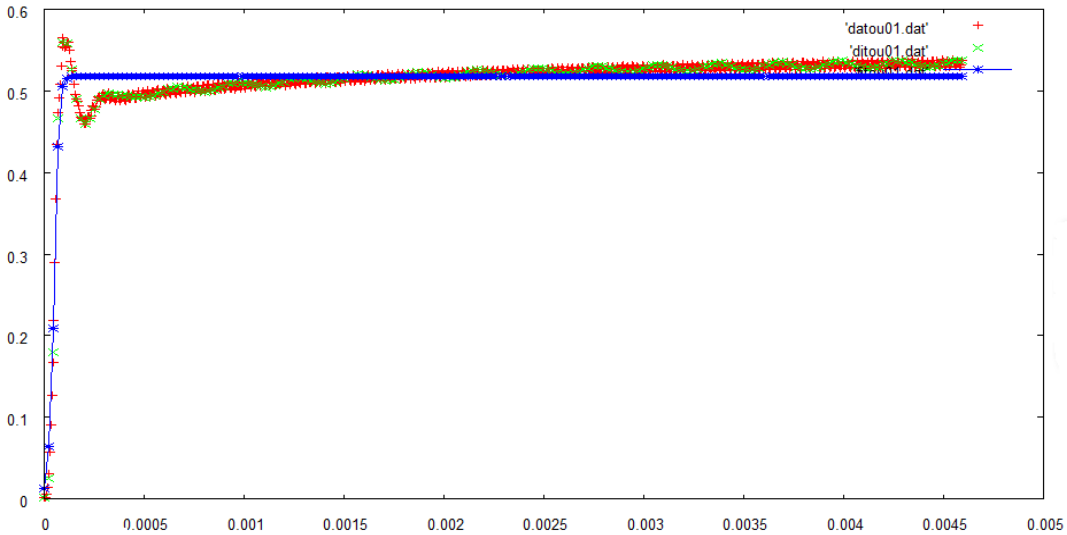

Graph 6.19 - Kinetic Behavior of Orientation

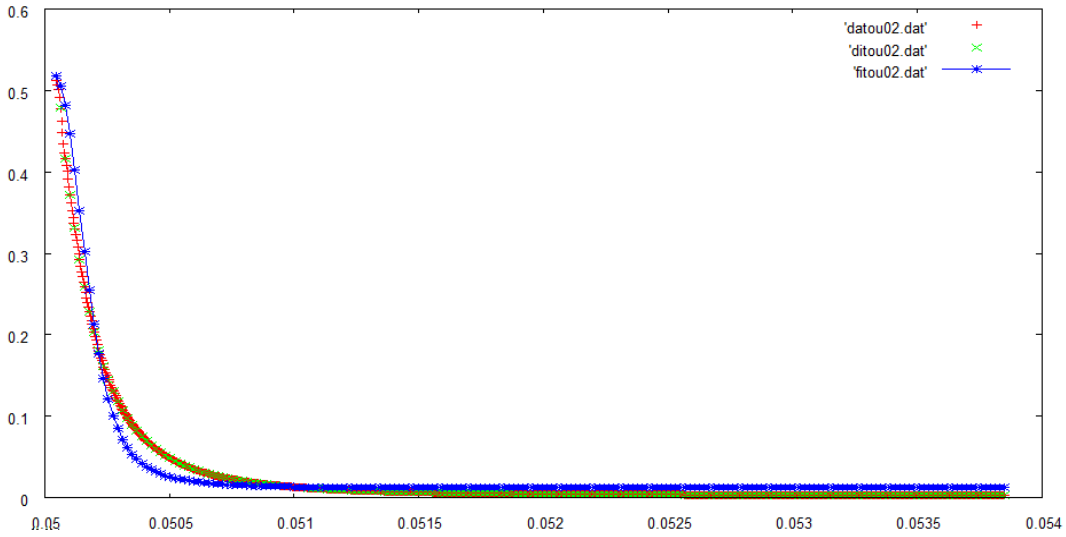

Graph 6.20 - Kinetic Behavior of desorientation

- **TRIEGDMA (1%AIBN) + E7 with 30/70% (w/w) and 10%TX100 of the total solution**

Table 6.4 - Value of the parameters before and after optimization

Parameter	Before Optimization	After Optimization
t_{is}	0,00	0,00
t_{fs}	49,78	49,87
t_{id}	50,04	50,04
t_{fd}	84,33	84,33
n_v	1,33	1,33
n_p	1,50	1,50
n_o	1,52	1,52
n_e	1,74	1,74
e_{po}	4,75	4,90
e_{no}	5,20	5,20
e_{pa}	19,00	19,00
K	25,89	25,65
d_K	34,91	35,80
n_K	8,00	8,00
γ	0,39	0,39
d_{CL}	25,00	25,00
r_{CL}	2,33	2,33
a_1	1362,45	1373,86
te_0	0,76	0,76
dte	0,0001	0,0001
nte	8,50	8,50
vef	42,00	42,00

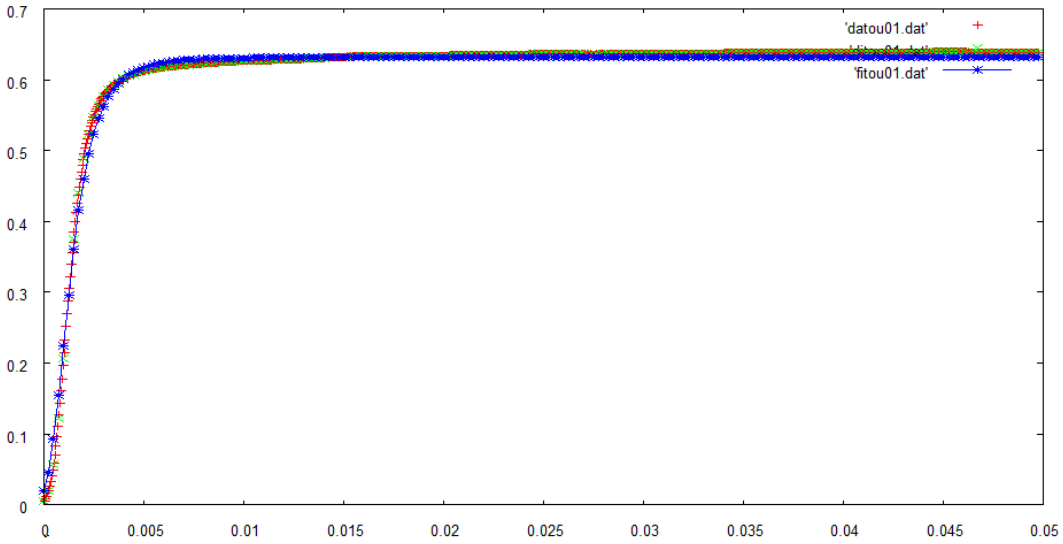

Graph 6.21 Kinetic Behavior of orientation

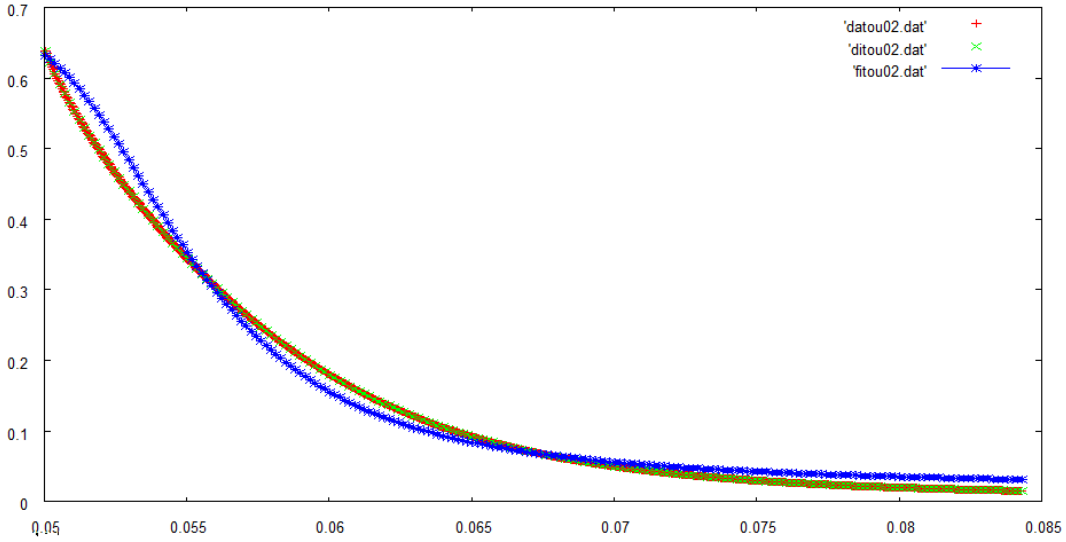

Graph 6.22 - Kinetic Behavior of desorientation

POLYEGDMA$_{875}$

- **POLYEGDMA$_{875}$ (1%AIBN) + E7 with 30/70% (w/w) without TX100**

Table 6.5 - Value of the parameters before and after optimization

Parameter	Before Optimization	After Optimization
t_{is}	0,00	0,00
t_{fs}	20,03	20,03
t_{id}	50,03	50,03
t_{fd}	100,00	100,00
n_v	1,33	1,33
n_p	1,47	1,47
n_o	1,52	1,52
n_e	1,74	1,74
e_{po}	1,50	1,50
e_{no}	5,20	5,20
e_{pa}	19,00	19,00
K	30,19	30,19
d_K	50,00	50,00
n_K	8,00	8,00
γ	0,15	0,15
d_{CL}	25,00	25,00
r_{CL}	2,33	2,33
a_1	463,94	463,80
te_0	0,77	0,77
dte	0,20	0,20
nte	8,00	8,00
vef	41,00	41,00

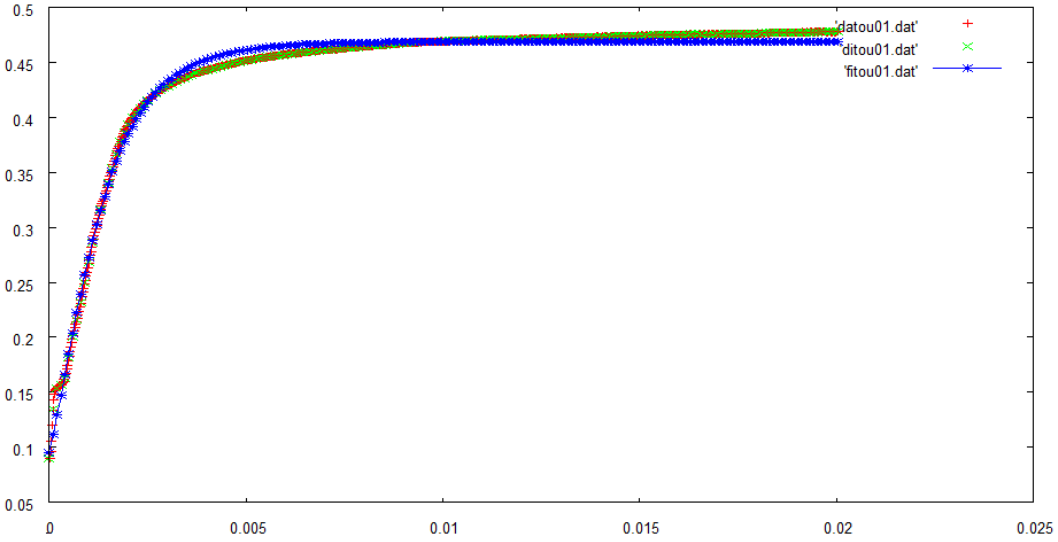

Graph 6.23 - Kinetic Behavior of orientation

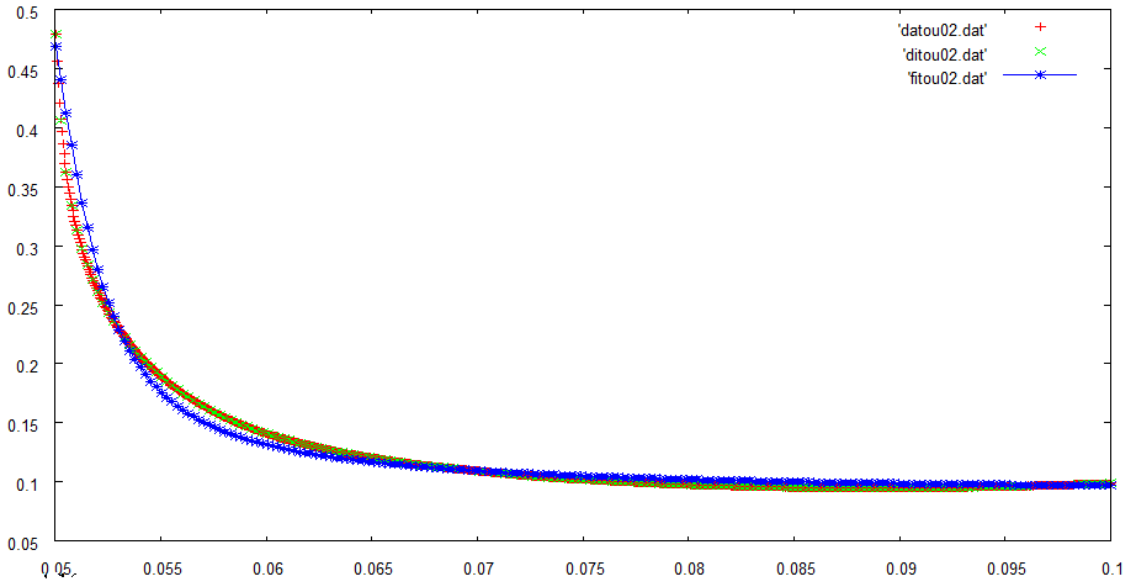

Graph 6.24 - Kinetic Behavior of desorientation

- **POLYEGDMA$_{875}$(1%AIBN) + E7 with 30/70% (w/w) and 1%TX100 of the total solution**

Table 6.6 - Value of the parameters before and after optimization

Parameter	Before Optimization	After Optimization
t_{is}	0,00	0,00
t_{fs}	20,03	20,03
t_{id}	50,03	50,03
t_{fd}	100,00	100,00
n_v	1,33	1,33
n_p	1,51	1,51
n_o	1,52	1,52
n_e	1,74	1,74
e_{po}	1,48	1,47
e_{no}	5,20	5,10
e_{pa}	19,00	19,00
K	103,05	102,57
d_K	170,00	170,00
n_K	8,00	8,00
γ	0,24	0,24
d_{CL}	25,00	25,00
r_{CL}	2,33	2,33
a_1	423,19	423,23
te_0	0,89	0,89
dte	0,74	0,74
nte	8,00	8,00
vef	39,00	39,00

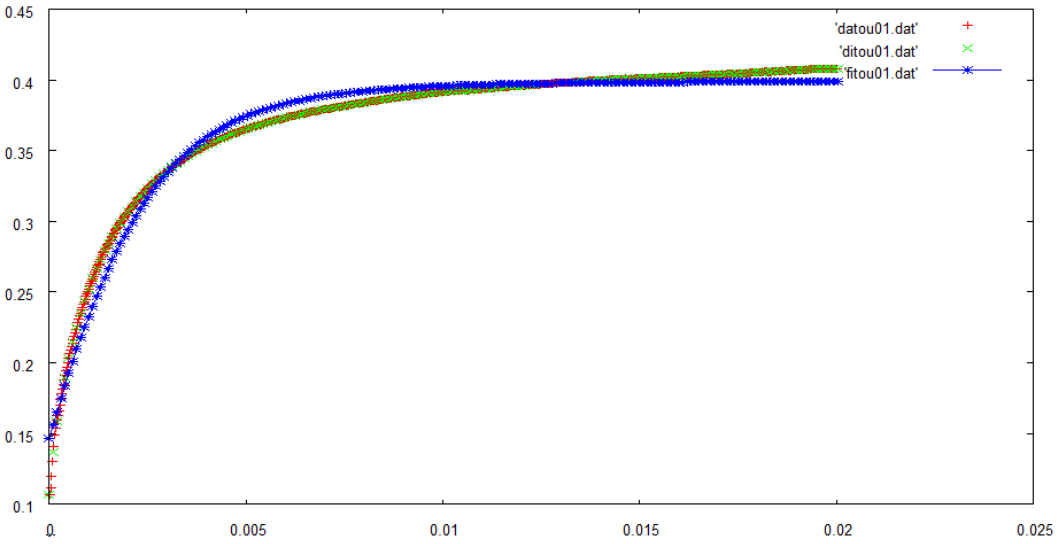

Graph 6.25 - Kinetic Behavior of orientation

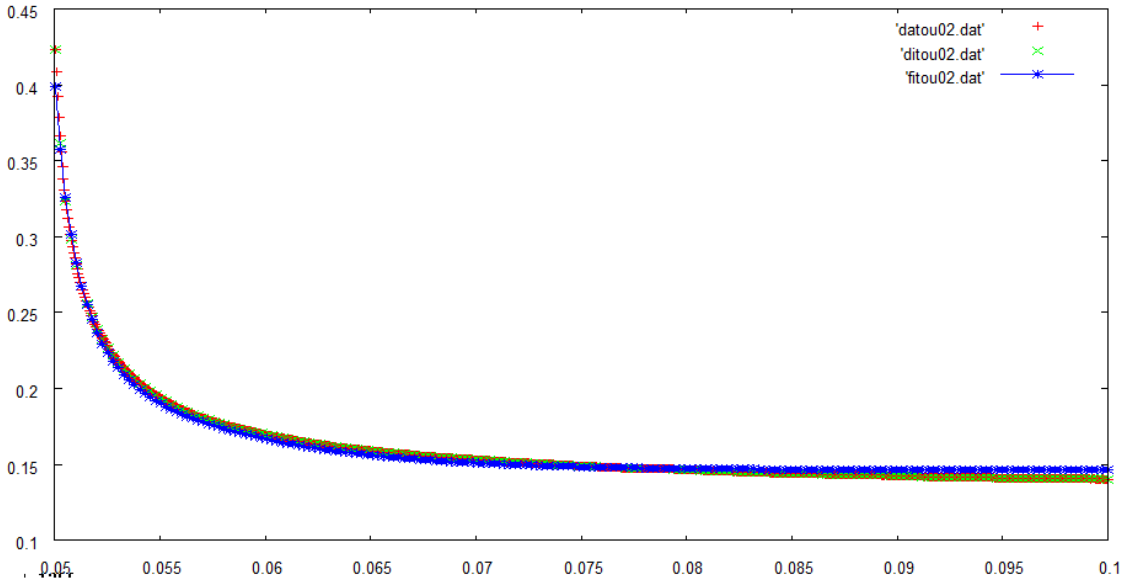

Graph 6.26 - Kinetic Behavior of desorientation

- **POLYEGDMA$_{875}$(1%AIBN) + E7 with 30/70% (w/w) and 5%TX100 of the total solution**

Table 6.7 - Value of the parameters before and after optimization

Parameter	Before Optimization	After Optimization
t_{is}	0,00	0,00
t_{fs}	20,03	20,03
t_{id}	50,03	50,03
t_{fd}	100,00	100,00
n_v	1,33	1,33
n_p	1,49	1,49
n_o	1,52	1,52
n_e	1,74	1,74
e_{po}	2,13	2,13
e_{no}	5,20	5,20
e_{pa}	19,00	19,00
K	34,52	34,46
d_K	55,00	54,99
n_K	8,00	8,00
γ	0,25	0,25
d_{CL}	25,00	25,00
r_{CL}	2,33	2,33
a_1	831,84	831,84
te_0	0,81	0,81
dte	0,0001	0,0001
nte	8,00	8,00
vef	39,00	39,00

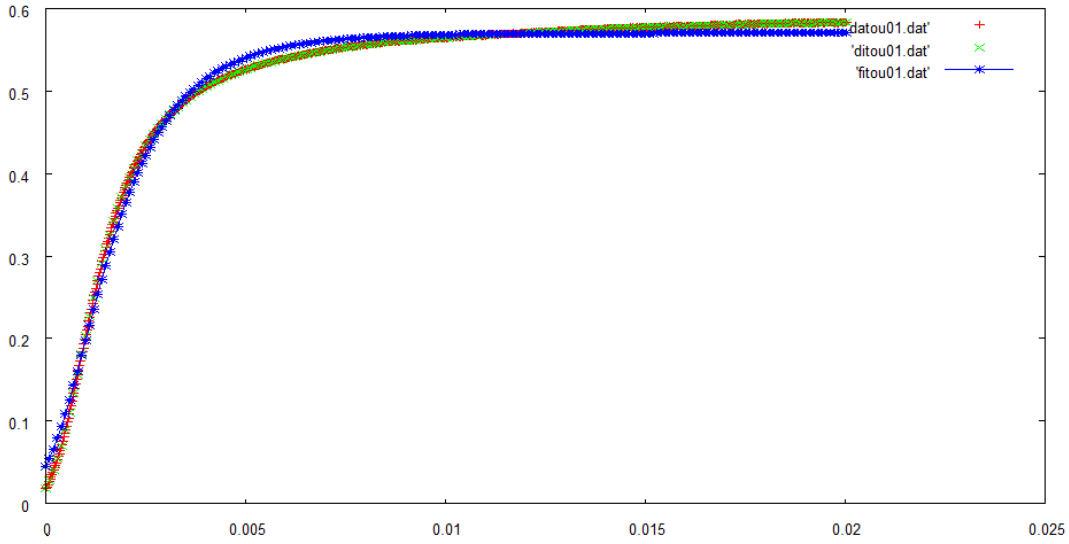

Graph 6.27 - Kinetic Behavior of orientation

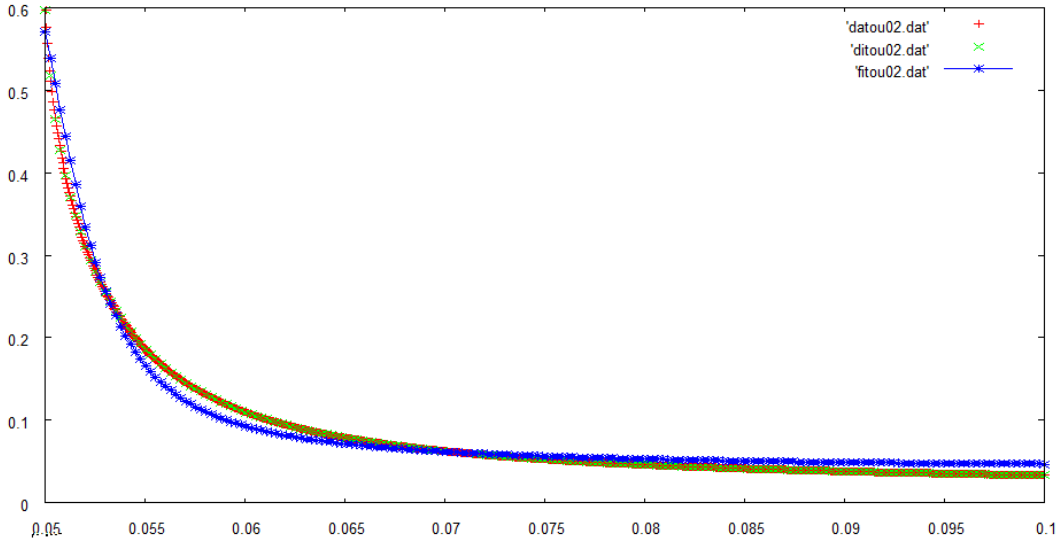

Graph 6.28 - Kinetic Behavior of desorientation

- **POLYEGDMA$_{875}$(1%AIBN) + E7 with 30/70% (w/w) and 10%TX100 of the total solution**

Table 6.8 - Value of the parameters before and after optimization

Parameter	Before Optimization	After Optimization
t_{is}	0,00	0,00
t_{fs}	30,00	30,00
t_{id}	50,00	50,00
t_{fd}	90,06	90,06
n_v	1,33	1,33
n_p	1,49	1,49
n_o	1,52	1,52
n_e	1,74	1,74
e_{po}	3,33	3,25
e_{no}	5,20	5,20
e_{pa}	19,00	19,00
K	17,60	17,70
d_K	29,57	29,57
n_K	8,00	8,00
γ	0,24	0,24
d_{CL}	25,00	25,00
r_{CL}	2,33	2,33
a_1	539,73	539,64
te_0	0,81	0,81
dte	0,0001	0,0001
nte	8,00	8,00
vef	38,00	38,00

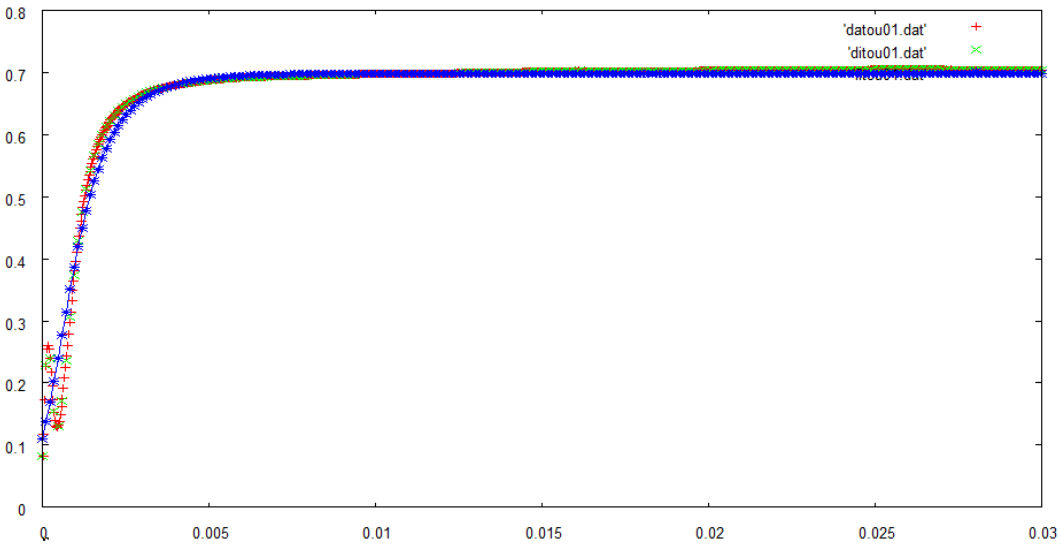

6.29 - Kinetic Behavior of orientation

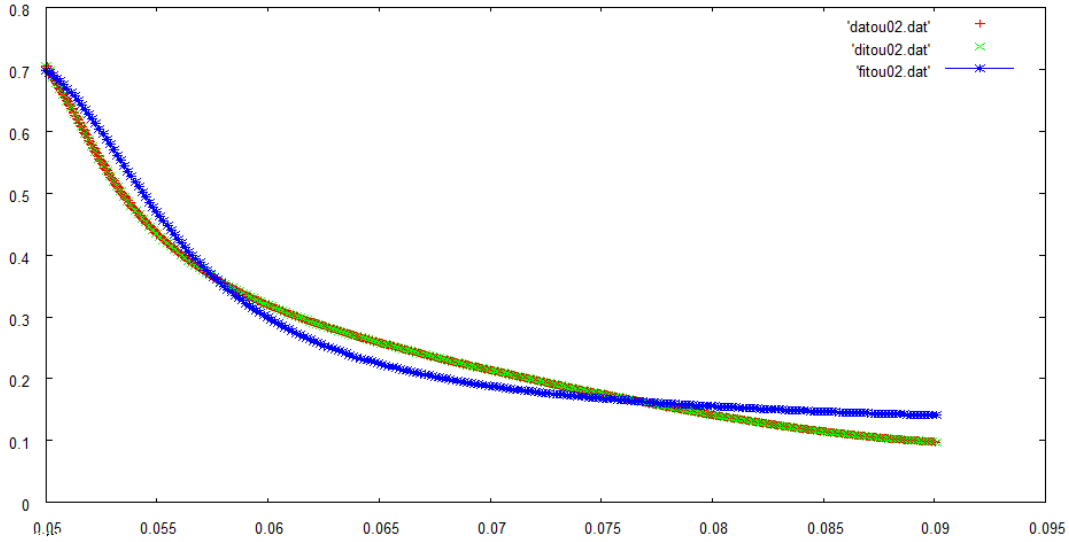

6.30 - Kinetic Behavior of desorientation

Appendix 4 - Additional DSC studies

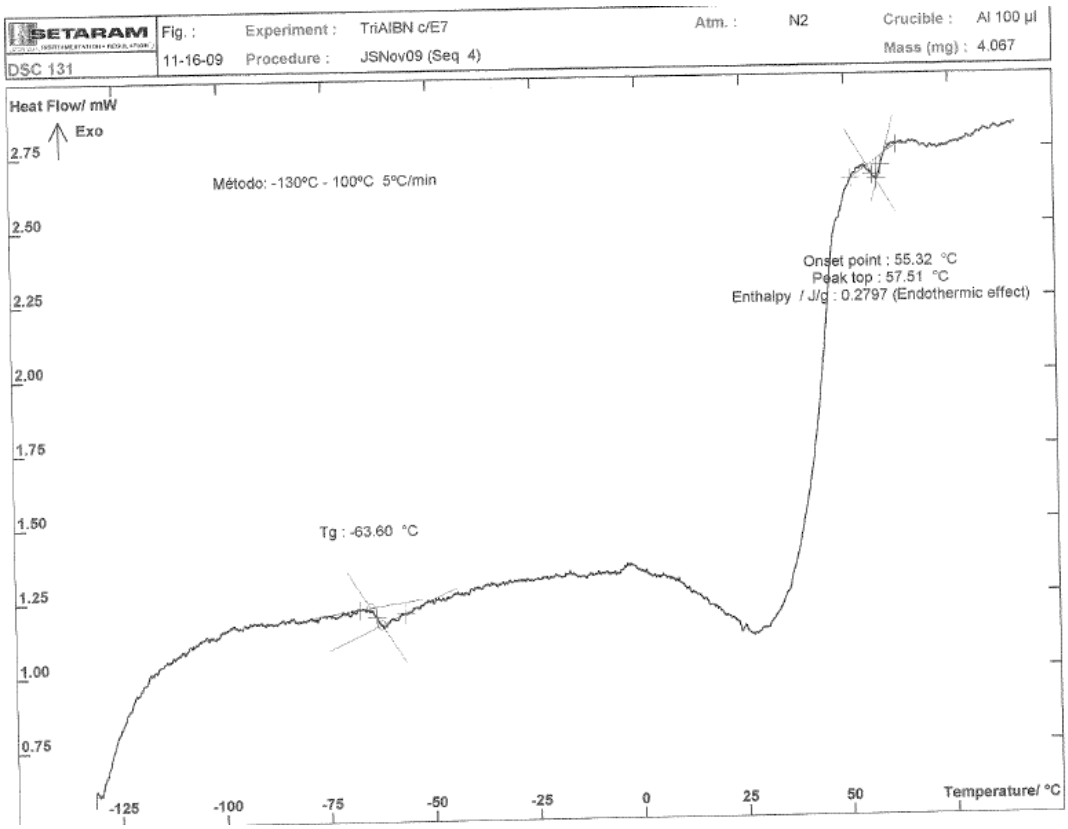

Graph 6.31 - DSC study of polymer TRIEGDMA with E7 in the proportion of 30/70 (%w/w)

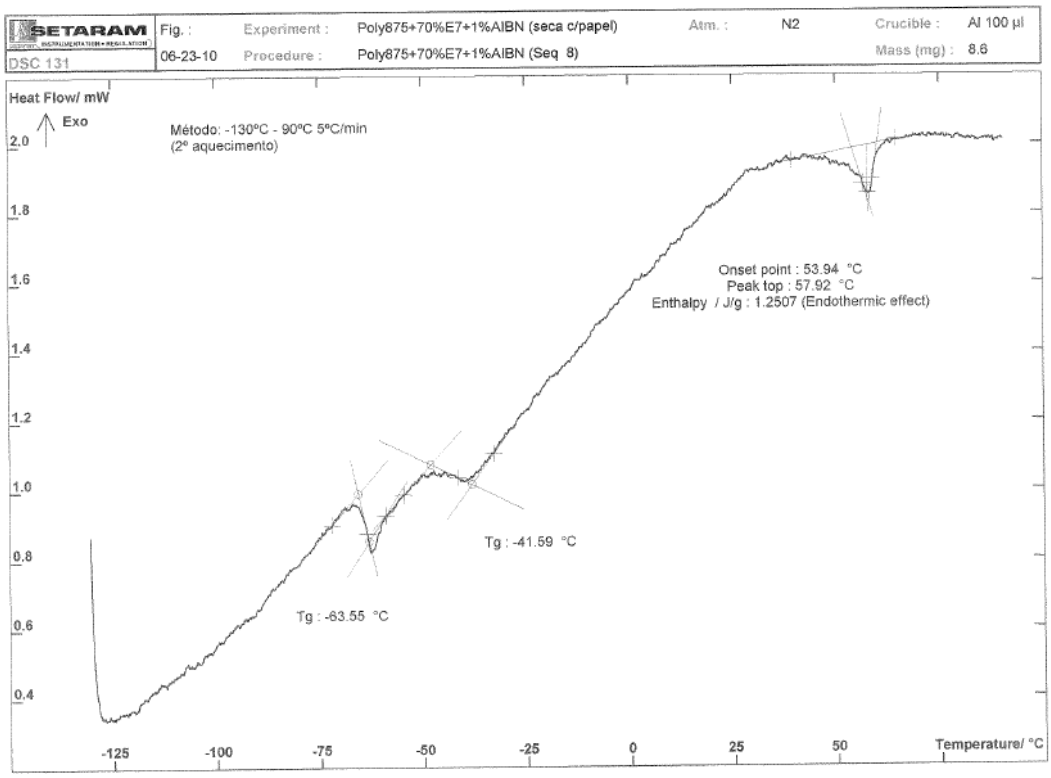

Graph 6.32 DSC study of polymer POLYEGDMA$_{875}$ with E7 in the proportion of 30/70 (%w/w)